NUREG/CR-3904
SAND84-1461
RG
Printed March 1985

A Comparison of Uncertainty and Sensitivity Analysis Techniques for Computer Models

Ronald L. Iman, Jon C. Helton

Prepared by
Sandia National Laboratories
Albuquerque, New Mexico 87185 and Livermore, California 94550
for the United States Department of Energy
under Contract DE-AC04-76DP00789

Prepared for
U. S. NUCLEAR REGULATORY COMMISSION

Available from

GPO Sales Program
Division of Technical Information and Document Control
U.S. Nuclear Regulatory Commission
Washington, D.C. 20555

and

National Technical Information Service
Springfield, Virginia 22161

NUREG/CR-3904
SAND84-1461
RG

A COMPARISON OF UNCERTAINTY AND SENSITIVITY ANALYSIS TECHNIQUES FOR COMPUTER MODELS

Ronald L. Iman
Jon C. Helton *

Printed: March 1985

Sandia National Laboratories
Albuquerque, New Mexico 87185
operated by
Sandia Corporation
for the
U.S. Department of Energy

Prepared for
Division of Risk Analysis and Operations
Office of Nuclear Regulatory Research
U.S. Nuclear Regulatory Commission
Washington, D.C. 20555
Under Memorandum of Understanding DOE 40-550-75
NRC Fin No. A-1339

*Arizona State University

ABSTRACT

Uncertainty analysis and sensitivity analysis are important elements in the development and implementation of computer models for complex processes. Typically, there are many uncertainties associated with both the development and the application of such models. Understanding of these uncertainties and their causes is required to effectively interpret model behavior. Many different techniques have been proposed for performing uncertainty and sensitivity analyses. The objective of the present study is to compare several widely used techniques on three models having large uncertainties and varying degrees of complexity in order to highlight some of the problem areas that must be addressed in actual applications. The following approaches to uncertainty and sensitivity analysis are considered: (1) response surface methodology based on input determined from a fractional factorial design, (2) Latin hypercube sampling with and without regression analysis, and (3) differential analysis. These techniques are compared on the basis of (1) ease of implementation, (2) flexibility, (3) estimation of the cumulative distribution function of the output, and (4) adaptability to different methods of sensitivity analysis. With respect to these criteria, the technique using Latin hypercube sampling and regression analysis gives the best results overall. The models used in the comparisons are well documented, thus making it possible for researchers to make comparisons of other techniques with the results in this study.

TABLE OF CONTENTS

TABLE OF CONTENTS (continued)

LIST OF FIGURES

LIST OF TABLES

LIST OF TABLES

ACKNOWLEDGEMENT

The authors would like to express their sincere appreciation to the following individuals whose careful review of a draft of this report contributed greatly to its present form.

David C. Aldrich	Science Applications, Inc.
Daniel J. Alpert	Sandia National Laboratories
Thomas A. Bishop	Battelle Columbus Laboratories
James E. Campbell	Intera Environmental Consultants
W. J. Conover	Texas Tech University
Darryl J. Downing	Oak Ridge National Laboratory
Robert G. Easterling	Sandia National Laboratories
Robert H. Gardner	Oak Ridge National Laboratory
William V. Harper	Battelle Columbus Laboratories
F. Eric Haskin	Sandia National Laboratories
Stephen C. Hora	Texas Tech University
Dale M. Rasmusson	Nuclear Regulatory Commission
Eric R. Ziegel	Standard Oil Company

1. INTRODUCTION

Computer models are used in many settings to implement mathematical models for complex processes. Typically, these models represent a variety of phenomena. For example, the Nuclear Regulatory Commission-sponsored MELCOR program at Sandia National Laboratories is developing a complex system of models that address accident progression, thermal-hydraulic phenomena, radionuclide behavior and transport, and environmental consequence analysis for severe reactor accidents (Sprung et al., 1983). There are many uncertainties associated with both the development and application of these models. Understanding of these uncertainties and their causes is required to effectively interpret the model predictions.

The analysis of uncertainties and sensitivities associated with such models plays an important part in their development and application. Typically, large systems such as MELCOR are too complex to permit a simple examination of uncertainty in its entirety. Hence, much effort is directed at examining the components of a system. At the first stage of an analysis, it is necessary to use some carefully designed procedure to determine the impact of uncertainty on individual models in the system, and then at the second stage to study the impact of uncertainty on the entire system. There are many techniques for uncertainty analysis and sensitivity analysis. The purpose of this study is to compare several widely used approaches for uncertainty and sensitivity analysis of individual models.

For this comparison, it is convenient to think of a model as a function $Y = f(X_1,...,X_k,t)$ of the independent variables $X_1,...,X_k$ and possibly also of time t. The variables $X_1,...,X_k$ can be used to represent a variety of phenomena within the model. For example, they might represent common properties such as temperature and pressure or other entities such as parameters in statistical distributions, branch points in the evolution of a process, or different submodels within a larger model. Uncertainty analysis is defined here to be the determination of the variation or imprecision in Y that results from the collective variation in the model variables $X_1,...,X_k$. Summarizing and displaying the uncertainty associated with Y is a problem of immediate concern since there are many questions of potential interest, such as (1) what is the range of Y, (2) what are the mean and median of Y, (3) what is the variance of Y, (4) what are the lower and upper 5% quantiles for Y, and (5) are there any discontinuities associated with the distribution of Y. A convenient tool for providing such information is the estimated cumulative distribution function (cdf) for Y since it summarizes the variability in computer model output which results from the input assumptions. However, the estimated distribution function of Y can only be interpreted in a probabilistic sense if the model variables $X_1, ..., X_k$ have meaningful probability distributions associated with them. Frequently, this is not possible as the model input variables may lack an adequate data base. We will proceed with the first stage of the uncertainty analysis using the estimated cumulative distribution function as a summary tool without being overly concerned about interpretations for the probability estimate it provides.

An area closely related to uncertainty analysis is sensitivity analysis. The importance of sensitivity analysis lies in the guidance it provides with respect to the identification of the important contributors to uncertainty in Y. Sensitivity analysis is defined here to be the determination of the change in the response of a model to changes in model parameters and specifications. Thus, sensitivity analysis is used to identify the main contributors to the variation or imprecision in Y.

The models to which uncertainty and sensitivity analyses are applied are often large and complex and frequently display many of the following properties:

- There are many input variables.
- The model is time consuming (i.e. expensive) to run on a computer.
- Alterations to the model are difficult and time consuming.
- It is difficult to reduce the model to a single system of equations.
- Discontinuities exist in the behavior of the model.
- Correlations exist among the input variables and the associated marginal probability distributions are often nonnormal.
- Model predictions (outputs) are nonlinear, multivariate, time-dependent functions of the input variables.
- The relative importance of individual input variables is a function of time.

For an approach to uncertainty and sensitivity analysis to be viable, it must be applicable to models possessing many of the preceding characteristics.

This study examines the following three often-used approaches to uncertainty and sensitivity analysis:

- Response surface replacement for the computer model
- Modified Monte Carlo as exemplified by Latin hypercube sampling
- Differential analysis.

This examination is implemented by applying these techniques to three existing models with large uncertainties. The following models are used:

- Pathways (a model for environmental radionuclide movement)
- MAEROS (a model for multicomponent aerosol dynamics)
- DNET (a model for salt dissolution in bedded salt formations).

These models were selected because each is well documented, has been extensively used in risk assessment applications associated with geologic isolation of radioactive waste or in risk studies for nuclear reactors, and displays many of the eight model characteristics indicated above.

Section 2 presents a brief description of the three techniques for uncertainty and sensitivity analysis that are compared in this study. Section 3 presents results from all three techniques utilizing the Pathways model. Section 4 presents a comparison of Latin hypercube sampling and differential analysis using the MAEROS model. The response surface replacement is not used with the MAEROS model due

to the difficulty of utilizing an experimental design with the complex multivariate input structure associated with this model. Response surface replacements and Latin hypercube sampling are compared in Section 5 with the DNET model. The differential analysis is not used with the DNET model due to feedback mechanisms within the model which make such an analysis difficult to implement. Additional techniques for sensitivity analysis and uncertainty analysis are discussed in Section 6. Section 7 contains a summary and conclusions.

2. METHODS TO BE COMPARED

Three methods for sensitivity analysis and uncertainty analysis are considered in this study. These methods are based on (1) a response surface replacement for the computer model, (2) modified Monte Carlo as examplified by Latin hypercube sampling both with and without regression analysis, and (3) differential analysis. A brief discussion of each of these methods is given in this section.

2.1 RESPONSE SURFACE REPLACEMENT FOR THE COMUTER MODEL

A response surface replacement for a computer model is based on using an experimental design to select a set of specific values and pairings of the input variables $X_1, \ldots, X_k$ that are used in making n runs of the computer model. The method of least squares is used with the model output Y_i and input $X_{1i}, \ldots, X_{ki}$, i = 1, ..., n, to estimate the parameters of a general linear model of the form:

$$Y = \beta_0 + \sum_j \beta_j X_j . \qquad (2.1)$$

The estimated model is known as a fitted response surface, and it is this response surface that is used as a replacement for the computer model. Thus, all inferences with respect to uncertainty analysis and sensitivity analysis for the computer model are derived from this fitted model. Two points are worth noting with respect to the model in (2.1). First, a linear model is usually written with an error term added on to represent stochastic variation. However, the computer models considered in the present analysis produce deterministic output, and therefore, differences between the model in (2.1) and the computer model are due to lack of fit rather than stochastic variation. The second point involves the individual X_j used in the model in (2.1). The actual fitting of such a model usually involves additional variables derived from the original variables, such as squares and crossproducts as well as transformations of the original variables.

The fitting of a response surface usually requires that some prescription be used to select the specific values of the inputs $X_1, \ldots, X_K$, and more importantly, to determine the manner in which the input are paired in each of the n computer runs. Experimental designs are commonly used to make this determination. The choice of available designs is quite large, and since this study is not intended to be a treatise on response surface techniques, only an often used approach based on factorial designs wil be used for purposes of illustration. References to more sophisticated attempts at fitting response surfaces are given at the end of this subsection.

Factorial experimental designs are well developed in the statistical literature and extensive discussions with respect to them may be found in textbooks on experimental design, for example see Box, Hunter and Hunter (1978). A factorial design utilizes two or more fixed values (i.e., levels) to represent each variable under consideration. Thus, if there are k input variables and if two levels are used for each variable, then there exist 2^k possible combinations of the k variables

while 3^k combinations are possible with 3 levels, or in general n^k combinations are possible with n levels. It is also possible to mix the number of levels used with each variable such as six variables at two levels paired with two variables at three levels and two variables at four levels. One of the features of a factorial design is that all pairwise correlations between the inputs are equal to zero (i.e., the input values are orthogonal to one another).

It is clear that the number of treatment combinations becomes quite large even for a small number of variables. Thus, in order for a factorial design to be useful with computer models having large numbers of input variables, an approach is needed that allows for a reduction in the number of treatment combinations. This is possible to some extent through the use of fractional factorial designs where some fraction of the total number of treatment combinations is used. That is, for each of k factors at n = 2 levels some fraction $(1/2)^m$, $m < k$, of the total number of treatment combinations is used. Thus, for k = 10 and n=2, fractional factorial designs could have 512, 256, 128, 64, 32, 16, 8, 4, or 2 treatment combinations corresponding to m = 1, 2, 3, 4, 5, 6, 7, 8, and 9, respectively. The number of required runs of the model would equal the number of treatment combinations. Of course, as m increases, the effects of some individual variables cannot be estimated because of confounding with interactions among variables. Thus, the selection of the fraction size and treatment combinations must be done with great care, keeping in mind which variable effects and interactions are of greatest interest. Selection of the actual design to be used in an analysis can be made only after a careful consideration of the model and the variables associated with it. The expense of evaluating the model (and subsequent limitation of the number of computer runs) may exert a strong influence on the selection of the design to be used.

A discussion of techniques for the development of fractional factorial designs is beyond the scope of this study. However, readable discussions on fractional factorial designs can be found in Box, Hunter, and Hunter (1978) and Finney (1960), with a more mathematical treatment of recent developments given by Raktoe, Hedayat and Federer (1981). Many textbooks on experimental design contain plans for fractional factorial designs for various numbers of levels and different values of m and k. The U. S. National Bureau of Standards (Applied Mathematics Series, 48 and 54; April 1957 and May 1959) has published one of the largest sets of plans and includes values of $k \leq 16$ for various values of m and n.

In the previous section, uncertainty analysis for an individual model output variable Y was focused on estimating the distribution function of Y. The distribution function for an output variable cannot be estimated directly from the set of output values resulting from input based on a fractional factorial design since the selection procedure used with the input values is not random. Therefore, to use a response surface replacement for the model in an uncertainty analysis, it is necessary to use Monte Carlo simulation with the response surface to estimate a distribution function for the dependent variable Y. The response surface can be used directly (i.e., without Monte Carlo) to estimate the expected value of Y by

$$\hat{E}(Y) = \hat{\beta}_0 + \sum_j \hat{\beta}_j E(X_j) \qquad (2.2)$$

where E is used to denote expected value and the hat represents the estimate of the quantity under the hat. Additionally, the variance associated with Y can be estimated by

$$\hat{V}(Y) = \sum_j \hat{\beta}_j^2 V(X_j) + 2 \sum\sum_{i<j} \hat{\beta}_i \hat{\beta}_j Cov(X_i, X_j) , \qquad (2.3)$$

where V and Cov are used to denote the variance and covariance, respectively.

As defined in Section 1, sensitivity analysis for an individual model output variable Y involves determination of the response of that variable to changes in system parameters and specifications. There are several ways explained in Section 3 in which the influence of individual variables or parameters can be measured. These measures include standardized regression coefficients, partial correlation coefficients, normalized partial derivatives, and contribution to variance. Many of these ways are closely related to response surfaces. The end result of these techniques is a ranking by importance of the input variables. These and other techniques are discussed and illustrated in the sections that follow.

Additionally, a useful preliminary nonquantitative screening technique is a sequence of scatterplots in which the values for the dependent variable appear on one axis and the values for each independent variable appear in turn on the other axis. Such plots provide an indication of which independent variables are important and may also provide guidance with respect to useful data transformations for the variables in (2.1) as well as other aspects of the analysis. Examples of scatterplots are given in Section 5.

If the output behaves in a linear fashion between the low and high values of each input variable, input based on a fractional factorial design with two levels works well for indicating major trends and the corresponding response surface replacement works well in both uncertainty analysis and sensitivity analysis. A simple application of this approach is given in Baybutt, Cox, and Kurth (1982). If the output does not behave in a linear fashion, then an improvement in the response surface fit can usually be obtained by using interior points in conjunction with the high-low values such as found in a central composite design as explained in Box, Hunter and Hunter (1978). In addition, a discussion of the application of a central composite design to a computer model that describes a scrubbing process which removes radioactive material from steam generated during a nuclear reactor melt down accident is given in Bishop (1983). Steck, Dahlgren and Easterling (1975) give an example of a sophisticated sequential attempt at fitting a response surface to product peak cladding temperature in a loss of coolant accident at a nuclear reactor. Myers (1971) provides an introduction to the use of fractional factorial designs in conjunction with response surface techniques. Additional information on response surface methodology can be found in references such as Box and Behnken (1960), Box and Draper (1959), Box, Hunter and Hunter (1978), Davies (1956), and DeBaun (1959). Draper (1982) and Box, Hunter and Hunter (1978) discuss designs with center points for fitting second order response surfaces and give several related references. Examples of the use of fractional factorial designs in uncertainty analysis and sensitivity analysis include Cox (1977), Steinhorst et al (1978) Kleijnen (1979), Nguyen (1980), Baybutt, Cox, and Kurth (1982) and Bishop (1983).

2.2 MODIFIED MONTE CARLO (LATIN HYPERCUBE SAMPLING)

A possible alternative to the response surface replacement approach is a type of stratified Monte Carlo sampling known as Latin hypercube sampling (LHS). As originally described in McKay, Conover, and Beckman (1979), LHS operates in the following manner to generate a sample of size n from the k variables $X_1, \ldots, X_k$. The range of each variable is divided into n nonoverlapping intervals on the basis of equal probability. One value from each interval is selected at random with respect to the probability density in the interval. The n values thus obtained for X_1 are paired in a random manner (equally likely combinations) with the n values of X_2. These n pairs are combined in a random manner with the n values of X_3 to form n triplets, and so on, until a set of n k-tuples is formed. Thus, for given values of n and k, there exist $(n!)^{k-1}$ possible interval combinations for a Latin hypercube sample. For example, with n = 3 and k = 2, there are $(3!)^{2-1} = 6$ possible interval combinations. The six interval combinations are indicated with asterisks in the following diagrams.

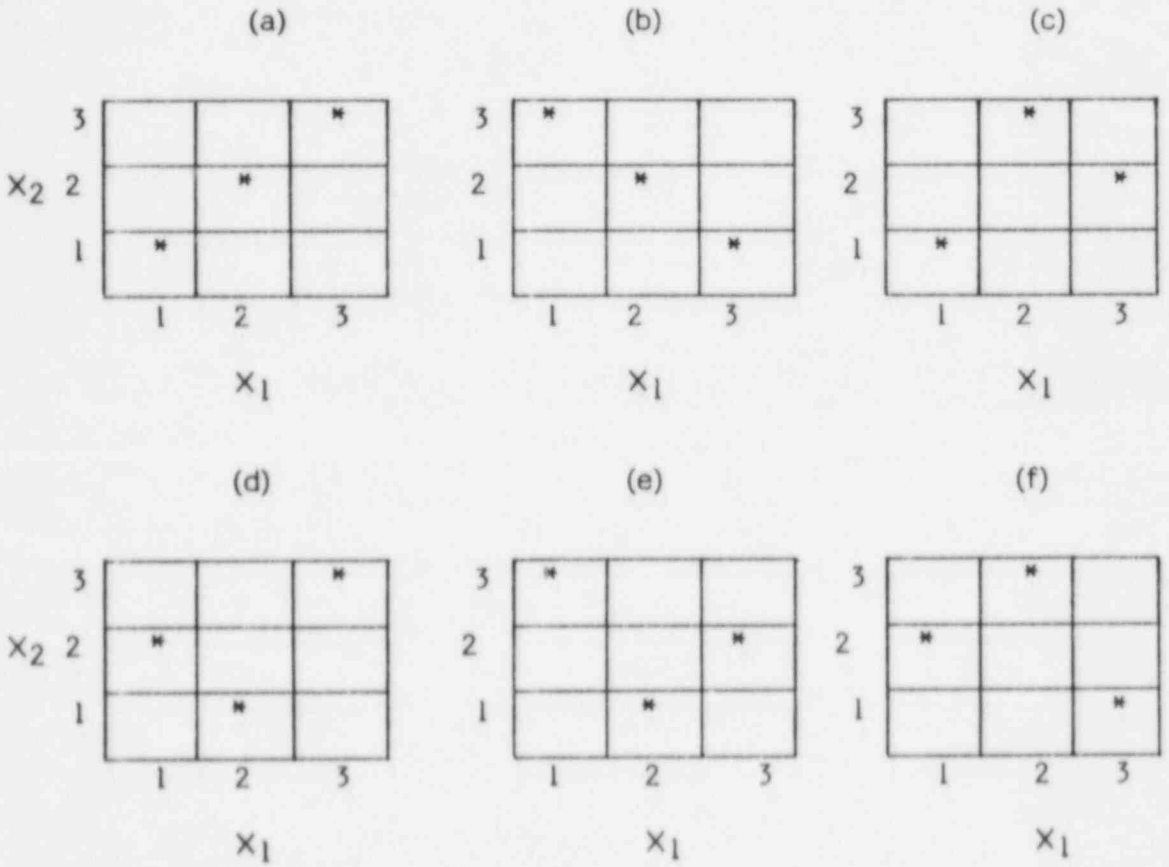

Thus, in diagram (a) a value of X_1 is randomly selected in interval 1 and paired with a value of X_2 selected at random from the first interval of X_2. Likewise, for intervals 2 and 3. In diagram (b) the value of X_1 from interval 1 is paired with the value of X_2 from interval 3. In each of these six diagrams, the full range of both X_1 and X_2 is sampled; whereas, in a simple Monte Carlo scheme all three pairs of values could easily come from the same subintervals for both X_1 and X_2.

It is convenient to think of the LHS as forming an n x k matrix of input where the ith row contains specific values of each of the k input variables to be used on the ith run of the computer model. Likewise, the jth column of the n x k input matrix from using Latin hypercube sampling contains the complete stratified sample for the jth input variable.

Due to the random pairing of intervals in the mixing process, there exists the possibility of inducing undesired pairwise correlations among some of the variables in a Latin hypercube sample. This is more likely to occur if n is small. Such correlations can be avoided by modifying the Latin hypercube sample by restricting the $(n!)^{k-1}$ possible interval pairings through the use of a technique introduced by Iman and Conover (1982a) and implemented by a computer program developed at Sandia National Laboratories (Iman and Shortencarier, 1984). Restricting the pairing in this manner preserves the fundamental nature of Latin hypercube sampling but replaces the random matching of intervals with a method that keeps all of the pairwise rank correlations among the k input variables very close to zero and thus ensures that no unwanted large pairwise correlations will exist between input variables. In the previous diagram, the interval pairings under (a) and (b) have rank correlations of 1 and -1, respectively. Both of these pairings are eliminated when the restricted pairing technique is used. In turn, this should result in more stable estimates of regression coefficients than simple random matching when the input-output values are used to fit a response surface. In addition, by selecting the proper combination of intervals, any desired rank correlation structure between variables can be induced (regardless of the distribution assigned to the variables) when it is known that there is correlation among the variables. When a sample generated by LHS is used, it is good practice to examine the associated correlation matrix for the presence of unwanted correlations among the variables under consideration. However, such correlations should not be a problem when the pairing is restricted.

The generation of a Latin hypercube sample requires that some thought must be given to the sample size n used. The choice of n depends on a number of considerations but will be dominated by the cost of making a single computer run and the number of input variables k. Our experience has shown that good results can be obtained with $n \geq (4/3)k$. However, this is not an absolute rule. If the model is inexpensive to run, then n could be larger such as between 2k and 5k. If k is quite large and the model is expensive to run, then it may be necessary to choose n considerably smaller than k. It should be kept in mind that, when k is large, only a small subset of the variables will turn out to be important (unless it is a very unusual model).

Another important aspect of selecting the sample size concerns the restricted pairing technique of Iman and Conover (1982a). This technique can be applied directly only if $n > k$; otherwise, it is necessary to use the technique in a piecewise fashion on subsets of the k variables where the number of variables used in each subset is less than n. A LHS of size n with the corresponding desired rank correlation structure is generated on each of the mutually exclusive and exhaustive subsets of the k variables. The resulting subsets are then combined to form the n x k input matrix. This piecewise approach assures that there are no unwanted correlations among variables within subsets but there could exist spurious correlations among variables belonging to different subsets. Hence, if such a piecewise approach is used, the resulting correlation matrix should be examined for unwanted correlations between variables in different subsets.

In uncertainty analysis associated with Latin hypercube sampling, it is desired to estimate the distribution function and the variance for the particular output variable(s) Y under consideration. Due to the probabilistic nature of Latin hypercube sampling, it is possible to estimate these entities directly from the model output associated with the sample just as in simple Monte Carlo sampling. Let (X_{i1}, ..., X_{ik}, Y_i) i = 1,...,n, denote the n individual sample elements, including the corresponding model output Y_i. Because each sample element has probability 1/n, an estimate of the cumulative distribution function for Y can be obtained directly from the values for the individual Y_i. Further, the expected value and variance for Y can be estimated by

$$\hat{E}(Y) = \sum_i Y_i/n \tag{2.4}$$

and

$$\hat{V}(Y) = \sum_i [Y_i - \hat{E}(Y)]^2/n, \tag{2.5}$$

respectively. These estimates are illustrated in the next section. As discussed by McKay, Conover, and Beckman (1979), the estimates for the distribution function and expected value associated with Y are unbiased. However, the estimator in (2.5) for the variance is biased; the exact amount of bias is small but unknown. Iman and Conover (1980) have shown that

$$[(n-1)/n]\, V(Y) \leq E[\hat{V}(Y)] \leq V(Y) \tag{2.6}$$

when Y is a monotonic function of each of the individual X_i. Use of the restricted pairing technique of Iman and Conover (1982a), while allowing correlations to be preserved and likely reducing the expected mean square $E(\hat{\theta} - \theta)^2$, removes the unbiasedness from the distribution function estimate. The amount of the bias is examined empirically in Figure 1 of Section 3.

The distribution function and variance for Y could also be estimated by fitting a response surface to the model input-output based on LHS and then proceeding as with factorial designs. However, there is little incentive to do this when the desired estimates can be obtained directly without the intermediate step of response surface construction. Techniques for sensitivity analysis for input generated with Latin hypercube samples are the same as those previously indicated for the response surface replacement approach.

Discussions of the use of LHS in uncertainty and sensitivity analysis are given by Iman and Conover (1980, 1982b), Iman, Helton, and Campbell (1981a, 1981b), and Harper and Gupta (1983). Applications of Latin hypercube sampling appear in Downing, Gardner, and Hoffman (1985), Helton and Iman (1982), Cranwell et al. (1982), and Helton, Iman, and Brown (1983). Beckman and Whiteman (1983) give examples showing good and bad features of LHS in uncertainty analysis.

2.3 DIFFERENTIAL ANALYSIS

The last method to be considered in the comparison in this study is based on a Taylor series expansion and the associated partial derivatives. With this approach, the dependent variable of interest is treated as a function f of the independent variables $X_1, \ldots, X_k$. Then, a first order Taylor series expansion for the model about some vector $\underset{\sim}{X}_0 = (X_{10},\ldots,X_{k0})$ of basecase values for the variables $\underset{\sim}{X} = (X_1,\ldots,X_k)$ approximates f as follows:

$$f(\underset{\sim}{X}) \doteq f(\underset{\sim}{X}_0) + \sum_j \frac{\partial f(\underset{\sim}{X}_0)}{\partial X_j} (X_j - X_{j0}). \tag{2.7}$$

The expression in (2.7) could be expanded to include terms with second order or higher derivatives, but is typically truncated after the first or second order derivatives. The expansion in (2.7) generates a model of the form in (2.1).

The Taylor series approximation shown in (2.7) is the starting point for uncertainty and sensitivity analysis techniques based on differentiation. The first step in such an analysis is the generation of the partial derivatives required in the series. If the function f appearing in (2.7) is relatively simple, then it may be possible to generate these derivatives analytically or by simple differencing schemes. Frequently, f is too complex to permit such simple approaches and more involved approaches tailored to the particular model under consideration must be used.

A typical analysis problem employing differential techniques involves a system of differential equations of the form

$$dY_j(\underset{\sim}{X},t)/dt = f_j[\underset{\sim}{Y}(\underset{\sim}{X},t),\underset{\sim}{X},t] \tag{2.8}$$

with the initial value condition $Y_j(0) = Y_{0j}(\underset{\sim}{X})$, where $\underset{\sim}{Y} = (Y_1,\ldots,Y_p)$ is a vector of unknown functions and $\underset{\sim}{X} = (X_1,\ldots,X_k)$ is a vector of variables that influence initial values or derivatives for $\underset{\sim}{Y}$. It is desired to determine $\partial\underset{\sim}{Y}/\partial X_i$ for each element X_i of $\underset{\sim}{X}$. In general, the equation in (2.8) is too complex to permit Y to be determined and then differentiated. Rather, it is necessary to formulate a new problem which enables a simultaneous numerical solution for both $\underset{\sim}{Y}$ and $\partial\underset{\sim}{Y}/\partial X_i$. This new problem is obtained by differentiating the expressions in (2.8) with respect to X_i, which yields

$$\partial[dY_j(\underset{\sim}{X},t)/dt]/\partial X_i = \partial\{f_j[\underset{\sim}{Y}(\underset{\sim}{X},t),\underset{\sim}{X},t]\}/\partial X_i$$

$$\partial[Y_j(0)]/\partial X_i = \partial[Y_{0j}(\underset{\sim}{X})]/\partial X_i \qquad j = 1,\ldots,p. \tag{2.9}$$

In turn, the preceding system can be reformulated as

$$d[\partial Y_j(\underset{\sim}{X},t)/\partial X_i]/dt = \partial\{f_j[\underset{\sim}{Y}(\underset{\sim}{X},t),\underset{\sim}{X},t]\}/\partial X_i$$

$$+ \sum_{q=1}^{p} \partial\{f_j[\underset{\sim}{Y}(\underset{\sim}{X},t),\underset{\sim}{X},t]\}/\partial Y_q \cdot \partial[Y_q(\underset{\sim}{X},t)]/\partial X_i$$

$$\partial[Y_j(0)]/\partial X_i = \partial[Y_{0j}(\underset{\sim}{X})]/\partial X_i \qquad j = 1,\ldots,p. \tag{2.10}$$

The systems in (2.8) and (2.10) can now be solved simultaneously to obtain $\underset{\sim}{Y}$ and $\partial\underset{\sim}{Y}/\partial X_i$. As it is necessary to solve the systems in (2.8) and (2.10) for each X_i, it is common for this procedure to require a large amount of computation to obtain the desired partial derivatives. It is sometimes possible to reduce the amount of required computation by the use of specialized numerical procedures; some of these procedures are discussed in Section 6.

Once the desired partial derivatives have been obtained, they can be used in a Taylor series of the form appearing in (2.7). For uncertainty analysis, the Taylor series approximation in (2.7) can be used in conjunction with Monte Carlo simulation to estimate distribution functions. Further, this approximation can be used with the relations in (2.2) and (2.3) to obtain expected value and variance estimates. For sensitivity analysis, the coefficients in a Taylor series can be normalized as will be discussed in section 3.4. Then, the values of these normalized coefficients can be used to develop rankings of variable importance. Further, the relation in (2.3) can be used to estimate the contribution of individual variables to the variance. The relations indicated in (2.2) and (2.3) are really properties of linear models and thus can be used with both linear regression models and Taylor series approximations. The application of the Taylor series in this manner will be demonstrated in later sections.

Differential techniques have been widely used in uncertainty and sensitivity analysis and several introductory treatments are available (e.g. Tomovic, 1963; Tomovic and Vukobratovic, 1982; Frank, 1978). Examples of the use of differential techniques include Morisawa and Inoue (1974), Atherton, Schainker, and Ducot (1975), Dickinson and Gelinas (1976), Lee, Gieseke, and Reed (1979), Cunningham, Hann, and Olsen (1980), Dunker (1981), Koda (1982), and Barhen et al. (1982). Harper and Gupta (1983) have made a comparison of LHS and differential analysis.

3. RESULTS BASED ON THE PATHWAYS MODEL

3.1 THE PATHWAYS MODEL

DESCRIPTION OF THE PATHWAYS MODEL

The Pathways model represents the environmental movement and human uptake of radionuclides. This model was developed at Sandia National Laboratories as part of a project funded by the Nuclear Regulatory Commission for the development of a methodology to assess the risk associated with the geologic isolation of high level radioactive waste. The Pathways model is divided into two submodels. One of these, the Environmental Transport Model, represents the long-term distribution and accumulation of radionuclides in the environment. This model is based on a mixed-cell approach and describes radionuclide movement with a system of linear differential equations. The other, the Transport-to-Man Model, represents the movement of radionuclides from the environment to man. This model is based on concentration ratios. In this study, only the environmental transport submodel is considered. Mathematically, this model is a system of linear, constant coefficient differential equations of the following form:

$$dq/dt = h + Cq \quad , \tag{3.1}$$

where q is a vector of unknown functions corresponding to the amount of each radio- nuclide in different environmental components, h is a vector of radionuclide source rates, and C is a coefficient matrix. The elements of C are functions of various variables which are considered as part of the sensitivity analysis in this section. When the system is suitably restricted and the input rate vector h is constant, the system in (3.1) has a unique asymptotic solution to which all other solutions converge. This solution is given by $-C^{-1}h$; it is this asymptotic solution that is considered in this paper.

The Pathways model has been well documented. A four volume set of NRC reports provides information about the Pathways model. A model description is given in Helton and Kaestner (1981), sensitivity results appear in Helton and Iman (1980), asymptotic properties appear in Helton, Brown, and Iman (1981) and effects of variable hydrologic patterns are examined in Brown and Helton (1981). Additionally, a two-part tutorial article on sensitivity analysis using the Pathways model for illustration is given in Iman, Helton, and Campbell (1981a, 1981b) with specific sensitivity results appearing in Helton and Iman (1982). A self-teaching curriculum for the Pathways model is given by Helton and Finley (1982). The specific form of the model considered in this analysis is described in Helton, Iman and Brown (1985).

VARIABLES CONSIDERED IN THE ANALYSIS OF THE PATHWAYS MODEL

The formulation of the Pathways model used in this example provides multivariate output for the movement of radionuclides in four environmental components: (1) groundwater, (2) soil, (3) surface water, and (4) sediment. For illustration in this study, these components are associated with a hypothetical hydrologic system consisting of a lake, the stationary sediments beneath the lake, an

area of irrigated land surrounding the lake, and the portions of a shallow aquifer which lie beneath the preceding areas of irrigated land and discharge into the lake. In the analysis, one radionuclide is considered in two of the preceding components. In particular, the following output variables are considered: Y_1 = amount (ci) of Ra226 in soil, Y_2 = concentration (ci/kg) of Ra226 in soil, and Y_3 = concentration (ci/L) of Ra226 in surface water. For this study the input to the Pathways model has been reduced to the 20 variables in Table 1 that describe various physical phenomena associated with the hypothetical hydrologic system as well as chemical properties of Ra226. The variables in Table 1 are discussed in Chapter 5 of Helton and Iman (1980), where the letter B is used in the designation of individual variables. The following correspondences exist:

$X_1 \sim B_1$,	$X_5 \sim B_5$,	$X_9 \sim B_{13}$,	$X_{13} \sim B_{20}$,	$X_{17} \sim B_{49}$
$X_2 \sim B_2$,	$X_6 \sim B_6$,	$X_{10} \sim B_{14}$,	$X_{14} \sim B_{23}$,	$X_{18} \sim B_{50}$
$X_3 \sim B_3$,	$X_7 \sim B_9$,	$X_{11} \sim B_{15}$,	$X_{15} \sim B_{26}$,	$X_{19} \sim B_{51}$
$X_4 \sim B_4$,	$X_8 \sim B_{12}$,	$X_{12} \sim B_{17}$,	$X_{16} \sim B_{28}$,	$X_{20} \sim B_{52}$

The variables in Table 1 are assumed to behave independently of one another and to have the distributions and ranges given in Table 2.

3.2 SELECTION OF THE VALUES OF THE INPUT VARIABLES USED IN THE ANALYSIS

THE FRACTIONAL FACTORIAL DESIGN

Prior to the actual analysis associated with a computer model, it is necessary to define specific values for each of the input variables to be used on each run of the model. For the portion of the analysis utilizing a fractional factorial design, two levels (low and high) are used to represent each variable with k = 20 and m = 13 (following the notation given in Section 2). The endpoints of each of the ranges given in Table 2 were used to represent the low and high values of each variable. Thus, a $1/2^{13}$ fraction of a 2^{20} factorial design was used to produce a fractional factorial design utilizing 2^7 = 128 computer runs, where each level of each variable is used exactly 64 times. The actual design used was the smallest design that would allow for the estimation of all main effects and 91 potentially important interactions indicated in Table 6-3 of Helton and Iman (1980).

THE LATIN HYPERCUBE SAMPLE

For the portion of the analysis utilizing a Latin hypercube sample (LHS), an n x 20 input matrix is created where n is the number of computer runs to be made. The value of n = 50 was used with the LHS, corresponding to n = 2.5k (since ½ = 20). Due to the random pairing of variables within the LHS, the correlation matrix associated with the LHS is <u>not</u> the identity matrix as is the case with the FFD input. However, the restricted pairing procedure of Iman and Conover (1982a) was utilized, which kept all off-diagonal rank correlations close to zero. In Section 5 of this paper, a

Table 1. Input Variables Used with the Pathways Model

X_1	Thickness of ground-water component (m)
X_2	Porosity of ground-water component (unitless)
X_3	Discharge from ground-water component to surface-water component (L/yr/m)
X_4	Thickness of soil component (m)
X_5	Porosity of soil component (unitless)
X_6	Annual rate at which water flows through soil component to ground-water component (m/yr)
X_7	Fraction of overland runoff that sufficiently mixes with soil component materials to permit radionuclide exchange (unitless)
X_8	Regional erosion rate (cm/1000 yr)
X_9	Fraction of solid material removed by erosion outside the soil component that sufficiently mixes with soil materials to permit radionuclide exchange (unitless)
X_{10}	Discharge of river 40 km above head of lake (L/yr)
X_{11}	Discharge of a lower aquifer into the surface-water component (L/yr/m)
X_{12}	Volume of water in surface-water component (L)
X_{13}	Thickness of sediment component (m)
X_{14}	Porosity of sediment component (unitless)
X_{15}	Scale factor such that product of X_{15} and the mass of solids contained in the sediment component is equal to the rate of sediment exchange between the sediment component and the surface-water component (yr^{-1}, when solid mass is expressed in kilograms)
X_{16}	Fraction of suspended sediments entering the surface-water component each year that are trapped in the lake and remain there permanently (unitless)
X_{17}	Distribution coefficient for Ra226 in the ground-water component (L/kg)
X_{18}	Distribution coefficient for Ra226 in the soil component (L/kg)
X_{19}	Distribution coefficient for Ra226 in the surface-water component (L/kg)
X_{20}	Distribution coefficient for Ra226 in the sediment component (L/kg)

Table 2. Distribution and Range Used with Each Input Variable to the Pathways Model

Variable	Distribution	Range
X_1	Uniform	15 to 45
X_2	Uniform	.1 to .4
X_3	Uniform	2.7×10^7 to 8.1×10^7
X_4	Uniform	.25 to .75
X_5	Uniform	.25 to .75
X_6	Uniform	.3 to .9
X_7	Uniform	0 to .1
X_8	Uniform	3 to 15
X_9	Uniform	0 to .1
X_{10}	Uniform	7.5×10^{12} to 2.3×10^{13}
X_{11}	Uniform	2.6×10^7 to 7.7×10^7
X_{12}	Uniform	9.5×10^{12} to 2.9×10^{13}
X_{13}	Uniform	.1 to .9
X_{14}	Uniform	.25 to .75
X_{15}	Loguniform	.01 to 1.0
X_{16}	Uniform	.2 to .8
X_{17}	Loguniform	20 to 2000
X_{18}	Loguniform	20 to 2000
X_{19}	Loguniform	20 to 2000
X_{20}	Loguniform	20 to 2000

measure for spurious correlations called the variance inflation factor is explained for use in conjunction with the DNET model. At this point, it is sufficient to state that an identity matrix has a variance inflation factor of 1.00 and that the associated rank correlation matrix for the LHS had a variance inflation factor of 1.07, which indicates negligible correlation within the sample.

THE DIFFERENTIAL ANALYSIS

The differential analysis approach does not have an associated scheme for selecting specific values of the input variables, rather it provides local information about each input variable at particular points that are deemed, a priori, to be of interest. A "basecase" vector consisting of the expected values of the variables listed in Table 2 was defined, and the first order partial derivatives of the dependent variables with respect to the independent variables were calculated at this "basecase" value. The Pathways model was sufficiently well-behaved so that it was possible to use a numerical differentiation scheme to obtain these partial derivatives. In addition, partial derivatives of the dependent variables were calculated at each of the 50 LHS input vectors in order to see how much variability would be encountered in local behavior from vector to vector. Thus, some indication of the reliability of extending local information to a global interpretation is provided.

A NOTE ON THE PROBABILISTIC NATURE OF THE INPUT

An important area worth noting at this point involves the probabilistic nature of the input and output as indicated by the probability distributions assigned to the variables in Table 2. If the objective of an analysis of a computer model is to gain an understanding of how it works and to identify important input variables, then some reasonably gross assumptions can be made with respect to the input distributions (such as treating them as uniform distributions). However, if the objective is to provide a meaningful estimate of a cdf of the output variables, then meaningful distributions must be assigned to the input variables and care must be taken to estimate the correlation structure among the input variables if it is other than the identity matrix (i.e., all input variables are independent of one another). The intent of this study is to demonstrate various techniques when a multivariate structure has been provided, and thus, we do not address the difficult question of whether or not the multivariate structure has been properly formulated for the problems under consideration.

SCATTERPLOTS OF THE INPUT-OUTPUT RELATIONSHIPS AS A GUIDE TO BETTER UNDERSTANDING OF THE MODEL BEHAVIOR

Once the specific input values have been defined, the computer runs are made. It is tempting after completing these runs to proceed immediately with response surface fits or whatever type of analysis is to be utilized. However, we strongly recommend that, prior to any such analysis, scatterplots of each input variable versus each output variable be made and carefully examined. Such scatterplots can aid in determining if the model is working as intended (i.e., does the input-output agree with engineering judgment?). Additionally, scatterplots

may aid in identifying the need for transformations (such as logarithmic) or may show how several variables jointly influence the output. Examples of scatterplots appear in Section 5 but are omitted for the Pathways model to conserve space.

3.3 UNCERTAINTY ANALYSIS FOR THE PATHWAYS MODEL

ESTIMATION OF THE DISTRIBUTION FUNCTION OF THE OUTPUT

LHS is based on a probabilistic input selection technique (as is a simple Monte Carlo procedure). When the actual output variable is graphed as an empirical cumulative frequency distribution, an estimate of the cdf is obtained directly. As was indicated in the previous section, the use of the restricted pairing with LHS removes the property of unbiasedness from the cdf estimate. The magnitude of the bias was investigated by generating cdfs for Y_1, Y_2 and Y_3 based on a random sample of size 500 and on a LHS of size 500 utilizing random pairing. As might be expected, graphs of the cdfs arising from these two methods showed excellent agreement. This process was repeated using a LHS with n=500 after incorporating the restricted pairing technique. The results from using LHS with random pairing and with restricted pairing were indistinguishable. Based on these results, it is felt that the amount of bias introduced by the restricted pairing in the LHS is probably negligible in problems of this type. A graph of the comparison of the random sample and the LHS with restricted pairing is shown in Figure 1 for Y_1.

Model output based on input selected through the use of fractional factorial designs cannot be used to provide a direct estimate of the output cumulative distribution function since the input values are not selected in a probabilistic manner. Rather, the output cdf is estimated by using a Monte Carlo simulation with a fitted response surface of the form indicated by the linear model in (2.1). Results of the response surface approach with $n = 100$ in the Monte Carlo simulation are shown in Figure 2 for Y_1 and Y_3 ; Y_2 was very similar to Y_1. Figure 2 also contains estimates based on a LHS utilizing restricted pairing with $n = 50$. For ease in comparing these estimates, an estimate of "truth" based on a random sample with $n = 100$ has also been included in Figure 2.

The results in Figure 2 show that the LHS estimate is quite close to the random sample estimate for both Y_1 and Y_3. The estimate for Y_3 in Figure 2 based on the response surface approach is in good agreement with the random sample estimate, but the estimate for Y_1 is not in good agreement. It is worth noting that the response surface estimate for Y_1 would undoubtedly be improved in a sequential manner through use of a more sophisticated experimental design. The only attempt to do so here was to add a center point to the design. However, we found that this had no affect on the results. No further attempts were made in this direction since we are not attempting to find the ultimate response surface fit, but rather to demonstrate what can happen with a well known and frequently used experimental design. It is also worth noting that a response surface can be fit based on the LHS input and corresponding output. Ordinarily, this would not be done to estimate a cdf since the output based on LHS yields such an estimate directly. However, we did fit such a response surface and used a Monte Carlo simulation with it to estimate the cdfs for Y_1 and Y_3. The results (not shown) were better than the FFD response surface estimate and in good agreement with the direct LHS estimate.

For the differential analysis (DA), the output cdf is estimated by approximating the underlying model with a first order Taylor series as given in equation (2.7) and then using a Monte Carlo simulation as was done with the response surface fits to yield the estimate of the output cdf. A potential problem with this method lies in the local nature of the Taylor series expansion. To examine this point, the Taylor series expansion at the so-called "basecase" vector was used with a Monte Carlo simulation and the results were compared with the direct estimate from LHS. These two results appear in Figure 3 and are in reasonably good agreement except for the lower 10% of the curves and some noticeable separation in the middle. One might be tempted to say at this point that "basecase" expansions give reasonable results. However, we caution the reader concerning the difficulty of determining a "basecase" in many real world situations and at the same time remind the reader of the very important point that this approach does not have a probabilistic basis. To further illustrate local behavior, we selected four of the 50 LHS input vectors to represent other possible "basecase" values and used Monte Carlo simulation with the Taylor series expansion about each of these points. The results are the curves labeled as 1, 2, 3, and 4 in Figure 4 along with the direct LHS estimate. Of these estimates the one labeled as "2" actually agrees better with the LHS estimate than does the "basecase" estimate in Figure 3. The estimate labeled as "1" is quite good in the lower tail but is not close in the upper tail. The estimates labeled as "3" and "4" are both extremely poor.

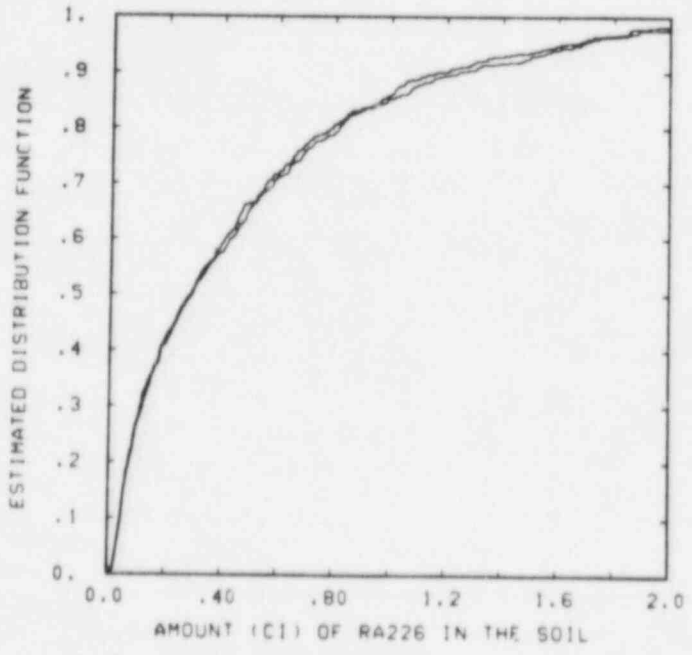

Figure 1. Estimates of the CDF for Y_1. Based on a Random Sample of Size 500 and a Latin Hypercube Sample of Size 500 Utilizing Restricted Pairing.

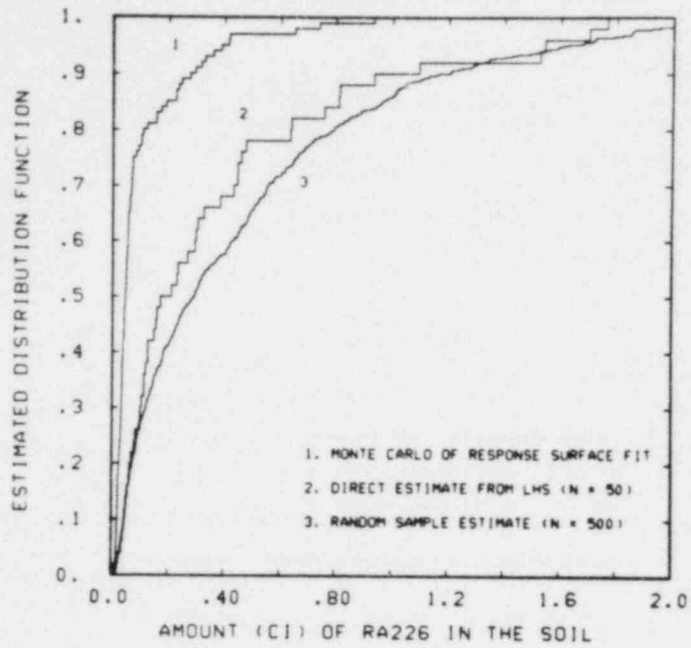

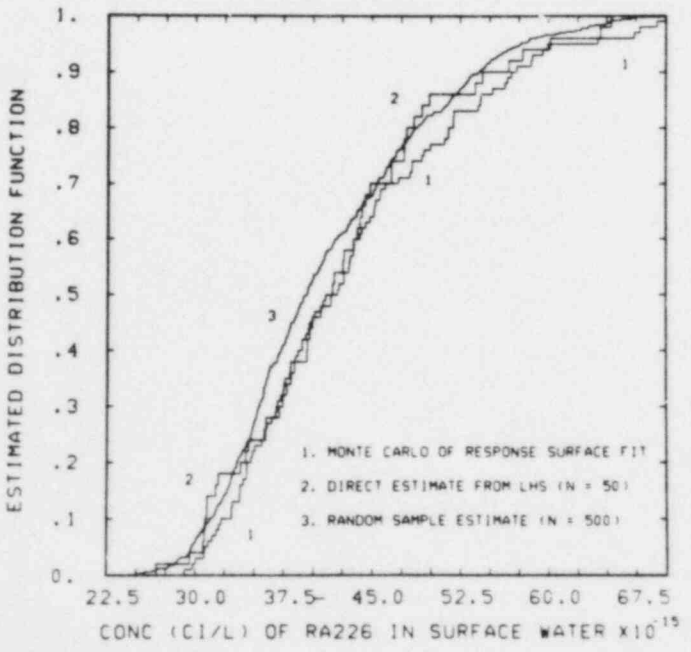

Figure 2. Response Surface Estimates of CDFs for Y_1 (amount of RA 226 in the soil) and Y_3 (concentration of RA 226 in the surface water)

ESTIMATION FOR THE OUTPUT VARIABLE

While a good estimate of the output cdf provides much information about the output variable, various characteristics or parameters are frequently used to describe the output variable. Some of the most frequently used characteristics are the expected value or mean, the median, and the variance. Clearly, if one can produce a good estimate of the output cdf, then it follows that these characteristics can be estimated as well. To shorten the discussion in this subsection, our comments will be restricted to estimating the variance, as problems encountered with estimating the variance carry over to estimating the mean.

There are two principal reasons for wanting to estimate the variance of the output variable. The first reason is to quantify the variability in the output. Estimation can be done directly from the output values if the input values are sampled according to their joint probability distribution or it can be done in conjunction with (2.3) utilizing a fitted model of some type. The second reason for estimating the variance of the output is to obtain a ranking of the input variables based on their percentage contribution to the variance in Y. The idea behind the ranking procedure is that, if a variable contributes only a negligible amount to the variance, then its effect can be safely ignored; whereas, an input variable making a significant contribution must be carefully considered. In this subsection, several methods of estimating the variance are compared while the ranking of the input variables on the basis of their individual contributions to the variance estimate is considered in the next subsection. It is important to recognize that the variables cannot be ranked if the variance is estimated directly as indicated above, i.e., the calculation of the direct estimate shown in (2.5) does not identify the contribution of the individual input variables as a byproduct.

To have a point of comparison for the various methods of estimating variance considered in this subsection, the variances of each of the output variables Y_1, Y_2, and Y_3 were estimated on the basis of a random sample. Since the Pathways computer model is relatively inexpensive to run, a random sample of size 100 was obtained from the variables in Table 2 and used to generate 100 runs of the model. From these runs, the following direct estimates were obtained for the variance of the three output variables:

$$V(Y_1) = .300,\ V(Y_2) = .195E\text{-}22, \text{ and } V(Y_3) = .888E\text{-}28$$

with corresponding 95% confidence intervals

$$(.231 \text{ to } .401),\ (.150E\text{-}22 \text{ to } .263E\text{-}22), \text{ and } (.685E\text{-}28 \text{ to } 1.198E\text{-}28).$$

If the output variables are normally distributed, then these confidence intervals are meaningful. Unfortunately, the normality assumption is difficult to satisfy for computer model output. For example, it is not satisfied for any of the output variables considered in this study. Thus, the above confidence intervals may be more than 95% or less than 95%. They will be referred to only as approximate 95% confidence intervals in the comparisons that follow.

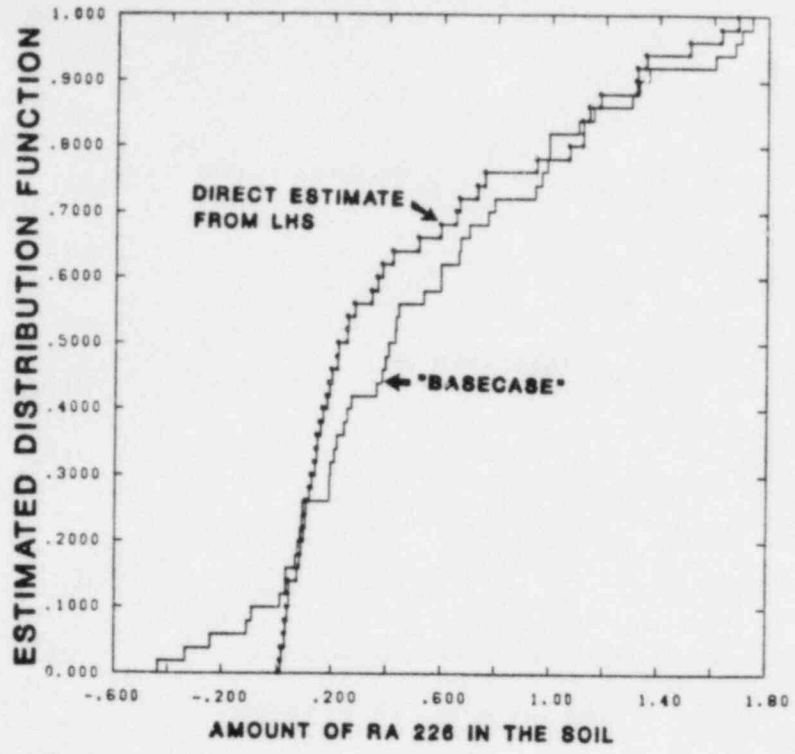

Figure 3. "Basecase" Taylor Series Expansion Used to Estimate the CDF for Y_1.

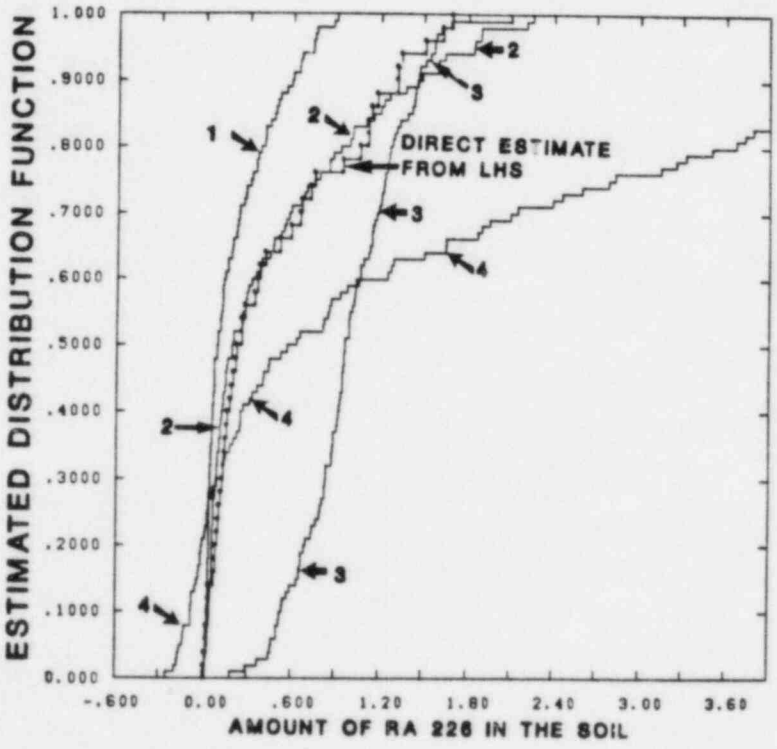

Figure 4. Estimates of the CDF of Y_1 for Various Potential "Basecases"

The reader may be concerned with the small size of the estimates for $V(Y_2)$ and $V(Y_3)$. The small values associated with Y_2 and Y_3 result from the fact that the system was modeled with a unit radionuclide release and therefore these estimates reflect the units being utilized.

In order to compare various methods of estimating the variance, the random sample estimates were used as a standard. The following methods for estimating the variance include one direct and two indirect estimates:

1. Direct estimate using (2.5) for output based on input generated by Latin hypercube sampling from the variables in Table 2.

2. Indirect estimate using (2.3) for a response surface (RS) of the form in (2.1) constructed using input-output generated through a fractional factorial design using the endpoints of the ranges in Table 2.

3. Indirect estimate using (2.3) for a Taylor series of the form in (2.7) constructed using partial derivatives evaluated at the expected values of the variables in Table 2.

Rather than listing the actual estimates obtained by each of these methods, the percentage errors in relationship to the random sample estimates are reported. The percentage error is calculated as follows:

$$\text{Percentage Error} = \frac{\hat{V}(Y) - \hat{V}_{RS}(Y)}{\hat{V}_{RS}(Y)} \times 100 , \qquad (3.2)$$

where $\hat{V}(Y)$ is the particular variance estimate under consideration and $\hat{V}_{RS}(Y)$ is the estimate from the random sample. Since $0 \leq V(Y) < \infty$, the percentage error is bounded by -100 on the low side and infinity on the high side. The percentage errors for the three methods are as follows:

Method	$V(Y_1)$	$V(Y_2)$	$V(Y_3)$
LHS	-18	16	-12
RS	-22	-80*	10
DA	2	23	-24*

The endpoints of the approximate 95% confidence interval given previously for the random sample estimate correspond to percentage errors of -22.9% to 30.0%. Therefore, any percentage error not falling inside this interval would correspond to an estimate outside of the approximate 95% confidence interval. Such percentages have been marked with an asterisk in the summary. These values show that only the direct estimate (LHS) gives all three estimates within the approximate 95% confidence bounds. The LHS method results from a calculation with equation (2.5) in relationship to an LHS. This calculation produces a biased estimate. The exact amount of the bias is small but unknown. However, if the assumption is made for the Pathways model that the output is a monotone function of the input (which is

probably true), the bounds on the expected value of the variance S^2, found from (2.6), are .98 $V(Y) < E(S^2) < V(Y)$ when n = 50 and the restricted pairing technique of Iman and Conover (1982a) is not used.

The RS method results from using equation (2.3) with fitted response surfaces. Two of the three estimates for this method are contained in the approximate confidence interval. In interpreting these results, it should be kept in mind that the output response is basically nonlinear and that the RS method was based on choosing the endpoints of the ranges in Table 2. If the response was linear, this strategy would be near optimal. In summary, for the LHS and RS methods, it would appear that more reliable estimates result from the direct LHS method than from the indirect estimates through the evaluation of (2.3).

The DA method is based on a Taylor series expansion as in (2.7) in conjunction with equation (2.3). The "basecase" evaluation in the DA method appears to give answers that are reasonable and competitive with those of the LHS method. However, in evaluating the estimates from the DA method, it should be kept in mind that this method does not have a probabilistic basis and that it may be difficult to define an appropriate "basecase" in most risk assessment settings. More importantly, however, these estimates are a measure of local behavior resulting from a Taylor series expansion about a single point and, as such, most likely cannot be safely extrapolated to a global interpretation. The nature of the local behavior was further explored by using a Taylor series expansion with each of the 50 points in the LHS and estimating the variance with each of these series. For $V(Y_1)$, 39 of the 50 estimates fell outside of the approximate 95% confidence interval (results not shown). For $V(Y_2)$ and $V(Y_3)$, the corresponding tabulations were 39 of 50 and 41 of 50, respectively, outside of the approximate 95% confidence interval.

In summary, the indirect estimates seem to be less reliable than the direct estimate. Thus, since input variable rankings based on contribution to variance are derived from indirect estimates, the resulting rankings may or may not be meaningful. This question is investigated in detail in the next subsection. As a final comment, the reader is again cautioned that comparisons involving the confidence intervals in this subsection have to be interpreted carefully since the normality assumption was not satisfied for the output variables.

3.4 SENSITIVITY ANALYSIS FOR THE PATHWAYS MODEL

There are several methods for quantifying the relative importance of the input variables to a computer model. However, these methods do not necessarily yield the same conclusions. In this subsection several different methods of quantifying input variable importance are presented and compared. It is natural to rank each of the input variables on the basis of its influence on the output variable. Some methods provide for such an overall ranking while others are designed to select subsets consisting of only the most influential variables. It should be realized at the onset that only a small subset of the input variables will tend to dominate individual outputs for most computer models. Therefore, techniques providing rankings of all input variables are best compared on the basis of the half dozen or so variables determined to be most important. Overall rankings and rankings within subsets are both considered in this subsection.

RANKING INPUT VARIABLES ON THE BASIS OF NORMALIZED COEFFICIENTS

A linear regression model and a finite Taylor series can each be thought of as a linear model of the form appearing in (2.1). The coefficients β_j in (2.1) depend on the units used for the input variables; as a result, the β_j will change as the units for the variables are changed. Therefore, it is difficult to obtain a meaningful ranking of the input variables based directly on the β_j. Rather, it is necessary to normalize the coefficients to remove the effect of the units.

One such normalization procedure explained in Draper and Smith (1981) involves normalizing the coefficients with respect to standard deviation. For linear regression, the normalized coefficients are produced by substituting $X_j = \bar{X}_j$ into (2.1), subtracting the resulting equation from (2.1), and finally dividing both sides of the equation by s_y to produce

$$(Y-\bar{Y})/s_y = \sum_j \beta_j\{s_{x_j}/s_y\}\ \{(X_j - \bar{X}_j)/s_{x_j}\}\ , \tag{3.3}$$

where $\bar{Y}$, $\bar{X}_j$, $s_y = [V(Y)]^{1/2}$ and $s_{x_j} = [V(X_j)]^{1/2}$ are the usual sample calculations. As σ_{x_j} is known for each X_j in this problem, σ_{x_j} could be used rather than s_{x_j}. However, it is convenient to use the values obtained from a regression program utilizing the individual observations rather than to make this substitution. Clearly,(3.3) could be expressed in a simpler notation as

$$\hat{Y}^* = \sum \hat{\beta}_j^* X_j^*\ . \tag{3.4}$$

The value of $\hat{\beta}_j^*$ is a unit free measurement and can be used to rank the relative importance of the individual X_j. The larger the absolute value of $\hat{\beta}_j^*$, the more influence the variable X_j has, while values of $\hat{\beta}_j^*$ close to zero indicate little importance for X_j. In a regression setting, $\hat{\beta}_j^*$ is referred to as a standardized regression coefficient. One way of thinking of β_j^* is as a measure of the fractional change in Y relative to its standard deviation when X_j is changed by some fixed fraction of its standard deviation. Therefore, an ordering of the absolute values of $\hat{\beta}_j^*$ provides a ranking of the variables on the basis of equal fractional changes relative to standard deviation.

For the differential analysis, the corresponding normalization is obtained by using the Taylor series expansion in (2.7). Each partial derivative in the expansion is standardized as follows:

$$(\partial Y/\partial X_j)(\sigma_{x_j}/\hat{\sigma}_y)\ , \tag{3.5}$$

where σ_{x_j} is the population standard deviation of X_j arising from the probability distribution in Table 2 and the estimate $\hat{\sigma}_y$ is obtained from (2.3). The rankings arising from (3.3) and (3.5) are given in Table 3 for each of the three Pathways output variables under the column headings DA (differential analysis), LHS (response surface from Latin hypercube sampling) and RS (response surface from the fractional factorial design). The actual standardized coefficients contain more information about relative variable importance than the simple ranks given in Table 3; for example, the signs and absolute values for the coefficients are important. However, use of the ranks makes comparisons within and across procedures easier.

Within Table 3, the DA and LHS techniques agree on the order of the top four variables for Y_1 and Y_3, but show considerable disagreement after rank 1 for Y_2. The RS technique agrees with DA and LHS on rank 1 for Y_1, Y_2 and Y_3 but shows moderate to severe disagreement on the other ranks. Noteable is the rank of 4 assigned to X_{16} under Y_1 by RS while the LHS technique assigns rank 20. Also, under Y_2, the RS technique assigns rank 17 to X_{11} while LHS assigns rank 3. In both of these latter cases the DA technique gives an intermediate rank. In general, the most disagreement within Table 3 for all variables occurs between the LHS and RS techniques. Additionally, the most disagreement between techniques occurs for the variable Y_2 while the best agreement is associated with variable Y_3.

In considering the entries in Table 3, it is important to keep in mind that disagreements among rankings by the three techniques for variables of lesser importance are of no practical concern since these variables have little or no impact on model output. For example, it is important when DA and LHS agree on the top three ranks for Y_3 while it is unimportant that these techniques assign ranks 8 and 20 to X_{17}. One way to measure agreement on the selection of the most important variables is to compute the ordinary correlation coefficient on scores based on the sum of the reciprocals of the assigned ranks in Table 3. For example, if there were only four ranks involved rather than 20, the scores used in computing the correlation coefficient would be $S_1 = 1 + 1/2 + 1/3 + 1/4$, $S_2 = 1/2 + 1/3 + 1/4$, $S_3 = 1/3 + 1/4$, and $S_4 = 1/4$. Thus, under Y_3 the correlation coefficient for DA and LHS would be calculated using the pairs of scores: $(1 + 1/2 + \ldots + 1/20, 1 + 1/2 + \ldots + 1/20)$, $(1/2 + 1/3 + \ldots + 1/20, 1/2 + 1/3 + \ldots + 1/20)$, ..., $(1/20, 1/6 + 1/7 + 1/8 + \ldots + 1/20)$ corresponding respectively to the pairs of ranks (1,1), (2,2), ..., (20,6). If these pairs of scores are plotted in a scatterplot, it is apparent that a premium is placed on agreement of the most important ranks while pairs of ranks such as (10, 6) have very little impact on the calculations. The correlation resulting for this case is .88, which compares with a much smaller value of .63 for the correlation computed simply on the ranks in Table 3. On the other hand, if the top ranks disagree considerably then the correlation on sums of reciprocals will likely be much smaller than the simple correlation on ranks. The scores based on the sum of the reciprocals of the ranks are commonly referred to in the statistical literature as Savage scores (see Savage, 1956); however, their use in that literature has not been in association with correlation as was done here. More information on measures of top-down correlation can be found in Iman and Conover (1985). The comments given on comparisons within and between techniques in Tables 3 and 4 are based on top-down correlations using Savage scores. The actual top-down correlations appear in Table 5. In evaluating the entries in Table 5, it is useful to know that a top-down correlation is statistically significant at approximately the .01 level for n=20 if it is greater than .53 and at approximately the .001 level if it is greater than .71.

Table 3. Rankings of the Input Variables to the Pathways Model Based On Standardized Coefficients

Input Variable	Y_1			Y_2			Y_3		
	DA	LHS	RS	DA	LHS	RS	DA	LHS	RS
1	18	17	17	18	19	18	13	16	10
2	19	14	13	19	9	12	19	19	20
3	10	11	10	8	6	10	3	3	2
4	2	2	3	11	20	8	17	11	17
5	3	3	2	10	17	9	18	18	8
6	6	8	12	4	10	6	14	10	13
7	5	7	11	3	4	5	10	14	19
8	8	9	6	6	8	4	6	5	6
9	9	5	7	7	2	3	16	17	18
10	4	4	5	2	5	2	1	1	1
11	11	10	18	9	3	17	4	4	3
12	17	16	20	17	18	16	12	12	15
13	13	6	8	13	7	14	7	8	7
14	15	19	14	15	15	13	9	15	9
15	16	12	19	16	11	20	11	7	12
16	12	20	4	12	12	7	5	9	5
17	14	13	15	14	13	15	8	20	11
18	1	1	1	1	1	1	15	13	14
19	7	15	9	5	16	11	2	2	4
20	20	18	16	20	14	19	20	6	16

A second normalization procedure involves multiplication by X_j/Y, where X_j and Y correspond to a basecase run of the computer model. In the case of regression, the coefficients are normalized as

$$\hat{\beta}_j(X_j/Y), \tag{3.6}$$

and in the differential analysis, the partial derivatives are normalized as

$$(\partial Y/\partial X_j)(X_j/Y) . \tag{3.7}$$

The resultant coefficients indicate the effect on the dependent variable of equivalent fractional changes of basecase values for the individual input variables. Such coefficients are frequently referred to as normalized sensitivity coefficients. The rankings from this normalization appear in Table 4 in a format similar to that found in Table 3.

Table 4. Rankings of the Input Variables to the Pathways Model Based on Normalized Sensitivity Coefficients

Input Variable	Y_1			Y_2			Y_3		
	DA	LHS	RS	DA	LHS	RS	DA	LHS	RS
1	16	14	15	16	16	17	10	13	10
2	18	13	13	18	7	11	17	18	20
3	8	9	7	6	4	10	2	2	2
4	1	1	2	11	19	6	14	7	13
5	2	2	1	10	13	7	15	15	6
6	5	7	10	3	9	4	12	6	11
7	6	11	11	4	6	9	13	16	19
8	7	10	5	5	8	3	6	4	5
9	10	6	8	8	5	5	16	17	16
10	4	4	3	2	3	1	1	1	1
11	9	8	16	7	2	16	3	3	3
12	15	12	19	15	15	15	9	9	12
13	13	5	9	13	10	14	7	10	8
14	14	16	14	14	12	12	8	12	9
15	19	15	20	19	14	20	18	14	15
16	12	19	4	12	11	8	4	8	4
17	17	17	17	17	17	18	11	20	14
18	3	3	6	1	1	2	19	19	17
19	11	18	12	9	20	13	5	5	7
20	20	20	18	20	18	19	20	11	18

The best agreement within Table 4 occurs for Y_3 where all three techniques pick the top three variables in order. Strong agreement also exists between DA and LHS for Y_1 but these techniques disagree after rank 1 for Y_2. The RS technique shows some degree of disagreement with both of these techniques under both Y_1 and Y_2. In the six cases in Table 3 and 4, LHS and DA always agree on the top rank and agree on the order of the top four ranks in three of the six cases. For these same cases, DA and RS agree on rank 1 in four of six cases. The same results also hold true for LHS and RS.

Although based on different criteria, it is also of interest to compare corresponding techniques and variables between Tables 3 and 4. For Y_1, all three techniques show considerable disagreement with their analogs between Tables 3 and 4. For Y_2, the DA has the best agreement with its analog from Table 3 to Table 4 while RS has the most disagreement. Under Y_3, all three techniques agree with their analogs on rank 1, but only RS shows agreement on the top three ranks.

Table 5. Correlations Computed on the Reciprocals of the Ranks in Tables 3 and 4.

Output Variable	Techniques	Within Table 3	Within Table 4	Technique	Between Tables 4 and 5
Y_1	DA and LHS	.92	.91	DA	.87
	DA and RS	.87	.82	LHS	.87
	LHS and RS	.83	.76	RS	.78
Y_2	DA and LHS	.71	.79	DA	.97
	DA and RS	.89	.83	LHS	.91
	LHS and RS	.72	.56	RS	.90
Y_3	DA and LHS	.87	.90	DA	.93
	DA and RS	.92	.95	LHS	.89
	LHS and RS	.85	.90	RS	.97

RANKING INPUT VARIABLES ON THE BASIS OF THEIR CONTRIBUTION TO THE VARIANCE OF THE OUTPUT

Another way of quantifying the relative importance of the individual input variables is by the percentage contribution each makes to the estimated variance of the output variable(s). For both the Latin hypercube sampling and response surface methods, the percentage contribution is obtained through the indirect variance estimate from equation (2.3) in conjunction with the response surface fit obtained from (2.1). For the Taylor series expansion, equation (2.3) is utilized in conjunction with (2.7).

If the input variables are independent of one another so that the covariance term in (2.3) is zero, then it is easy to show that the rankings based on contribution to variance from (2.3) and standardized regression coefficients from (3.3) are equivalent. The same is true for similar rankings based on the differential analysis. Thus, rather than simply showing the same results over again, the ranking based on contribution to variance will be illustrated after some improvements are made to the regression model.

The regression-based rankings presented in Tables 3 and 4 were based on the model in (2.1) and included all 20 input variables, thus providing rankings for all 20 input variables. This approach has some drawbacks. First, as previously mentioned, rankings beyond the first few variables usually have little meaning in an absolute ordering since only a few of the 20 variables actually turn out to be significant.

Thus, it seems reasonable to consider ranking only within a subset containing the most important input variables. Second, since regression techniques are easily influenced by extreme observations and nonlinearities, more reliable rankings can sometimes be obtained by first transforming the data.

Thus, some modifications are made in the regression for this analysis. First, the model in (2.1) is modified to be of the form

$$\log Y = \beta_0 + \sum \beta_j X_j^* + \sum \sum \beta_{ij} X_i^* X_j^*, \tag{3.8}$$

where $X_j^* = (X_j - \bar{X})/s_{X_j}$ has a mean of zero and a variance of one. In the case of X_j having a loguniform distribution, X_j^* was computed on log X_j. Next, the model in (3.8) is fit using stepwise regression (see Draper and Smith, 1981). Stepwise regression is a procedure for selecting only the most influential variables at a predetermined level of significance in the construction of the fitted model. Thus, not all input variables appear in the final fitted model. One way of measuring the adequacy of the fitted model is through the calculation of a value called R^2 (see Draper and Smith, 1981, for details), which indicates the fraction of variation in the output variable explained by the independent variables appearing in the fitted model.

As an example of stepwise regression, consider the following results for Y_2 based on the LHS input:

Step Number	Variable Entering	Model R^2
1	X_{18}	.912
2	X_7	.943
3	X_{10}	.969
4	X_{11}	.977
5	X_6	.982

Thus, after five variables have entered into the regression model, 98.2% of the variation in Y_2 has been accounted for. The order in which variables enter a stepwise regression and corresponding changes in R^2 values that take place with the entry of successive variables also provide insight into relative variable importance.

The percentage contribution to the estimate of the variance of Y through (2.3) appears in Table 6 along with the model R^2 where appropriate. However, since the model in (3.8) involved log Y, it is necessary to convert the estimate of V(log Y) obtained from the regression model to V(Y). The first step in this conversion is straightforward:

$$\hat{V}(\ln Y) = (\ln 10)^2 \hat{V}(\log Y). \tag{3.9}$$

The second step involves an approximation arising from a Taylor series expansion of ln Y and is given as follows:

$$\hat{V}(Y) = [\hat{E}(Y)]^2 \hat{V}(\ln Y), \tag{3.10}$$

where $\log \hat{E}(Y) = \hat{E}(\log Y)$ and $\hat{E}(\log Y)$ is determined as indicated in equation (2.2) for $\hat{E}(Y)$.

The percentages given in Table 6 do not total to 100 for each value of Y. In the case of the fitted models (LHS and RS), the remainder is due to lack of fit. For the DA method, only those variables are shown that contributed at least 1% to the total variation. If the variables are ranked according to the percentages for the DA method, the results are the same as those shown earlier in this section. The percentages in Table 6 for Y_1 lead to the selection of the four most important variables as determined by LHS in Table 3 and to the selection of the three most important variables as determined by the RS in Table 3. For Y_2, the variable X_{18} is identified as dominant in Table 6 which is in agreement with the results in Table 3; however, the ordering on the less influential variables is different for both the LHS and RS approaches in Table 3. The disagreements among the rankings in Tables 3 and 6 can be attributed to the model used in (3.8). Generally speaking, more reliable rankings can be obtained through an improved model such as appears in (3.8) unless the input-output relationships are very well behaved in a linear sense.

An examination of the values within Table 6 shows an overall good agreement on variable ranking for all three methods, particularly for Y_1 and Y_2. For Y_3, the best agreement is between the LHS and DA methods but with no great areas of disagreement. One might expect the LHS and RS methods to show reasonably good agreement depending on the degree of nonlinearity in the output; however, agreement of the LHS and RS methods with the DA method may or may not be a desirable objective. The reason for this lies in the local nature of the Taylor series expansion and the selected "basecase." This will be examined in detail later in this section but first comments will be made on the interpretation of the values in Table 6.

The percentage contributions of the variables in Table 6 have to be interpreted very carefully due to the complexity of the model and the inherent dangers of linear extrapolation. To illustrate this point, it would appear that X_{18} contributes approximately 80% to the variance in Y_1 and thus it would seem reasonable to ask if the variance will decrease if X_{18} is held constant. To answer this question, the random sample of size 100 used in the previous subsection was modified by setting the value of X_{18} equal to 25 on all 100 computer runs of the model. The value of 25 corresponds to the .05 quantile for X_{18} on the basis of the probability distribution given in Table 2. Two additional sets of 100 runs were made by first setting X_{18} equal to 200 and then to 1589, corresponding to its .50 and .95 quantiles, respectively. The percentage change in the variance of Y_1, Y_2, and Y_3 was recorded in relationship to the random sample estimates given in the previous subsection. This procedure was repeated using the same quantiles for X_{10}. The results are summarized in Table 7.

The values in Table 7 clearly indicate that X_{10} plays an important role in influencing $V(Y_1)$ and $V(Y_2)$ but has no significant effect on $V(Y_3)$. However, the percentage change in the $V(Y_1)$ varies from a reduction of 99.8% to an increase of 70.1% as X_{18} increases. The percentage change in $V(Y_2)$ varies from a reduction of 99.9% to an increase of 39.7%.

Table 6. Percentage Contribution to the Estimate of the Variance of the Output for Three Different Methods of Estimating the Variance Using the Model in (3.8)

Output Variable	Input Variable	LHS	RS	DA
Y_1	X_4	6	6	6
	X_5	6	5	6
	X_7	3	2	2
	X_{10}	3	2	2
	X_{18}	80	80	77
	Model R^2:	97.4%	94.5%	--
Y_2	X_6	1	1	1
	X_7	3	2	2
	X_8	0	1	0
	X_9	0	1	0
	X_{10}	3	2	3
	X_{11}	1	0	1
	X_{18}	91	89	90
	Model R^2:	98.2%	96.3%	--
Y_3	X_3	5	8	6
	X_{10}	75	66	77
	X_{11}	8	5	5
	X_{19}	7	6	8
	$X_{16}X_{19}$	3	0	0
	X_3X_{10}	0	6	0
	Model R^2:	97.0%	91.2%	--

Table 7. Percentage Change in the Variance Estimates When X_{18} and X_{10} Are Held Constant at Each of Three Different Quantiles

VARIABLE	QUANTILE	$V(Y_1)$	$V(Y_2)$	$V(Y_3)$
X_{18}	.05	-99.8	-99.9	0.1
	.50	-91.5	-95.0	0.0
	.95	70.1	39.7	-0.1
X_{10}	.05	51.9	55.4	-43.0
	.50	-16.0	-11.4	-80.9
	.95	-48.9	-45.1	-92.5

In the case of X_{10}, the percentage reduction in $V(Y_3)$ ranged from 43.0% to 92.5%. It is interesting to note that X_{10} played a minor role in Table 6 with respect to Y_1 and Y_2. However, Table 7 indicates that when X_{10} is held fixed at either of its .05 or .95 quantiles it has a major influence on $V(Y_1)$ and $V(Y_2)$. Hence, estimates such as given in Table 6 must be interpreted carefully, keeping in mind the complexity of the underlying model, as they could be misleading.

One should not concentrate only on the change in variance of the output variable, but should also consider the change in location as measured by the mean or median, or the effect on the distribution function. This is important because changes in variables are frequently accompanied by changes in means. To demonstrate this point, estimated CDF's for Y_1 have been plotted in Figure 5 for a random sample of size 100 and for the random sample modified by fixing X_{18} at each of its .05, .50, and .95 quantiles. Figure 5 makes it clear that there has been a large (99.8%) reduction in the $V(Y_1)$ with X_{18} held at its .05 quantile; however, the location has changed dramatically. Likewise, with X_{18} held at its .95 quantile, the variance increases by 70% but the location changes considerably, as indicated by the median increasing by a factor of 5. Figure 6 is similar in construction to Figure 5 except that X_{10} has been held fixed at each of the three quantiles rather than X_{18}. Since X_{10} has a minor influence on Y_1, as indicated in Table 6, the change in the estimated CDF's is much less than in Figure 5; that is, neither the variance or location are influenced much by X_{10}. Results for Y_2 and Y_3 are not shown. However, Y_2 was affected in a manner similar to Y_1, while Y_3 was influenced heavily by X_{10} and not at all by X_{18}.

RANKING THE INPUT VARIABLES ON THE BASIS OF PARTIAL RANK CORRELATION COEFFICIENTS

Methods presented thus far in this subsection have ranked either all of the variables or a subset utilizing stepwise regression with an improved model in an effort to obtain more reliable results. The last method to be considered is hybrid in the sense that it is regression based but avoids the transformations appearing in (3.8) and can be used to rank either all variables or only those within a subset.

If runs of a computer model are made with many input variables changing simultaneously, it can be difficult to see the sensitivity of the output variable Y to the individual variables X_j. One way of quantifying such sensitivity is by

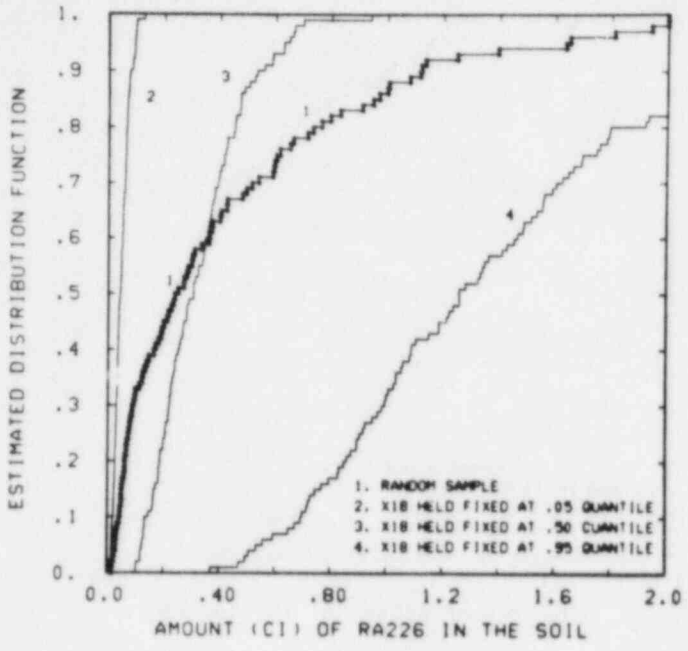

Figure 5. CDF Estimates for Y_1 Showing the Impact of Holding X_{18} Fixed at different Quantiles Versus the Estimate from a Simple Random Sample of Size 100.

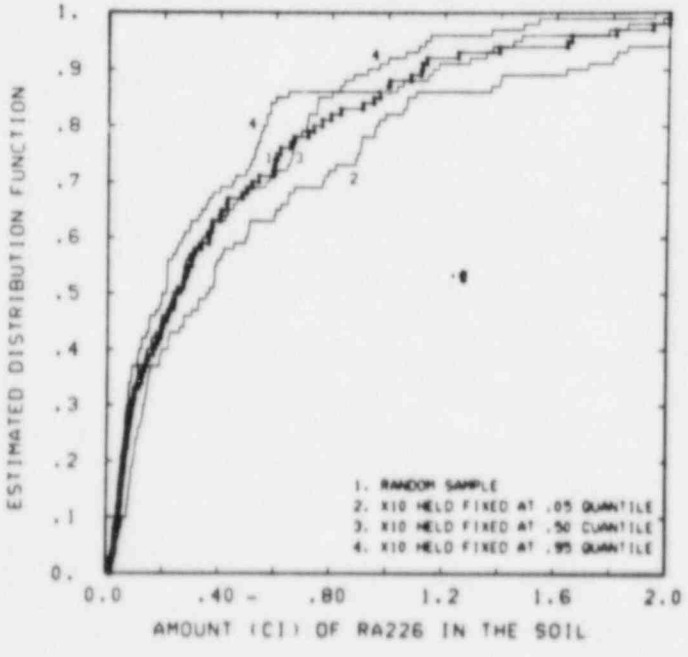

Figure 6. CDF Estimates for Y_1 Showing the Impact of Holding X_{10} Fixed at different Quantiles Versus the Estimate from a Simple Random Sample of Size 100.

calculating the partial correlation coefficient. The partial correlation coefficient differs from a simple correlation coefficient in that it measures the degree of linear relationship between the X_j and Y after making an adjustment to remove the linear effect of all of the remaining variables. The actual calculation involves finding the inverse of the correlation matrix C between the individual X_j's and Y based on n computer runs. The inverse matrix can be written as follows:

$$C^{-1} = \begin{bmatrix} 1/(1-R^2_{x_1}) & c_{12} & \cdots & c_{1k} & b_1/(1-R^2_y) \\ c_{21} & 1/(1-R^2_{x_2}) & \cdots & c_{2k} & b_2/(1-R^2_y) \\ \cdots & \cdots & & \cdots & \cdots \\ c_{k1} & c_{k2} & \cdots & 1/(1-R^2_{x_k}) & b_k/(1-R^2_y) \\ b_1/(1-R^2_y) & b_2/(1-R^2_y) & \cdots & b_k/(1-R^2_y) & 1/(1-R^2_y) \end{bmatrix}$$

The value b_j in C^{-1} is the standardized regression coefficient in equation (3.4); the value R^2_y is the coefficient of determination (i.e., R^2 value) from regressing Y on $X_1, \ldots, X_k$, and the value $R^2_{x_j}$ is the coefficient of determination from regressing X_j on $Y, X_1, \ldots, X_{j-1}, X_{j+1}, \ldots, X_k$.

The partial correlation coefficient for X_j and Y is obtained directly from C^{-1} as

$$\rho_{x_j} = -c_{jy}/(c_{jj}c_{yy})^{1/2}$$

Therefore, the partial correlation coefficient can be written as

$$\rho_{x_j y} = \frac{b_j/(1-R^2_y)}{\sqrt{[1/(1-R^2_{x_j})][1/(1-R^2_y)]}} = b_j\sqrt{\frac{1-R^2_{x_j}}{1-R^2_y}} \qquad (3.11)$$

Equation (3.11) shows the close relationship between $\rho_{x_j y}$ and b_j; however, it is

important to recognize that they yield different types of information. Standardized regression coefficients are derived from a conditional univariate distribution, while partial correlation coefficients come from a conditional bivariate distribution. Partial correlation coefficients allow one to judge the unique contribution that an explanatory variable can make. Standardized regression coefficients are equivalent to partial derivatives in the standardized model.

It is important to recognize that the quantity in (3.11) will not provide a reliable measure of sensitivity when the relationship between X_j and Y is basically monotonic but nonlinear or if there are outliers (extreme observations) present. To avoid this problem, each of the individual variables X_j and Y can be replaced by their corresponding ranks from 1 to n and (3.11) can be computed on these ranks. This transformation converts the sensitivity measure from one of linearity between X_j and Y to one of monotonicity between X_j and Y. The result of this calculation is called the partial rank correlation coefficient (PRCC). A computer program for making such calculations has been developed at Sandia National Laboratories (Iman, Shortencarier and Johnson, 1985). This program will also calculate the standardized regression coefficients on either the original observations or their ranks.

The PRCC provides a number between -1 and 1 such that PRCCs near -1 indicate the Y decreases as X increases while values near 1 indicate that X and Y increase together. Values near zero indicate no monotonic relationship exists. Thus, the PRCC can be used to provide a ranking of the input variables. The PRCCs have been calculated on the basis of input from LHS (n = 50), random sampling (n = 100) and a fractional design (n = 128). The resulting rankings of the more important variables appear in Table 8. The rankings under Y_1 are in absolute agreement for all three methods. For Y_2, the three methods agree on the top three rankings with some disagreement for lower ranks. For Y_3, agreement exists on the most important variable, but some permutation occurs among ranks 2, 3, and 4. However, the rankings overall are in good general agreement with those of the methods presented earlier in this subsection. Before summarizing the results of this section, the local behavior of results based on partial derivatives will be examined in more detail.

EFFECTS OF THE CHOICE OF THE BASECASE FOR A DIFFERENTIAL SENSITIVITY ANALYSIS

The selection of a "basecase" value in differential analysis was brough up earlier in this section. The following discussion is intended to illustrate the effects that "basecase" selection can have on the outcome of a sensitivity analysis. Figure 7 illustrates the effect of changing one variable while all the remaining variables are held fixed. The horizontal dashed line in Figure 7 shows $\partial Y_1/\partial X_5$ calculated at the expected values for all 20 variables and normalized as in (3.7). The curve in Figure 5 is generated by fixing all independent variables except X_5 at their expected values while X_5 is assigned the values selected for it in the previously used LHS.

Table 8. Rankings of the five most influential input variables affecting Y_1, Y_2, and Y_3 based on the PRCC computed on a LHS with n = 50, a random sample (Random) of size n = 100 and 128 fractional factorial points (FFD).

Input	Y_1			Y_2			Y_3		
Variable	LHS	Random	FFD	LHS	Random	FFD	LHS	Random	FFD
3							2	3	2
4	2	2	2						
5	3	3	3						
6				(14)	4	4			
7	5	5	5	3	3	3			
8				5	(6)	(6)	(7)	5	5
9				8	9	5			
10	4	4	4	2	2	2	1	1	1
11				4	(9)	(11)	3	4	4
16							5	(6)	(8)
18	1	1	1	1	1	1			
19				(9)	5	(7)	4	2	2

Then, $\partial Y_1/\partial X_5$ is calculated and normalized as before. As indicated by the two curves in Figure 7, a large amount of variation can be induced by changing the value of a single independent variable in the calculation of a normalized partial derivative.

Figure 8 provides another illustration of the effect of the "basecase" point on the calculation of partial derivatives. This figure shows $\partial Y_2/\partial X_9$ calculated at each of the 50 points in the previously used LHS and normalized as in (3.7). Thus, in contrast to the situation shown in Figure 7, all 20 independent variables are changing for each partial derivative. That is, the "basecase" point is moved about in a 20-dimensional space to 50 different locations. As readily seen, the value for the normalized partial derivative varies from approximately 0 to - .5 Each of these normalized derivatives is correct at the particular location selected; however, it clearly would not be safe to extrapolate away from any local point.

The effect of the choice of a "basecase" value on the estimation of the variance is illustrated by using a Taylor series expansion at each of the 50 LHS points and using these expansions to estimate the variance of Y_1, Y_2, and Y_3. Results for Y_1 are given in Table 9, where the vectors have been ordered from the smallest input value used for X_{18} to the largest input value used for X_{18}. Results are given for each variable that contributed at least 1% to the variation in Y for some run. The last column of this table contains the percentage error of the variance estimates as calculated from equation (3.2) using the previously indicted random sample of size 100.

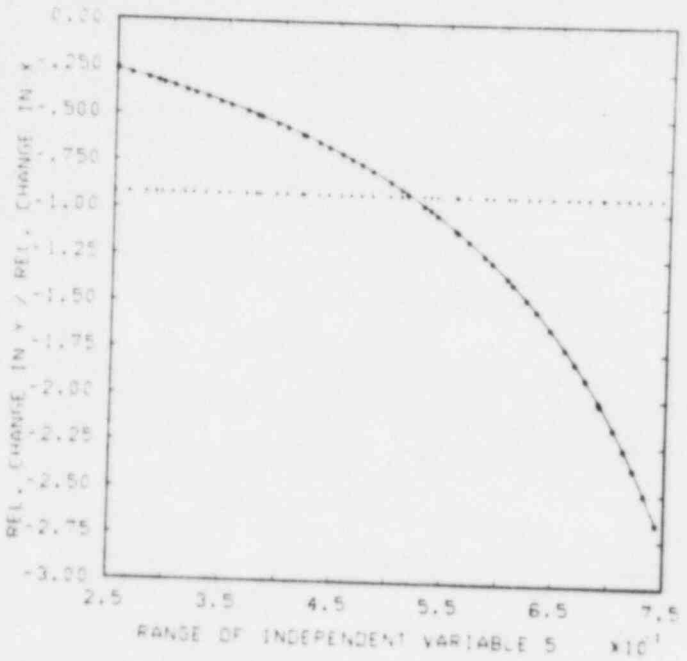

Figure 7. Behavior of $(\partial Y_1/\partial X_5)(X_5/Y_1)$ as a function of X_5. The horizontal line represents the partial derivative calculated at the expected values of the X_i.

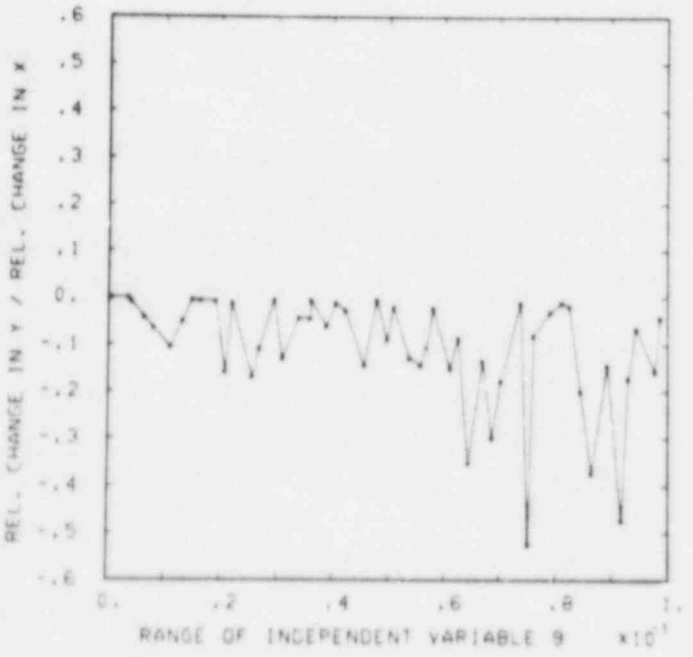

Figure 8. Behavior of $(\partial Y_2/\partial X_9)(X_9/Y_2)$ at 50 points in a LHS.

Table 9. Percent contribution to the variance of Y_1 listed by run number and input variable number. The order of the table entries has been determined by the input values used for X_{18} (from smallest to largest). The last column contains the percentage error on the variance estimate.

Run No.	X_4	X_5	X_6	X_7	X_8	X_9	X_{10}	X_{18}	X_{19}	P.E.
1	0	0	0	0	0	0	0	99	0	43
2	0	0	0	0	0	0	0	99	0	-62
3	0	0	0	0	0	0	0	99	0	-78
4	0	0	0	0	0	0	0	99	0	75
5	0	0	0	0	0	0	0	99	0	2041
6	0	0	0	0	0	0	0	99	0	34
7	0	0	0	0	0	0	0	99	0	-45
8	0	0	0	0	0	0	0	99	0	906
9	0	0	0	0	0	0	0	99	0	728
10	0	0	0	0	0	0	0	99	0	1400
11	0	0	0	0	0	0	0	99	0	133
12	0	0	0	0	0	0	0	99	0	240
13	0	0	0	0	0	0	0	99	0	31
14	0	0	0	0	0	0	0	99	0	14
15	0	0	0	0	0	0	0	98	0	-82
16	0	0	0	0	0	0	0	98	0	-47
17	0	0	0	0	0	0	0	98	0	0
18	1	0	0	0	0	0	0	97	0	-35
19	0	0	0	0	0	0	0	99	0	35
20	1	0	0	0	0	0	0	97	0	-21
21	0	0	0	0	0	0	0	98	0	64
22	0	2	0	0	0	0	0	94	0	124
23	1	2	0	0	0	0	0	95	0	-29
24	0	2	0	0	0	0	0	95	0	20
25	1	1	0	0	0	0	0	96	0	69
26	5	2	0	0	0	0	1	89	0	-59
27	1	2	0	1	0	0	0	93	0	61
28	2	4	0	0	0	0	1	90	0	-54
29	1	1	0	0	0	0	2	92	0	356
30	5	2	0	0	0	0	1	86	1	-23
31	9	2	0	1	0	0	2	82	1	17
32	13	9	1	3	0	1	1	69	0	-50
33	16	4	1	3	1	2	4	61	2	-2
34	3	18	1	2	1	0	2	69	0	-4
35	5	7	1	3	0	0	7	72	0	524
36	5	6	1	2	0	2	6	71	3	184
37	5	8	0	1	1	0	12	67	0	328
38	19	6	1	2	2	0	5	59	1	-5
39	8	6	2	5	2	10	8	49	2	195
40	14	8	1	3	6	0	8	54	0	79

Table 9 (Continued)

Run No.	X_4	X_5	X_6	X_7	X_8	X_9	X_{10}	X_{18}	X_{19}	P.E.
41	35	24	0	2	4	4	3	22	1	-87
42	9	17	2	6	8	1	6	46	0	17
43	11	26	2	5	1	13	6	28	2	50
44	7	56	1	2	6	3	4	16	0	-46
45	31	15	2	5	8	1	11	20	0	150
46	36	10	2	6	12	4	6	19	0	43
47	18	21	2	5	0	19	9	18	1	113
48	27	12	1	3	1	22	12	12	4	234
49	19	32	0	1	10	7	14	4	7	-9
50	44	17	0	1	9	13	6	2	2	-57

The results in Table 9 are quite revealing with respect to local behavior and its extendibility to global interpretation. In Tables 3, 4, 6, and 8, X_{18} was identified as the dominant variable influencing Y_1. In Table 9, the influence of X_{18} on $V(Y_1)$ decreases from 99% to 2% as X_{18} increases. In eight of 50 cases, X_{18} was not designated as the dominant variable. Furthermore, in those cases where X_{18} was identified as contributing 99% to the variation in Y_1, the percentage error on the variance estimate ranged from -78% (run 3) to 2041% (run 5). There does not seem to be any discernible pattern in the behavior of the percentage error as X_{18} increases. Other wide variations on percentage contributions are noted for X_4 (0% to 44%) and X_5 (0% to 56%). Similar results occurred with the analysis on Y_2.

An interesting result appeared in the analysis for Y_3. The variables contributing to $V(Y_3)$ for the 50 LHS runs are listed in Table 10, where the entries have been listed in increasing order of the input values used for the dominant variable X_{10}. First, the percentage contribution from X_{10} varies between 50% and 86% with no discernible pattern as X_{10} increases. This is much more stable than the results shown in Table 9 for X_{18}. Second, a very definite pattern does appear in the column containing the percentage error of the estimates. The first 22 entries show 21 positive entries and the last 28 show 27 negative entries. Hence, small values of X_{10} lead to an overestimate of the variance calculated from the random sample, while large values lead to an underestimate of this variance. In this example, the observed behavior of estimates for $V(Y_3)$ is due to the fact that estimates for $E(Y_3)$ derived from Taylor series expansions are decreasing as X_{10} increases. In this regard, it is important to recognize that variance estimates for Y_3 are being made with respect to different estimates for $E(Y_3)$. This is also true for Y_1. Overall, it can be quite precarious to extend estimates of variance based on local behavior to a global interpretation.

The preceding results indicate a difficulty with differential analysis based on behavior at a single point in the input variable space. Such an analysis might be appropriate in a setting where all of the input parameters were essentially fixed and one was interested in the effects of small perturbations in the input parameters or when the model is essentially linear. However, this is generally not the case in risk

Table 10. Percent contribution to the variance of Y_3 listed by run number and input variable number. The order of the table entries has been determined by the input values used with X_{10} (from smallest to largest). The last column contains the percentage error on the variance estimate.

Run No.	X_3	X_8	X_{10}	X_{11}	X_{16}	X_{19}	P.E.
1	6	0	77	5	0	9	112
2	6	0	82	5	0	4	406
3	5	0	67	4	0	22	79
4	6	0	84	5	0	2	416
5	5	1	70	4	14	2	119
6	6	0	81	5	0	6	157
7	6	0	79	5	0	8	76
8	5	4	69	4	4	11	35
9	6	0	82	5	0	3	36
10	5	0	64	4	0	25	155
11	6	0	85	5	0	1	128
12	5	0	69	4	0	20	49
13	5	0	74	5	0	14	128
14	5	1	75	5	6	5	0
15	4	0	63	4	0	26	50
16	6	0	78	5	0	10	54
17	6	5	80	5	1	1	25
18	6	0	79	5	0	8	52
19	4	12	56	3	13	7	-55
20	6	0	86	5	0	0	94
21	5	1	72	5	2	13	34
22	6	0	86	5	0	1	30
23	6	0	77	5	0	10	-18
24	6	2	78	5	1	6	-4
25	3	8	50	3	11	21	-59
26	6	0	85	5	0	1	-36
27	6	0	86	5	0	1	-25
28	6	0	83	5	0	3	5
29	6	0	81	5	5	0	-56
30	6	0	77	5	0	10	-20
31	5	3	73	5	2	9	-41
32	6	0	85	5	0	0	-45
33	5	0	71	4	1	17	-18
34	6	0	82	5	2	2	-59
35	5	8	73	5	4	3	-75
36	5	0	74	5	0	13	-33
37	4	1	63	4	0	25	-41
38	4	0	63	4	0	26	-19
39	5	9	74	5	3	1	-61
40	6	0	78	5	0	9	-58

Run No.	X_3	X_8	X_{10}	X_{11}	X_{16}	X_{19}	P.E.
41	4	0	55	3	1	34	-42
42	6	0	82	5	3	1	-56
43	6	0	82	5	0	5	-71
44	5	0	66	4	0	23	-58
45	5	0	72	5	0	16	-47
46	5	0	76	5	0	12	-69
47	6	0	86	5	0	1	-69
48	5	0	76	5	0	12	-73
49	5	0	72	5	0	16	-76
50	6	2	79	5	0	5	-78

assessment problems where a great deal of uncertainty is associated with the input values. The analysis shows the value of using multiple points with a differential analysis, such as the points generated by the LHS in the present example.

3.5 SECTION SUMMARY

In this section, three frequently used techniques for performing uncertainty analysis and sensitivity analysis were compared on the basis of estimating the cdf(s) of an output variable(s) from a computer model given input cdfs and on the ability to rank the input variables to the model by each of several different criteria. The computer model used in these comparisons, called the Pathways model, represents the environmental movement and human uptake of radionuclides. The version of the Pathways model used in these comparisons is relatively simple, consisting of a system of four linear, constant coefficient differential equations. The Pathways model requires 20 input variables that behave independently of one another and produces nonlinear output which is a monotone function of each of the input variables.

UNCERTAINTY ANALYSIS

The response surface replacement for the Pathways model used 128 computer runs based on input selected by a fractional factorial design which, when used with a Monte Carlo simulation according to the input distributions in Table 2, produces an indirect estimate of the output cdf. A Monte Carlo simulation of the Taylor series expansion about a point also yields an indirect estimate of the output cdf. On the other hand, a direct estimate of the output cdf is obtained from the LHS generated from input values which have the multivariate input structure described in Table 2. When this input is supplied to the computer model, an estimate of the output cdf, conditional on the assumptions in Table 2, can be produced directly.

Figures 2 contains three estimates (two direct and one indirect) of the output cdfs for Y_1 and Y_3. The estimates from LHS (n = 50) and random sampling (n = 100) are in good agreement for both Y_1 and Y_3. The estimate for Y_3 based on a Monte Carlo simulation with the fitted response is quite good while the corresponding estimate for Y_1 is quite poor.

Figure 3 shows the indirect estimate of the output cdf obtained by using a Monte Carlo simulation with the Taylor series expansion about the "basecase" to be in good agreement with the LHS direct estimate. However, Figure 4 shows that other choices of basecase points can produce widely varying results, and as such, it would be difficult to place much faith in estimates such as these. More detail on estimates arising from Taylor series expansions about basecase values is provided in the next section.

The estimation of the variance of the output by several different indirect and direct methods was considered in this section. In general, as one might suspect, the direct variance estimates tend to produce a more reliable measure of spread than do the indirect variance estimates. However, since variance is not a robust measure of spread for output of the type considered in this paper, its use is precarious at best.

SENSITIVITY ANALYSIS

Four methods of measuring variable influence were considered in this section. These methods are as follows:

1. The relative size of the absolute value of standardized coefficients (see Table 5).

2. The relative size of the absolute value of normalized sensitivity coefficients (see Table 4).

3. Contribution to variance after improving the fitted regression model (see Table 6).

4. The relative size of the absolute value of the partial rank correlation coefficient (see Table 8).

Ranking of the input variables is important because it allows research efforts to be guided in the proper direction to reduce uncertainties. Although each of these methods can be used to rank the relative importance of all input variables, it is usually sufficient to compare different techniques for ranking on the basis of their ability to identify the most influential variables. That is, if a variable is not important, then there is no need to concern oneself with the fact that it received ranks of 13, 17, and 20 by three different methods of ranking.

Methods 1 and 3 above are based on the same calculation and are therefore equivalent. Thus, the apparent difference in rankings between Tables 5 and 6 is not attributable to a difference in methods but rather to the fact that Method 1 was used to rank all variables utilizing the original variables, while Method 3 was used to rank a subset of the variables after an attempt had been made to improve the fit of the model, as indicated in (3.8).

Method 2 utilizes a different criterion for ranking than the other methods considered, and hence will not necessarily produce rankings in agreement with the other methods. Specifically, Method 1 is based on ranking variable importance due to the effects of changing variables by equal fractions of their standard deviations while Method 2 is based on ranking variable importance due to the effects of

changing variables by equal fractions of their basecase values. This point is quite evident when rankings in Table 4 are compared with rankings in Tables 3, 6, and 8. Method 2 provides good information with respect to variable influence about a point and is therefore most likely to be used with a differential-based analysis. However, there is great potential for providing erroneous results when this local information is extrapolated to a global interpretation. This point is clearly demonstrated in Figures 7 and 8.

Method 4 relies on the use of ranks to overcome difficulties with relationships that may not be well behaved in the sense of either extreme observations or monotonic nonlinear relationships being present. Standardized regression coefficients can also be computed on ranks to overcome these same difficulties. These methods cannot be used with a differential analysis, but are quite effective when used with either a LHS or a random sample. The calculation in (3.1') is quite easy to do and can be performed on either the original variables or on their ranks. This method is demonstrated with time-dependent output in the next section with the MAEROS model.

The variability of the cdf estimates in Figures 2, 4 and 5 might lead one to suspect that the rankings of input variables would vary greatly from LHS to RS to DA for a given method of ranking. This did not occur as each method of ranking proved to be fairly robust with respect to different approaches to sensitivity analysis. This result is mainly attributable to the simplicity of the Pathways model and to the fact that a single input variable tended to dominate each output variable. In the next section it will be shown that this robustness may not hold up with a more complex model.

4. RESULTS BASED ON THE MAEROS MODEL

4.1 THE MAEROS MODEL

DESCRIPTION OF THE MAEROS MODEL

The MAEROS model represents multicomponent aerosol dynamics. Mathematically, the model is a system of differential equations of the form

$$dY_j(\underset{\sim}{X},t)/dt = f_j[Y(\underset{\sim}{X},t), \underset{\sim}{X},t]$$

$$= s_j(\underset{\sim}{X}) + \sum_k a_{jk}(\underset{\sim}{X})\, Y_k(\underset{\sim}{X},t) + \sum_k \sum_\ell b_{jkl}(\underset{\sim}{X})\, Y_k(\underset{\sim}{X},t)\, Y_\ell(\underset{\sim}{X},t) \qquad (4.1)$$

with the initial value condition $Y_j(0) = Y_{0j}(\underset{\sim}{X})$, where some zero coefficients are included for notational convenience and $\underset{\sim}{X}$ is used to represent model input. This model was developed at Sandia National Laboratories under NRC sponsorship to represent aerosol behavior in reactor accident assessments. The model calculates aerosol composition and mass concentration as a function of particle size and time. The processes that may be incorporated are (1) coagulation due to Brownian motion, gravity and turbulence; (2) particle deposition due to gravitational settling, diffusion, and thermophoresis; (3) particle growth due to condensation of a gas, typically water vapor; and (4) time varying sources of particles of different sizes and chemical compositions. Operation of the model involves two numerical steps. The first step is numerical evaluation of a number of single and double integrals to generate the coefficients for the system of differential equations. These integrations involve functions of the input variables which will be considered as part of the comparison contained in this section. The second step is the generation and numerical solution of the system of equations. Documentation for the MAEROS model includes a user's guide by Gelbard (1982) with the numerical procedure given in Gelbard and Seinfeld (1980). Additional background with respect to the analysis problem considered in this section is given in Helton et al. (1985).

Whereas the Pathways model of the previous section consisted of a set of linear differential equations, MAEROS consists of a set of nonlinear differential equations. Additionally, MAEROS produces time-dependent output rather than the single values of the dependent variables obtained with Pathways. Another important difference between the two models lies in the additional complexity of the multivariate input structure for MAEROS.

VARIABLES CONSIDERED IN THE ANALYSIS OF THE MAEROS MODEL

The problem considered in the analysis with the MAEROS model involves the behavior of a two-component aerosol in a reactor containment building. The first component is assumed to have been released early in a reactor accident; the second component is assumed to be continuously released as the accident progresses. For this analysis, no water vapor condensation is assumed. Ten particle size classes are used in representing particle behavior; this results in the use of a system of 20

differential equations to represent the behavior of suspended particles. In addition, unknown functions defining integrated concentration and integrated depositions on ceiling, wall, and floor for each component were also added to the system of equations. This resulted in a system containing a total of 28 equations.

The output from MAEROS is multivariate as was the case with the Pathways model. However, unlike the Pathways model, the output from MAEROS is also time dependent. For this comparison, the following four output variables were selected for consideration:

Y_1 = Total integrated concentration of the second component (kg-sec/m^3)

Y_2 = Total integrated deposition on the wall for the first component (kg)

Y_3 = Total suspended mass for the first component (kg)

Y_4 = Geometric expected value of particle diameter (m).

The variables Y_1 and Y_2 are integrated over time (72,000 seconds), while Y_3 is examined primarily at 20 minutes. However, Y_3 and Y_4 are examined at multiple time steps later in this section when illustrating results for the partial rank correlation coefficient. Various system variables are required as input in formulating the preceding system of equations. Certain of these variables were taken to be uncertain and were assigned ranges and distributions. The variables used in the analysis are listed in Table 11 with the corresponding ranges, distributions, and restrictions given in Table 12.

Examination of the restrictions in Table 12 shows that the multivariate structure of the input is more complex than is the case when all variables are independent of one another. The input structure in Table 12 requires a correlation between X_2 and X_5 and also between X_5 and X_6. Further, the restrictions specify that rank correlations of .5 be used in both correlations (as opposed to correlations on original values). The correlation is specified on ranks since this correlation measure is meaningful for both normal and nonnormal distributions; in contrast, the ordinary correlation coefficient is sensitive to the nature of the underlying distributions. A second problem associated with the formulation of the input structure to MAEROS occurs with the input pairs (X_8, X_9) and (X_{12}, X_{16}). The manner in which this problem is handled is explained in the next subsection under the heading of Latin hypercube sample.

4.2 SELECTION OF THE VALUES OF THE INPUT VARIABLES USED IN THE ANALYSIS

THE RESPONSE SURFACE REPLACEMENT

A response surface analysis on the MAEROS model was not performed using input values associated with a fractional factorial design. The reason for this decision lies in the complexity of the multivariate structure of the input including correlated variables and conditional distributions as described in the previous subsection. That is, a basic reason for using fractional factorial designs is that they provide orthogonal (uncorrelated) input and hence are not really intended for use in situations such as exist with MAEROS.

Table 11

Input Variables Used with the MAEROS Model

X_1	Geometric standard deviation for diameter of first component (unitless)
X_2	Mass median diameter for first component (m)
X_3	Total released mass for first component (kg)
X_4	Geometric standard deviation for diameter of second component (unitless)
X_5	Mass median diameter for second component (m)
X_6	Total mass source rate for second component (kg/sec)
X_7	Release duration for second component (sec)
X_8	Containment temperature (K)
X_9	Containment pressure (Pa)
X_{10}	Ratio of ceiling area to volume (m^{-1}) (also the ratio of floor area to volume)
X_{11}	Ratio of wall area to volume (m^{-1})
X_{12}	Dynamic shape factor (unitless)
X_{13}	Diffusion boundary layer thickness (m)
X_{14}	Particle density (kg/m^3)
X_{15}	Constant associated with thermal accommodation coefficient (unitless)
X_{16}	Agglomeration shape factor (unitless)
X_{17}	Probability sticking factor (unitless)
X_{18}	Temperature gradient (K/m)
X_{19}	Ratio of thermal conductivity of gas to that of particle (unitless)
X_{20}	Turbulence dissipation rate (m^2/sec^3)
X_{21}	Molecular weight of gas (kg/kg-mole)

Table 12

Distribution, Range, and Restrictions Used
with Each Input Variable to the MAEROS Model

Variable	Distribution	Range	Restrictions
X_1	Uniform	1.3 to 4	
X_2	Loguniform	2×10^{-7} to 5×10^{-6}	0.5 rank correlation with X_3
X_3	Loguniform	100 to 1000	0.5 rank correlation with X_2
X_4	Uniform	1.3 to 4	
X_5	Loguniform	5×10^{-8} to 5×10^{-6}	0.5 rank correlation with X_6
X_6	Loguniform	0.1 to 1	0.5 rank correlation with X_5
X_7	Uniform	7.2×10^{-3} to 1.8×10^{4}	
X_8	Uniform	375 to 600	
X_9	Triangular with apex at $4\times10^{5} + 500\ X_8$	$1000X_8$ to 8×10^{5}	$1000\ X_8 \leq X_9$
X_{10}	Uniform	0.025 to 0.075	
X_{11}	Uniform	0.08 to 0.24	
X_{12}	Uniform	1 to 3	
X_{13}	Loguniform	5×10^{-5} to 8×10^{-3}	
X_{14}	Normal	2000 to 8000	
X_{15}	Uniform	1 to 3	
X_{16}	Uniform	X_{12} to 3	$X_{12} \leq X_{16}$
X_{17}	Uniform	0.5 to 1	
X_{18}	Uniform	0 to 5×10^{4}	
X_{19}	Triangular with apex at 0.5	0.05 to 1	
X_{20}	Uniform	0.001 to 0.03	
X_{21}	Uniform	20 to 40	

It is conceivable that a fractional factorial design could be altered in some manner for use with a multivariate input structure such as specified with MAEROS, but it is doubtful that it could be done and still retain the spirit or intent of the design. A possibility that might be suggested is to ignore the multivariate input structure and generate a response surface utilizing a fractional factorial design in the usual manner. The next step would be to use a Monte Carlo simulation with the response surface with input incorporating the required multivariate input structure. The problem with such an approach is that pairs of variables may be created by the design that the modeler knows to be physically impossible or meaningless and for which the model will likely not run or if it does run, the results may be useless. These points would have influence equal with all other points in determining the fitted response surface and could therefore lead to meaningless response surface predictions even when the input is meaningful . The response surface approach based on fractional factorial designs is utilized again in the next section with the DNET model.

THE LATIN HYPERCUBE SAMPLE

With the Pathways model, the input variables were independent of one another and the LHS approach attempted to generate an input structure having a correlation matrix close to the identity matrix. However, specific nonzero rank correlations are required for two pairs of variables in the input to MAEROS. The required correlations are induced by generating a LHS in the usual sense and then controlling the individual pairing of variables to produce specific rank correlations as explained in Iman and Conover (1982a). A LHS of size n = 50 was used with the 21 MAEROS input variables and produced rank correlations of .48 and .43 for the pairs (X_2, X_3) and (X_5, X_6), respectively, where the target values were each .50. At the same time, among the 187 remaining pairs of variables in the rank correlation matrix with a target of zero correlations, only three correlations were larger than .10 with the largest being a nonsignificant value of .23.

The condition $X_{12} \leq X_{16}$ was handled by generating the required uniform marginal distribution for X_{12} in the usual manner. A uniform distribution was generated for X_{16} on the interval (1,3) followed by a transformation of X_{16} to X_{16}^* = $.5(X_{16}-1)(3-X_{12}) + X_{12}$. After X_{16} is transformed in this manner, the new variable X_{16}^* satisfies the restriction that $X_{12} \leq X_{16}^*$. That is to say, the distribution of X_{16}^* becomes conditional upon the value of X_{12}. After this transformation, the marginal distribution of X_{12} remains uniform on the interval (1,3) but the distribution of X_{16}^* is uniform, conditional on the value of X_{12}, that is, X_{16}^* is uniform on the interval (X_{12}, 3). Moreover, it is easily shown that the generation of this conditional distribution creates a population correlation of .65 between X_{12} and X_{16}^*. The actual correlation observed between this pair of variables in the LHS of size 50 was .58. The pair (X_8, X_9) was treated in a similar manner.

THE DIFFERENTIAL ANALYSIS

Some modifications had to be made to the MAEROS computer model in order to include input variables X_1 through X_7 and to generate integrated concentrations as output. It was possible to calculate the inputs to the computer

model associated with X_1 through X_7 externally and to supply them when needed. Further, it was easy to add the capability to calculate integrated concentrations. Modifications such as these cause no serious problems in setting up the input for an analysis such as associated with LHS, nor are any problems created in processing the output. However, these modifications did cause the differential analysis to be much more difficult to implement.

The differential analysis was performed at a "basecase" set of input values consisting of the expected values of the variables in Table 12. The differential analysis requires the implementation of the system of equations shown in (2.10). This required exact knowledge of the system of equations in (4.1). The documentation for the MAEROS computer program did not give a statement of the equations and it was necessary to go to the computer program itself to determine exactly how the equations were implemented. Ultimately, parts of this implementation had to be changed in order to perform the differential analysis. For example, desired dependent variables included integrated depositions on ceiling, walls, and floor. The MAEROS program used an interpolation procedure to determine these quantities that did not lend itself to inclusion in a differential analysis. To implement the system of equations in (2.10) for determining the derived partial derivatives, additional differential equations were added that had these quantities as solutions. Once a system of equations was determined that included all the dependent variables of interest, it was necessary to formulate the system of equations in (2.10). This required writing a subroutine to define the Jacobian matrix for the system in (4.1). Further, it was necessary to calculate various partial derivatives with respect to the X_i. These partial differentiations were often coupled with numerical integrations. For example, the coefficients a_{jk} and $b_{jk\ell}$ appearing in (4.1) are actually single and double integrals of functions of the X_i. To calculate the partial derivatives for the a_{jk} and $b_{jk\ell}$, a routine for numerical differentiation was used in conjunction with a routine for numerical integration. Once the machinery was in place to calculate all the needed pieces appearing in (2.10), a program was written to combine the equations in (2.10) and (4.1). This combined system had to be solved 21 times, once for each independent variable. As the details of the system were not the same for each independent variable, assorted logic had to be built in to account for differences associated with individual variables. For example, X_7 had a discontinuity associated with it which required special treatment. Once the preceding systems had been developed, they had to be solved. As might be expected, they turned out to be stiff and as such required use of a solver for stiff systems (Shampine and Watts, 1980). The original MAEROS model used a Runge-Kutta solution method.

Our original, perhaps naive, intent for the MAEROS differential analysis had been to add the system in (2.10) to the original MAEROS computer model. By the time the differential analysis was actually completed, we had developed a separate computer program that was considerably more complicated than the original program for MAEROS. As the preceding discussion might lead one to suspect, the differential analysis required significantly more human and computer time than the Latin hypercube analysis. Further, due to the complexity of the implementation, it is also more likely to contain errors. In retrospect, it might have been better to have approximated the desired derivatives with difference quotients. However, the given approach to differential analysis does have the advantage that it provides a useful leadin to the discussion of adjoint sensitivity analysis techniques given in Section 6.

4.3 UNCERTAINTY ANALYSIS FOR THE MAEROS MODEL

ESTIMATION OF THE DISTRIBUTION FUNCTION OF THE OUTPUT

Figure 3 contained two estimates of the output cdf for Y_1 from the Pathways model. These estimates were obtained directly from the LHS analysis and indirectly by using a Monte Carlo simulation with the Taylor series expansion at the basecase. Analogous results appear in Figures 9, 10, and 11 for Y_1, Y_2, and Y_3, respectively, from the MAEROS model. As a check on the adequacy of these methods, a third estimate has been added to each of these figures. The third estimate was based on a simple random sample of size 100.

Results in Figure 9 show reasonably good agreement for all three procedures except for the lower tail. In Figure 10, the LHS and random sample estimates coincide throughout, while the Taylor series expansion is not close for cumulative probabilities $< .4$. In fact, over 35 percent of the predictions from this latter approach were negative (these values have been set equal to zero in Figure 10). Results in Figure 11 show good agreement between the LHS estimate ($n = 50$) and the random sample estimate ($n = 100$) except for some noticeable separation above the .90 quantile. The Taylor series expansion procedure agrees with the other two estimates below the .10 quantile but disagrees significantly for all quantiles above .10.

Two summary comments can be made about the results in Figures 9 through 11. First, the results based on LHS and random sampling are in good agreement as was the case with the Pathways model. The second point concerns the estimate from the Taylor series expansion. The estimate in Figure 9 from this approach shows good agreement with the other methods but the results in Figures 10 and 11 show areas of disagreement. This points out that the result from the Taylor series expansion may or may not be good. One never knows a priori. As mentioned in the previous section, the reason for this lies with the danger of trying to extrapolate local information to a global interpretation.

ESTIMATION FOR THE OUTPUT VARIABLE

Comments were made in the previous section with respect to the influence of extreme observations on estimates of the mean and variance. This point is illustrated in this section using the variables Y_1, Y_2, and Y_3. Estimates of both location and scale were obtained for each of these variables on the basis of (1) direct estimation from a random sample of size 100, (2) direct estimation from a LHS of size 50, (3) indirect estimation from Monte Carlo simulation with Taylor series expansions about the "basecase" point, and (4) indirect estimation from Taylor series expansions as indicated in (2.3).

The sample mean and median provide direct estimates of location. The sample standard deviation provides a direct estimate of scale. A robust measure of scale known as the median absolute deviation (MAD) was also calculated directly. The MAD estimator is calculated as follows for a sample of size n:

$$MAD_n = \text{median} \{ |Y_i - \text{median } Y| \} \quad . \tag{4.2}$$

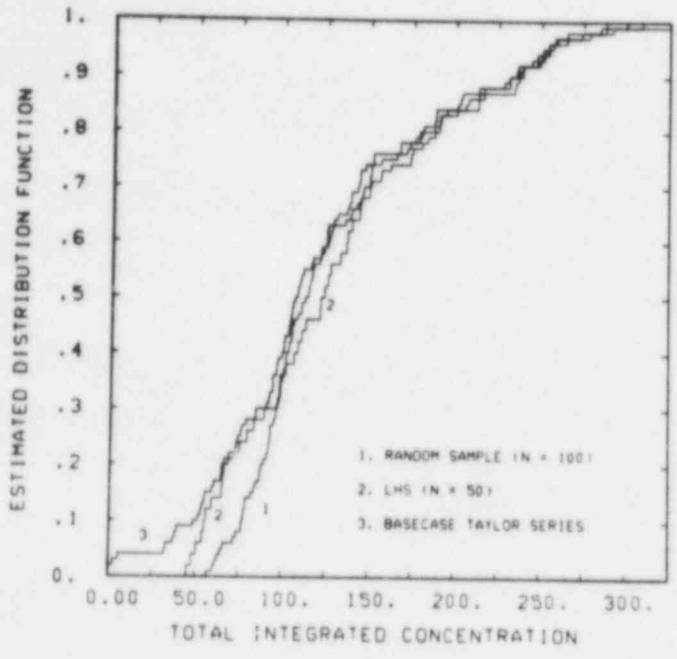

Figure 9. A Comparison of Three Estimates of the CDF for Y_1 for the MAEROS Model

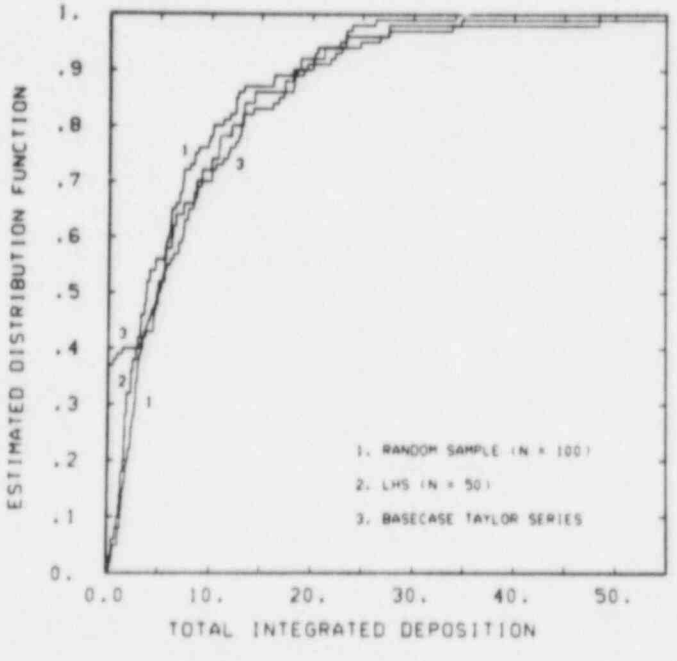

Figure 10. A Comparison of Three Estimates of the CDF for Y_2 for the MAEROS Model

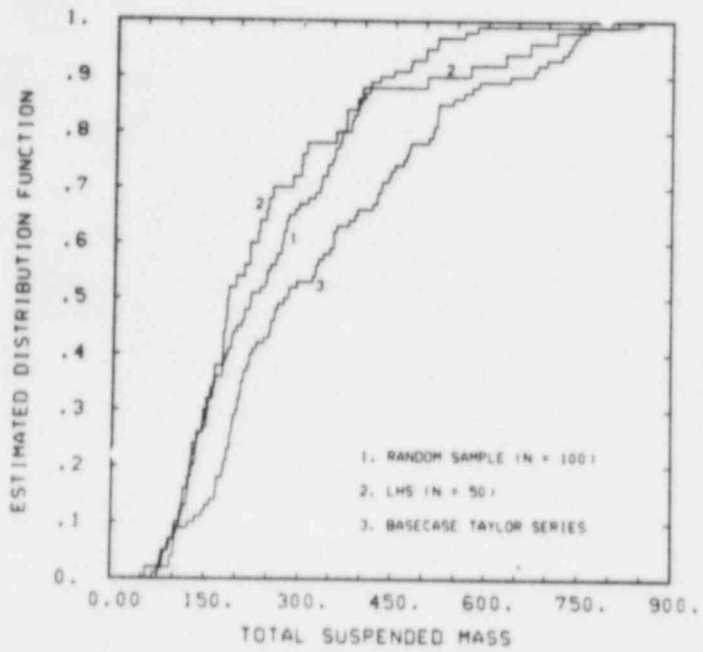

Figure 11. A Comparison of Three Estimates of the CDF for Y_3 for the MAEROS Model

Table 13

Estimate of Location and Scale for the Output Variables Y_1, Y_2, and Y_3

ESTIMATES OF LOCATION

Output Variable	RANDOM SAMPLE		LHS		DA (Monte Carlo)		DA (Indirect)
	Mean	Median	Mean	Median	Mean	Median	Mean
Y_1	134	113	130	123	129	112	171
Y_2	7.6	4.9	7.5	3.7	-6.1	-7.7	10.6
Y_3	254	220	252	183	341	278	343

ESTIMATES OF SCALE

	Var	MAD	Var	MAD	Var	MAD	Var
Y_1	3868	26	3810	41	4736	41	5175
Y_2	87	2.9	76	2.6	68.6	5.2	109
Y_3	19,808	95	30,505	67	36,679	111	34,044

The MAD estimator is not influenced by extreme observations and Huber (1981) has stated, "...the median absolute deviation has emerged as the single most useful ancillary estimate of scale." While the MAD estimator can be used to quantify the variability in the output, it cannot be used to rank input variables. That is, as with the direct calculation of the sample variance, the calculation of the MAD estimator does not in and of itself produce a ranking of the variables as a byproduct. Results of all estimates with respect to Y_1, Y_2, and Y_3 are summarized in Table 13.

It is not possible to estimate the median with the DA approach, but in the other cases where a median estimate is available, it is always less than the mean estimate of location. This is due to the skewness of the distributions given in Figures 9, 10, and 11. The random sample and LHS estimates of location show good agreement with one another in all cases while the Monte Carlo of the Taylor series expansion is sometimes in agreement and sometimes in disagreement with the other estimates. The indirect estimate from the Taylor series expansion shows behavior similar to the Monte Carlo estimate.

There are two reasons for wanting to use variance as a measure of scale. The first is to quantify the variability in the output and the second is to rank the input variables on the basis of their contribution to the variance estimates. The form of the output, in particular the presence of extreme observations, has a large impact on the reliability of these calculations. This point will now be discussed in reference to quantifying variability by using the results shown in Figures 9, 10, and 11. In Figure 11, the cdf estimated from the random sample shows only one extreme value compared to the heavier upper tails of the other two cdf estimates. This results in the random sample providing a variance estimate that is 35 to 42 percent less than the other estimates. However, another random sample could change the results dramatically depending on the number of extreme observations. In Figure 10, the cdfs of the random sample and LHS show excellent agreement; yet, the variance estimate from the random sample is 15 percent higher than the LHS estimate principally because the random sample has the most extreme observation. When the variance estimates are made after discarding the upper 2 percent of each curve, the random sample produces an estimate of 45.7 compared to 43.8 for the LHS. Hence, the estimates almost double in size with the addition of one or two extreme values. In Figure 9, the basecase estimate increases because of the extreme observations; however, they still show some variability between the random sample and the LHS.

4.4 SENSITIVITY ANALYSIS FOR THE MAEROS MODEL

In the previous section, the input variables to the Pathways model were ranked using (a) two types of normalized coefficients, (b) contribution to variance, and (c) the partial rank correlation coefficient. These same ranking methods are presented in this subsection for the output variables Y_1 and Y_2 from the MAEROS model. An expanded discussion is also presented on the usefulness of the partial rank correlation coefficient with time-dependent output utilizing the output variables Y_3 and Y_4.

RANKING THE INPUT VARIABLES

The results of using the ranking methods listed above were summarized in the previous section for the Pathways model in Tables 3, 4, 6, and 8. In the interest of shortening the discussion, all of the rankings in this subsection appear simultaneously in Tables 14 and 15 for Y_1 and Y_2, respectively. In addition to the ranks, the value of the PRCC is also given in parentheses in order to provide more information about the relative rankings.

Table 14 shows good agreement between the DA and LHS rankings within each ranking criterion. This agreement might have been anticipated since the DA approach provided a reasonably good estimate of the cdf for Y_1 in Figure 9. Likewise, there is good agreement between the random sample and LHS results under the PRCC criterion. However, as with the Pathways model, there is a noticeable disagreement on the relative importance of the variables between ranking criteria. In particular, X_6 ranks fourth and fifth by the normalized coefficients and first by all other criteria. The ties occurring within the rankings for contribution to variance occur because some of the variables are correlated with one another and their individual contribution cannot be separated from their joint contribution. The PRCC handles the correlated variables by adjusting for the presence of all other variables.

The results in Table 15 for Y_2 show more disagreement both within and between ranking criteria than the results presented in Table 14. This disagreement might have been anticipated somewhat on the basis of the poor cdf estimate of Y_2 in Figure 10 by the DA approach and the corresponding parameter estimates in Table 13. For the standardized coefficients criterion, the top three ranks for both the DA and LHS approaches agree, but there is disagreement on X_{11} where ranks of 4 and 11 are assigned. This is probably not a major concern since the dominant three variables have been identified. More noticeable is the disagreement between the rankings for normalized coefficients. These rankings disagree considerably after rank 1, and the rankings as a whole disagree with the other ranking criteria, particularly on X_{18}. The rankings under contribution to variance for LHS agree very well with those found under PRCC, but the agreement is not quite as good for the DA based rankings. Once again, the random sample and LHS rankings under PRCC agree very well with each other.

USE OF THE PRCC WITH TIME-DEPENDENT OUTPUT

The PRCC is particularly useful when the output is time dependent and the relative importance of the input variables changes with respect to time. For example, the MAEROS output for Y_3 and Y_4 was recorded at 65 time points. The PRCC as computed from (3.11) can be calculated for each input variable versus each output variable at each of the 65 time points. The influence of a particular input variable X_j on a particular output variable Y is easily summarized by plotting r_{jy} from (3.11) on the vertical axis versus time on the horizontal axis. Two such plots appear in Figures 12 and 13 for X_7 and Y_3 and X_7 and Y_4. A value of the PRCC near 1 or -1 indicates a strong influence while a value near 0 indicates little influence. Thus, in Figure 12, X_7 has little influence on Y_3 during the first 10,000 seconds but quickly shows a strong negative correlation after 10,000 seconds. In Figure 13, X_7 shows a negative correlation developing between X_7 and Y_4 out to 10,000 seconds and then very quickly changes to a strong positive correlation.

Table 14

Rankings of the Input Variables to the MAEROS Model for the Output Variable Y_1

Input Variable	Standardized Coefficients DA	Standardized Coefficients LHS	Normalized Coefficients DA	Normalized Coefficients LHS	Contribution to Variance DA*	Contribution to Variance LHS**	PRCC LHS(n=50)	PRCC RS(n=100)
1	18	17	18	16				
2	17	18.5	17	20				
3	14	8	14	11				
4	10	20	12	19				
5	4	6	9	12	1.5[c]	1.5[a]	8(-.57)	5(-.64)
6	1	1	4	5	1.5[c]	1.5[a]	1(.91)	1(.89)
7	3	3	2	2	5	3	2(.89)	2(.82)
8	9	11	6	4				
9	13	12	11	10				
10	19	21	19	11				
11	15	10	15	9				
12	6	5	5	6	3.5[d]	4.5[b]	7(.59)	7(.48)
13	21	13	21	15				
14	8	9	7	8	8	8	5(.66)	8(.43)
15	20	18.5	20	18				
16	2	2	1	1	3.5[d]	4.5[b]	3(-.82)	3(-.68)
17	7	7	3	3	7	7	6(-.61)	6(-.52)
18	12	15	13	17				
19	16	14	16	14				
20	5	4	8	7	6	6	4(-.72)	4(-.64)
21	11	16	10	13				

$R^2 = 96.5\%$

[a] X_5 and X_6 jointly contribute 35.7%.
[b] X_{12} and X_{16} jointly contribute 18.5%.
[c] X_5 and X_6 jointly contribute 36.8%.
[d] X_{12} and X_{16} jointly contribute 24.4%.

* Estimate obtained directly from coefficients
** Estimate obtained by regression with LHS output

Table 15

Rankings of the Input Variables to the
MAEROS Model for the Output Variable Y_2

Input Variable	Standardized Coefficients DA	Standardized Coefficients LHS	Normalized Coefficients DA	Normalized Coefficients LHS	Contribution to Variance DA*	Contribution to Variance LHS*	PRCC LHS(n=50)	PRCC RS(n=100)
1	16	16	15	16				
2	7	6	14	11	2.5[a]			10(-.34)
3	2	2	7	4	2.5[a]	2	2(.83)	2(.80)
4	18	10	18	10				
5	14	21	16	21				
6	5	4	11	7		4	5(-.52)	5(.57)
7	20	14	20	14				
8	13	12	2	5	6			
9	9	19	4	15			9(-.37)	
10	19	20	19	20				
11	4	11	5	12			4(.61)	3(.70)
12	10	18	9	19	4.5[b]		10(-.32)	8(-.40)
13	21	9	21	13				
14	15	7	12	6				
15	17	17	17	17				
16	3	3	1	1	4.5[b]		8(-.39)	7(-.40)
17	12	13	8	9			6(-.45)	9(-.35)
18	1	1	6	3	1	1	1(.95)	1(.89)
19	8	8	10	8			7(.42)	6(.40)
20	11	15	13	18				
21	6	5	3	2		3	3(-.65)	4(-.60)

$R^2 = 75.8\%$

[a] X_2 and X_3 jointly contribute 18.6%.
[b] X_{12} and X_{16} jointly contribute 17.2%.

*Estimate obtained directly from coefficients
**Estimate obtained by regression with LHS output

The graphs in Figures 12 and 13 show quite clearly the influence of a single input variable and, in particular, point out the fact that the importance of input variables may be time dependent. One convenient way of summarizing the relative importance of the input variables is to rank each of them on the basis of the absolute value of their PRCC at each of several time steps. Such a summary is presented in Table 16 for Y_3 and Y_4 for 11 different time steps. This summary shows that X_3 is the most influential variable through 20 minutes and then decreases in importance with respect to Y_3. In contrast, X_6 has no influence (rank 19) on Y_3 at 2 minutes but starting at 40 minutes it becomes the most important variable. Other measures of sensitivity such as standardized regression coefficients could also be used here rather than the PRCC.

4.5 SECTION SUMMARY

The comparisons in the last section were continued in this section with the MAEROS computer model. MAEROS models multicomponent aerosol dynamics and is more complex in a mathematical sense than is the Pathways model. Mathematically, the model is a system of nonlinear differential equations of the form given in (4.1). The complexity of the analysis was also increased by the fact that the multivariate nonlinear output from MAEROS is time dependent. This means that the relative importance of the input variables may change as a function of time. Another important difference from the Pathways analysis involves the complexity of the multivariate input structure. Whereas the input variables for the Pathways model were all independent of one another, the input to the MAEROS model involved dependences among some of the input variables. These dependences manifested themselves in the form of required correlations for two pairs of variables and in conditional distributions for two other pairs of variables, which created correlations for these variables also. Thus, eight of the 21 input variables had required correlations.

The complexity of the multivariate input structure forced us to drop the response surface approach utilizing a fractional factorial design from consideration in this analysis since the basic idea underlying the fractional factorial design is to generate orthogonal input. It may be possible to alter a fractional factorial design in some manner to satisfy the requirements of the input structure. However, such alterations would not be straightforward and it is doubtful that such alterations, if possible, would be able to retain the spirit and intent of a fractional factorial design. The suggestion may be made to ignore the conditional distributions and required correlations and construct the fractional factorial design in the usual manner. The basic problem with this approach is that it may generate some input combinations that are physically impossible and yet would be used along with all other combinations runs in fitting a response surface; this assumes that the model will even run for such combinations or, if it does run, that meaningful results will be produced.

UNCERTAINTY ANALYSIS

Estimates of the output cdf are given in Figures 9 through 11 for three output variables. These estimates include one made directly from a simple random sample of size 100. This estimate was included to provide a standard for comparison with the other estimates. Of the other two estimates, one is obtained directly from 50

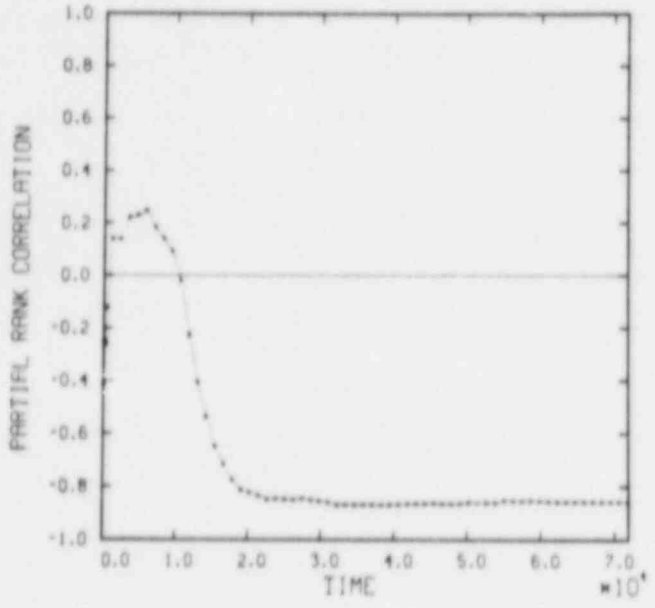

Figure 12. A Plot of the PRCC Showing the Influence of X_7 on Y_3 Over Time

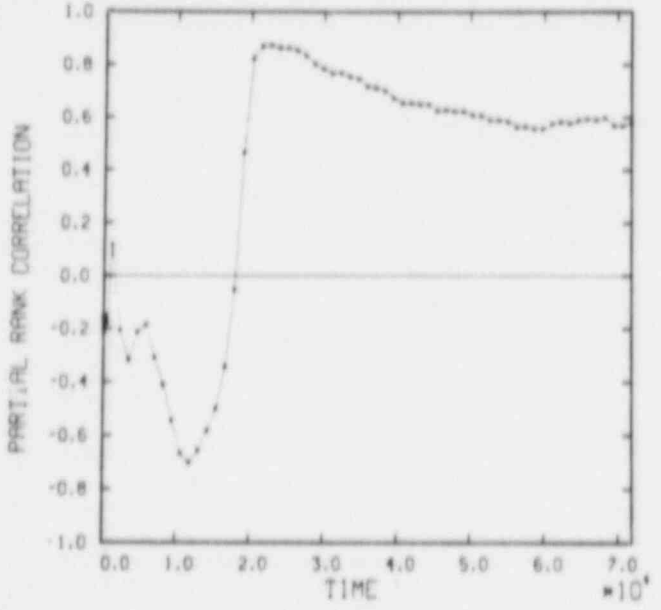

Figure 13. A Plot of the PRCC Showing the Influence of X_7 on Y_4 Over Time

Table 16

Ranking of the Influence of the Input Variables
on Y_3 and Y_4 at 11 Selected Time Steps

		TIME (MIN)										
	X	2	4	6	8	10	20	40	60	120	180	240
Y_3	1	4	4	5	5	5	7	12	20	20	17	17
	2	3	2	4	3	3	9	6	6	6	6	9
	3	1	1	1	1	1	1	5	7	8	8	10
	4	13	13	7	6	7	15	10	8	7	7	12
	5	20	19	21	21	17	21	19	16	10	9	7
	6	19	11	6	7	6	3	1	1	1	1	1
	7	6	8	8	10	12	13	16	11	13	19	6
	8	14	14	14	12	21	10	8	9	11	13	16
	9	16	17	16	15	14	18	15	17	15	18	21
	10	15	6	9	8	9	8	20	21	21	20	20
	11	8	18	18	19	11	14	14	14	16	12	15
	12	5	5	3	4	4	4	9	10	9	11	11
	13	11	15	13	14	13	19	21	15	19	15	14
	14	9	9	15	16	19	6	4	4	4	3	3
	15	18	10	11	11	10	11	13	19	17	14	13
	16	2	3	2	2	2	2	3	3	2	2	2
	17	12	21	17	17	16	16	7	5	5	5	5
	18	17	20	19	13	15	17	17	18	14	16	19
	19	21	7	12	9	8	12	11	12	18	21	18
	20	7	12	10	18	20	5	2	2	3	4	4
	21	10	16	20	20	18	20	18	13	12	10	8
Y_4	1	4	5	5	5	5	12	18	19	19	11	16
	2	1	1	1	1	3	5	15	13	16	15	14
	3	5	4	3	2	1	2	3	4	8	6	17
	4	11	12	12	14	16	17	16	17	11	21	7
	5	2	2	2	3	2	1	1	1	1	1	3
	6	8	15	20	17	18	6	6	14	4	4	5
	7	12	10	10	13	10	14	13	5	10	3	2
	8	10	11	9	6	7	20	8	6	17	18	6
	9	6	6	6	7	6	8	14	20	20	13	15
	10	13	8	14	12	12	4	4	3	3	5	4
	11	16	21	18	21	20	15	11	10	6	12	18
	12	18	18	17	19	21	19	12	12	9	16	11
	13	14	14	15	15	14	18	5	8	7	9	8
	14	3	3	4	4	4	3	2	2	2	2	1
	15	9	7	8	9	9	21	7	16	12	17	13
	16	17	13	13	11	11	11	21	11	15	8	12
	17	20	19	21	18	17	7	9	21	18	14	10
	18	19	20	16	16	15	16	17	18	14	10	19
	19	15	16	19	20	19	10	19	9	13	20	20
	20	21	17	11	10	8	9	10	7	5	7	9
	21	7	9	7	8	13	13	20	15	21	19	21

LHS computer runs and the other is an indirect estimate obtained by using a Monte Carlo simulation with the Taylor series expansion about a basecase point. The basecase point consisted of the expected values of each of the input variables from the distributions listed in Table 12.

The direct LHS (n = 50) and random sample (n = 100) estimates show reasonably good agreement in Figures 9 through 11. In Figure 9 the Taylor series expansion about the basecase shows good agreement except at the lower tail. This result is reminiscent of the outcome in Figure 3 for the Pathways model. Although the basecase input remains unchanged, Figure 10 shows the estimate arising from the Taylor series expansion to be poor, similar to some of the poorer showings in Figure 4 for the Pathways model. The estimate from the Taylor series expansion in Figure 11 is an improvement over the corresponding estimate in Figure 10; however, it shows a constant bias in being shifted significantly to the right of the random sample estimate.

The results in Figures 9 through 11 show that although the basecase for MAEROS was selected in the same manner as with the Pathways model, namely using the means of the input variables, the resulting estimates range from reasonably good to poor. One can never realiy be comfortable with such estimates.

SENSITIVITY ANALYSIS

The four methods of ranking variable importance used with the Pathways model were also used with the MAEROS model. In addition, the partial rank correlation coefficient was also calculated on the basis of a random sample of size 100. Results for all ranking techniques are summarized in Table 14 for Y_1 and in Table 15 for Y_2. The reasonably good agreement between the LHS and differential analysis estimates of the cdf in Figure 9 might lead one to suspect that these procedures will show good agreement on input variable importance for a given method of ranking. Table 14 shows this to indeed be the case for each method of ranking. Within the table, the normalized coefficients again show disagreement with the rankings of the other methods. The rankings under contribution to variance show ties for X_5 and X_6 and again for X_{12} and X_{16}. The ties occur because it was only possible to determine the joint contribution to variance of these two variables. That is, because these variables are correlated, their individual contributions to variance could not be determined. However, the other three ranking techniques all indicate that X_5 is less important than X_6 and that X_{12} is less important than X_{16}.

In a similar line of reasoning, the disagreement between the LHS and differential analysis estimates of the cdf in Figure 10 might lead one to suspect some disagreement on ranking within a given method in Table 15. This suspicion is somewhat justified by observing the rankings in Table 15. The rankings under normalized coefficients show more than their usual disagreement with other methods of ranking (see, for example, X_{18}), but there is also disagreement between the LHS and differential analysis ranks. For example, X_8 receives ranks of 2 and 5; X_9 receives ranks of 4 and 15. Under contribution to variance, ranks 1 and 2 agree for the LHS and differential analysis approaches, but the remaining selections disagree. The LHS and random sample rankings under PRCC again agree very well, but it is worthwhile to note the ranks assigned to X_{16} since the PRCC rankings for this variable disagree with rankings from other techniques. Such

disagreements are not unusual with monotonic nonlinear output or when extreme observations are present as the PRCC is not influenced by these situations.

The PRCC can be plotted with respect to time when the output is time dependent. Plots of the PRCC appear in Figures 12 and 13 and show the changing influence of X_7 on Y_3 and Y_4, respectively. Graphs such as these can be constructed for each input variable versus each output variable. Moreover, the PRCC can be used to rank the input variables at any given point in time. Table 16 gives such rankings and clearly demonstrates the changing of the sensitivity of the output to the input variables. The PRCC has provided reliable rankings in a variety of applications with computer models and in addition is easy to calculate. There is no reason why the other methods of ranking such as standardized regression coefficients could not also be plotted over time. However, the partial correlation coefficient does have a natural bounding between -1 and +1. Such graphs make it easy to interpret the coefficient associated with a single variable and to compare the coefficients associated with a number of variables. Downing, Gardner and Hoffman (1985) give a comparison of PRCC with three importance measures for ranking 24 variables in a dose assessment model which demonstrates the usefulness of ranks in identifying the most influential variables.

5. RESULTS BASED ON THE DNET MODEL

5.1 THE DNET MODEL

DESCRIPTION OF THE DNET MODEL

The final model considered in the comparison of techniques for uncertainty analysis and sensitivity analysis is a dynamic network (DNET) flow model used in simulating dissolution in bedded salt formations. DNET evolved as part of an NRC-sponsored program at Sandia National Laboratories for the development of a methodology to assess the risk associated with geologic isolation of high-level radioactive waste. DNET simulates several physical processes including the following: (1) fluid flow, (2) salt dissolution, (3) thermal expansion, (4) fracture formation and closure, (5) subsidence and (6) salt creep. In addition to this multivariate aspect, the output is nonlinear and time dependent. Submodels within DNET are applied sequentially to represent various processes. Because of feedback mechanisms governing the selection of different submodels and the complexity involved in treating various processes, the governing equations are not solved in an implicitly coupled fashion (i.e., simultaneously). This feature makes it difficult to implement a differential analysis. Thus, in this section only the techniques based on response surface replacement and Latin hypercube sampling are considered.

The DNET model has been well documented. A user's manual for DNET was written by Cranwell, Campbell, and Stuckwisch (1982), and sensitivity results are given in Cranwell, Iman and Stuckwisch (1985). A self-teaching curriculum for the DNET model is provided by Cranwell, et al. (1983).

VARIABLES CONSIDERED IN THE ANALYSIS OF THE DNET MODEL

The DNET model provides multivariate output for the process of salt dissolution in bedded salt formations. However, only one output variable has been selected for the comparison given in this section in order to simplify the presentation. The selected output variable is the rate of dissolution of a cavity of in a bedded salt formation at 20 different time periods from 5 to 10^5 years. These time periods correspond to the following times in years: 5, 10, 30, 150, 200, 500, 1000, 5000, 10000, 20000, 50000, and 100000. The input to the DNET model considered in this application consists of the 10 independent variables listed in Table 17 that describe various physical phenomena associated with the bedded salt formation. Also given in Table 17 for each variable is a probability distribution and an associated range.

5.2 SELECTION OF THE VALUES OF THE INPUT VARIABLES USED IN THE ANALYSIS

THE RESPONSE SURFACE REPLACEMENT

For the response surface analysis, a fractional factorial design with two levels (low and high) is utilized for each variable with $k = 10$ and $m = 5$ (following the notation given in Section 2). Thus, 32 computer runs are required. The fractional

factorial plan calls for each level of each variable to be used exactly 16 times in the 32 computer runs. This is the smallest number of runs that could be used and still allow for an estimate of each main effect and the following interactions selected a priori by the model developers as potentially important:

$$\begin{array}{lllll} X_1X_2 & X_1X_8 & X_2X_3 & X_2X_5 & X_2X_6 \\ X_2X_8 & X_2X_{10} & X_3X_8 & X_3X_{10} & X_5X_6 \\ X_5X_7 & X_6X_7 & X_7X_8 & X_8X_9 & X_8X_{10} \end{array} \qquad (5.1)$$

THE LATIN HYPERCUBE SAMPLE

For the portion of the analysis utilizing a Latin hypercube sample, the value of $n = 32$ is used. This corresponds to $n = 3.2k$ (since $k = 10$). This value of n was selected to keep the sample size the same as used with the fractional factorial design. The sample was generated using the restricted pairing technique of Iman and Conover (1982a) to control the correlations between variables within the sample.

The rank correlations among the 10 input variables for this particular LHS with $n = 32$ appear in matrix form in Table 18. To calculate these correlations, the values in each column of the 32 x 10 input matrix are ranked from 1 (smallest) to 32 (largest) and then the usual correlation coefficient is computed on the ranks rather than the original values. The result is a Spearman's rho, a well-known nonparametric measure of correlation as explained in Iman and Conover (1983). This measure is used since it remains meaningful in the presence of nonnormal distributions on the input variables. Examination of the rank correlation matrix in Table 18 shows that 35 of the 45 pairwise entries are $< .05$ in absolute value, 43 of 45 are $< .10$ and the largest element is .1379. However, this latter value is a nonsignificant correlation for $n = 32$. Additionally, there is nothing to prevent the user from generating other LHSs and choosing the one that most nearly fits his or her requirements.

If the off diagonal elements in the matrix in Table 18 were all zero, then the input variables would all be orthogonal and the matrix would be an identity matrix as is the case with the fractional factorial design. However, it is virtually impossible to obtain an exact identity matrix when using LHS. A commonly used measure for detecting large pairwise correlations comes from inverting the correlation matrix and then examining the largest element on the diagonal of the inverted matrix. This element was referred to in Section 3 as the variance inflation factor (VIF). When the correlation matrix is an identity matrix, then its inverse is also an identity matrix, and therefore, the VIF will be equal to its minimum value of 1. As discussed in Marquardt and Snee (1975) when the VIF becomes larger than 1, a measure of unwanted correlation is generated. Another way of obtaining the VIF is by calculating $1/(1-R^2)$, where R^2 is the maximum R^2 one gets by regressing each independent variable on the others. Marquardt and Snee (1975) deal with some very large VIFs ($>2 \times 10^6$) and provide a readable explanation on reasonable sizes for VIFs. Marquardt (1970) indicates that there can be serious collinearity for VIF > 10, which corresponds to a maximum $R^2 > .90$ among the independent variables. There is certainly no problem as long as the VIF is close to 1. For the matrix in Table 18 the VIF is 1.03.

Table 17. Distribution and Range* Used with Each Input Variable to the DNET Model

Variable	Distribution	Range
X_1 : Crack spacing (ft)	Uniform	3 to 20
X_2 : Conductivity of the upper shale (ft/day)	Loguniform	1.1×10^{-7} to .57
X_4 : Conductivity of the upper aquifer (ft/day)	Lognormal	.01 to 50
X_4 : Conductivity of the lower aquifer (ft/day)	Lognormal	.01 to 40
X_5 : Coefficient of thermal expansion of salt (ft/°F)	Normal	10^{-5} to 10^{-4}
X_6 : Coefficient of thermal expansion of shale (ft/°F)	Normal	5×10^{-6} to 1.3×10^{-5}
X_7 : Thermal conductivity of salt (BTU/yr·ft·°F)	Normal	40 to 85
X_8 : Exponent in salt creep law (unitless)	Lognormal	2.5 to 7
X_9 : Maximum width of the sum of the solution channels (ft)	Uniform	1500 to 4500
X_{10}: Salt dissolution rate constant (yr^{-1})	Uniform	100 to 500

* For normal and lognormal distributions, the lower and upper values of the range are interpreted as representing the .001 and .999 quantiles, respectively.

For the variables in Table 17 having uniform and loguniform distributions, the low and high values used in the fractional factorial design correspond to the endpoints of the range, while the .05 and .95 quantiles were used for all other variables.

Table 18. Rank Correlations Among the Input Variables Used in the Latin Hypercube Sample with n = 32.

1	1.0000									
2	-.0411	1.0000								
3	.0352	-.0620	1.0000							
4	-.0257	-.0271	.0007	1.0000						
5	.0341	-.0018	.0176	-.0957	1.0000					
6	.0121	.0279	.1122	.0590	-.0147	1.0000				
7	.0183	-.0792	-.0121	-.0249	-.0550	.0213	1.0000			
8	.0363	.0370	.0469	-.0172	.0337	-.0403	-.0092	1.0000		
9	.0583	.0440	-.0198	-.0011	.0099	-.0389	.0279	.0576	1.0000	
10	.1397	-.0363	.0279	-.0253	.0601	.0814	.0491	-.0216	-.0088	1.0000
	1	2	3	4	5	6	7	8	9	10

5.3 SCATTERPLOTS OF THE INPUT-OUTPUT RELATIONSHIPS AS A GUIDE TO BETTER UNDERSTANDING OF THE MODEL BEHAVIOR

As mentioned in Section 3, scatterplots can be a great aid in determining if the model is working as intended, i.e. does the input-output agree with engineering judgment? Additionally, scatterplots may aid one in identifying the need for transformations (such as logarithmic), or when placed side-by-side, may show how several variables jointly influence the output. The DNET model provided a good illustration of the value of scatterplots as some unexpected model behavior was detected through their use. Side-by-side scatterplots for DNET output appear in Figures 14 to 16 for X_2, X_3, and X_8 at the time steps of 5, 500 and 5000 years, respectively. The left-hand one-third of each of these graphs shows a scatterplot of log X_2 versus log Y; the middle one-third has ln X_3 versus log Y; the right-hand one-third shows ln X_8 versus log Y. The top half of each figure was based on fractional factorial input while the bottom half was based on input selected by Latin hypercube sampling. The three variables X_2, X_3, and X_8 were selected from among the 10 input variables because they appeared as the dominant variables when considered over all time steps. With fractional factorial input, each variable takes on only two values; thus, the plot appears as 16 points (half of the 32 runs) above each of the two values for each variable. In the top portion of Figure 14, the numerals appearing with the graphs indicate the multiplicity of the various points.

Examination of the top half of Figure 14 shows that X_2 is dominant in controlling the value of Y in conjunction with X_3. When the low value of X_2 is present, the output was constant at approximately 10^{-4} regardless of X_3. When the high value of X_2 was used, the output was either 10^5 or 10^7 depending on whether the high value of X_2 was paired with the low value of X_3 or the high

value of X_3, respectively. The side-by-side scatterplots of X_2 and X_3 make this relationship easy to see. Additionally, X_8 has no effect at either its high or low value.

The plot of X_2 versus Y in the bottom half of Figure 14 (5 years) shows an interesting phenomenon. The points appear in two distinct clusters separated by several orders of magnitude on the Y axis. These clusters are determined by large and small values of X_2 which represents the conductivity of a shale layer directly above the bedded salt formation and directly below an aquifer. In a simplified sense, the higher the conductivity of the shale, the greater the water flow through the shale and in turn the greater the dissolution of the salt cavity. Thus, the six points in the cluster at the top of the graph represent "breakthrough" runs. That is, conditions exist on these runs that allow the salt cavity to undergo rapid dissolution and thereby creating a discontinuity in the output. The LHS plot of X_3 versus Y in Figure 14 shows that when a "breakthrough" occurs, the rate of dissolution is controlled by X_3, the conductivity of the aquifer directly above the shale layer. Further, Figure 14 indicates that X_8 has little or no effect on dissolution regardless of whether or not a breakthrough occurs.

In Figure 15 (500 years) X_2 is still the dominant variable in determining if a breakthrough occurs, but none of the three variables seems to have much influence on determining the rate of dissolution for those cases in which a breakthrough fails to occur. However, both X_2 and X_3 are influencing the dissolution rate in those cases where a breakthrough occurs. Figure 16 (5000 years) shows some interesting results. The variable, X_2 is still dominant in determining if a breakthrough occurs. When a breakthrough occurs, X_3 is the dominant variable while X_8 (the creep law exponent) is dominant when a breakthrough does not occur.

The scatterplots in Figures 14 to 16 make it readily apparent that the occurrence or nonoccurrence of a breakthrough has a direct bearing on any regression based analysis whose purpose is to determine the relative importance and contribution of the input variables. For example, a straight line or even a quadratic fit to the points in the LHS plot of X_2 versus Y in Figure 14 will be less than satisfactory. This is true because while the lower cluster (no breakthrough) of the graph can be fit nicely by a quadratic in X_2 the upper cluster (breakthrough) shows no relationship to X_2. Rather, the behavior of the upper portion seems to be dominated by X_3.

While the results of the two sets of scatterplots corresponding to the two approaches give good general agreement, it is impossible for plots based on two fixed levels to show the true pattern of the input-output relationship for this model. That is, one must assume that the output behaves in a linear fashion between the high and low values of X_2 with the exact placement of the linear relationship being dependent upon the value of X_3. The discontinuity present in the LHS portion of Figure 14 cannot be discovered in the fractional factorial portion of Figure 14 nor can the nonlinear relationship between X_2 and Y for about 80% of the range of X_2. This is a price that must be paid for the simplifying assumptions that go along with the use of two levels for each variable. At this point, one might consider a modification of the fractional factorial design to include points other than those found at the two levels. For instance, a central composite design would use $2k + 1$ additional points with one point being in the center for each variable and $2k$ axial points. Details of such designs can be found in Myers (1971). For the

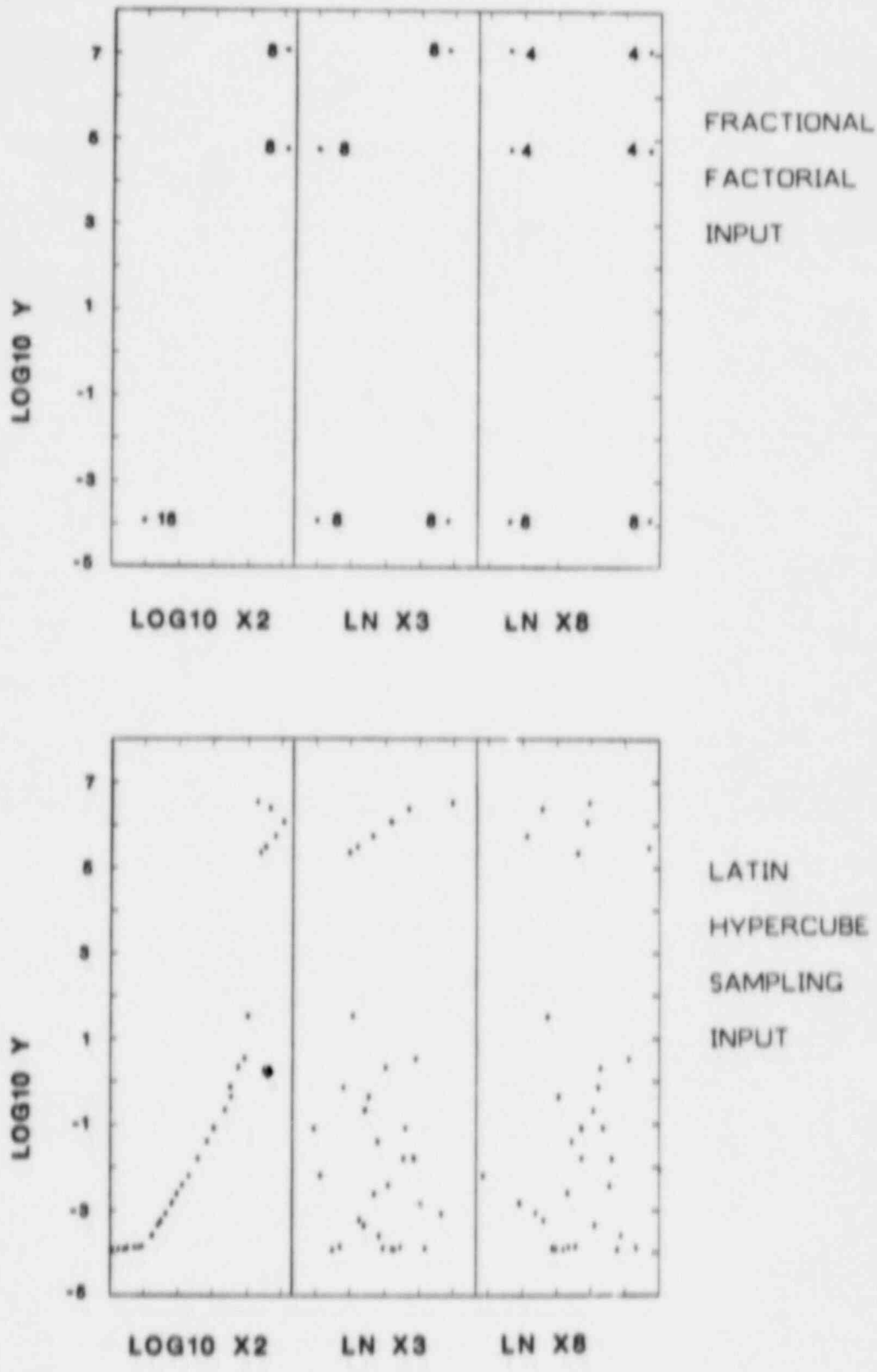

Figure 14. Scatterplots of log X_2, ln X_3, and ln X_8 versus log Y at 5 years.

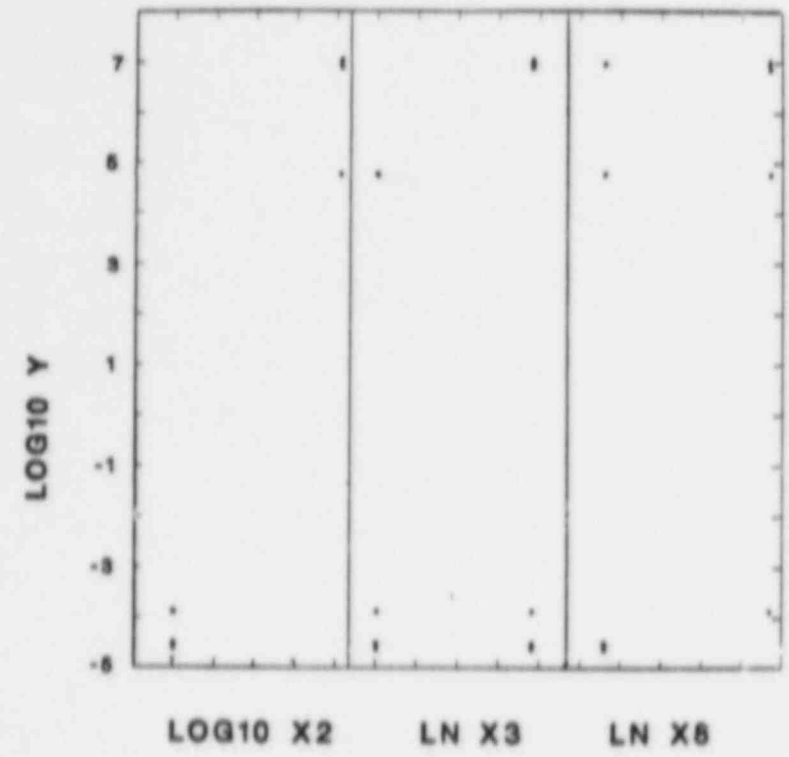

FRACTIONAL FACTORIAL INPUT

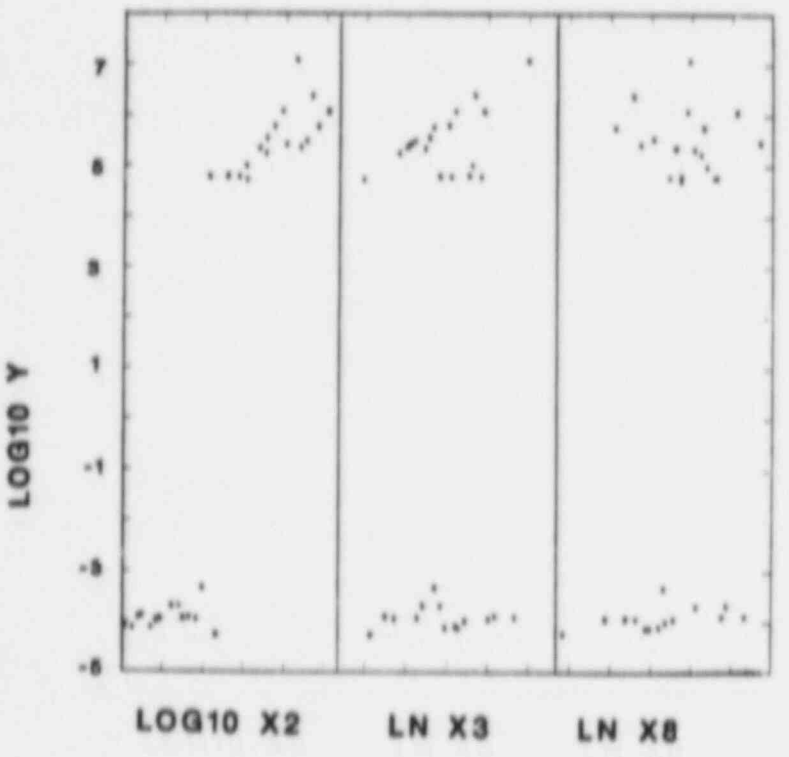

LATIN HYPERCUBE SAMPLING INPUT

Figure 15. Scatterplots of log X_2, ln X_3, and ln X_8 versus log Y at 500 years.

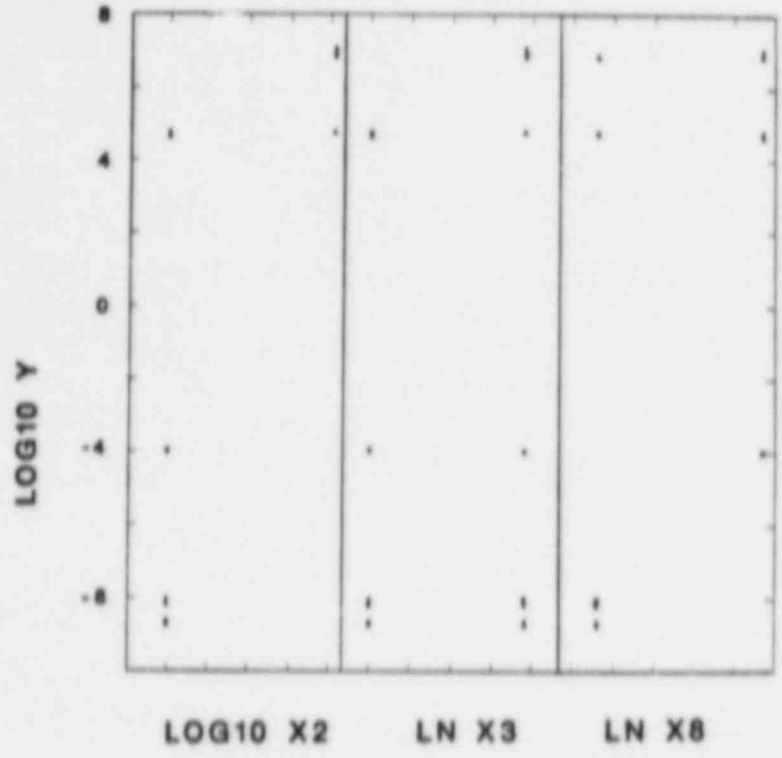

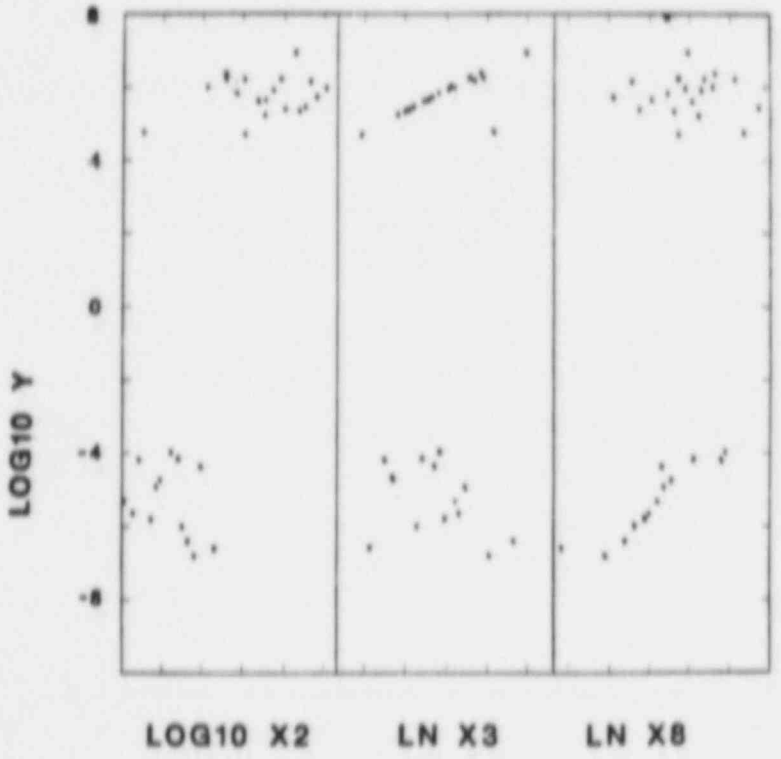

Figure 16. Scatterplots of log X_2, ln X_3, and ln X_8 versus log Y at 5000 years.

present analysis, an additional 21 computer runs would be needed. However, there would still be no guarantee that the information available in the lower half of Figures 14 to 16 would become apparent, whereas the LHS approach would have revealed the same information with fewer than 32 runs.

5.4 UNCERTAINTY ANALYSIS FOR THE DNET MODEL

ESTIMATION OF THE DISTRIBUTION FUNCTION OF THE OUTPUT

Response surfaces for the fractional factorial design were fit as indicated in (2.1) at each of the time steps and then evaluated 100 times based on random sampling from the probability distributions given in Table 17. The resulting estimated cdfs for 5 years and 500 years appear in Figure 17 with the label "RS." For ease in making comparisons, the LHS results also appear (with the label "LHS") in Figure 17. There are actually two cdf estimates based on LHS appearing within both portions of Figure 17. One is based on 32 runs and the other is based on 100 runs. The close agreement of the LHS estimates within each figure provides an indication of the precision associated with estimates arising from LHS.

Figure 17 shows that the LHS estimates of the output cdf disagree sharply with the response surface estimate obtained from using the fractional factorial input. In fact, most quantile estimates disagree by one or more orders of magnitude. The reason for this disagreement is that the phenomenon of a "breakthrough" and the corresponding discontinuity in the output mentioned earlier in the discussion of the scatterplots has gone undetected by the analysis of the input-output relationships based on the fractional factorial approach. That is, from the top half of Figures 14 through 16 it can be seen that the low and high values of the output differ by several orders of magnitude over the range of X_2. But what of the behavior of the output for intermediate values of X_2? The bottom half of Figures 14 through 17 as well as the LHS portion of Figure 18 make it clear that a discontinuity occurs in the output. This discontinuity is missed by the fractional factorial approach since a linear relationship must be assumed between the two levels used with each input variable. More complex response surfaces could be estimated, but only at increased computer costs, and even then it is likely that such surfaces would fail to accurately depict the discontinuity. This example identifies an underlying problem with the response surface approach, which is that the DNET computer model is too complex mathematically to be adequately represented by a simple response surface.

ESTIMATION FOR THE OUTPUT VARIABLE

At this point in the analysis in each of the previous two sections, the estimation of population parameters for the output variable has been considered. However, the cdf estimates in the previous subsection point out the potential for problems associated with estimating and interpreting population parameters. For example, the response surface fit from the fractional factorial design produced a less than satisfactory estimate of the output cdf in Figure 17. Hence, the associated estimates of location and scale may or may not be accurate, but more importantly these population characteristics may not have any real meaning in this problem. To explain further, consider the graph in Figure 17 corresponding to 500 years. What meaning should be attached to an overall measure of either location or scale here?

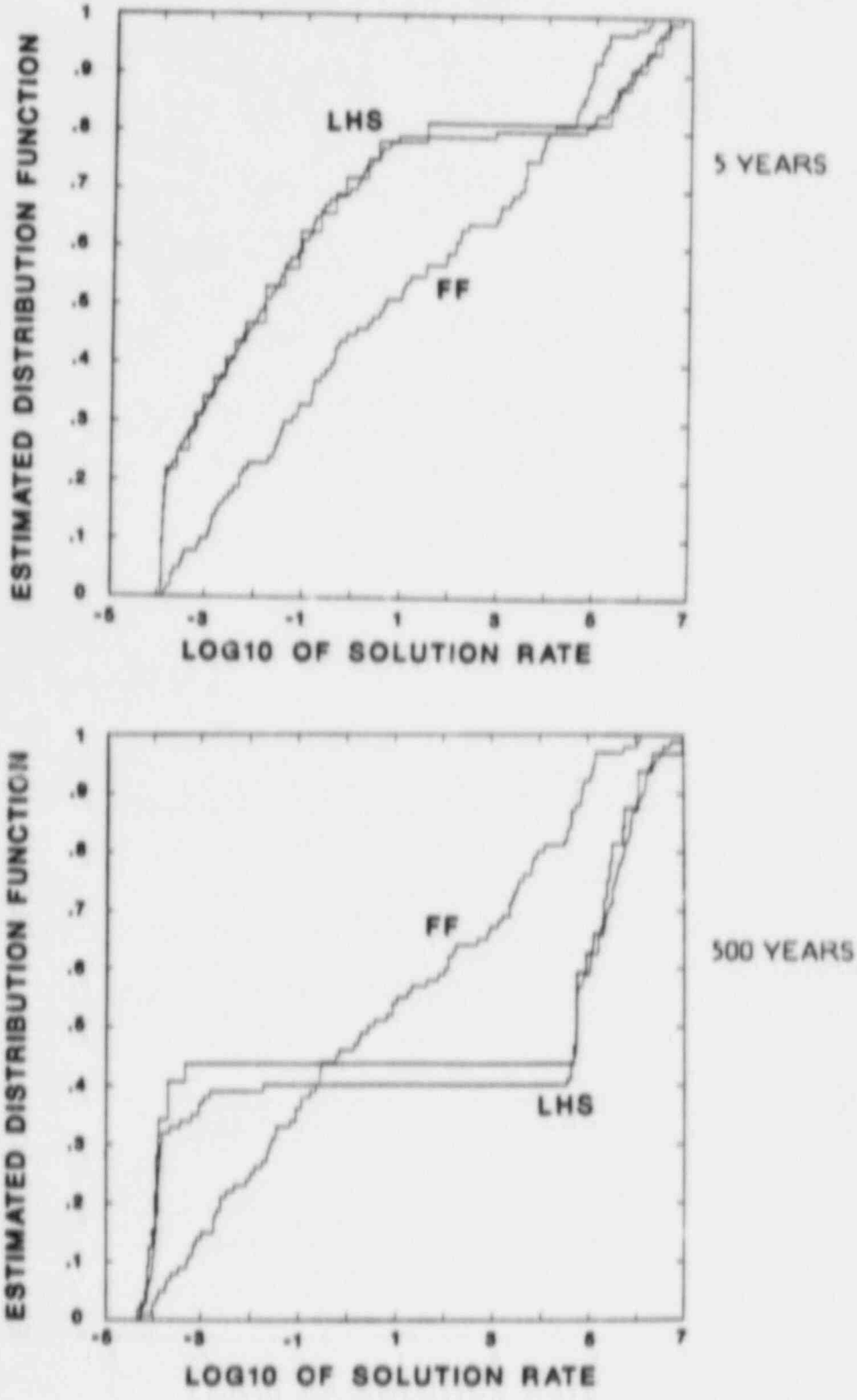

Figure 17. Response Surface and LHS Estimates of the CDF for log Y.

Certainly, the overall estimate of the variance of Y will be too large to be applied individually to either of the two groups of Y values based on the occurrence or nonoccurrence of a "breakthrough." Likewise, an overall measure of location will be too small to represent the large values of Y and too large to represent the small values of Y. More useful estimates would be made conditional on the occurrence or nonoccurrence of a "breakthrough." That is, one could estimate the location and scale for those cases where a "breakthrough" occurs and obtain separate estimates for those cases where a "breakthrough" fails to occur.

5.5 SENSITIVITY ANALYSIS FOR THE DNET MODEL

It is important to keep in mind that the discontinuity in the output was not anticipated a priori. In fact, the existence of a discontinuity was not clearly identified until the scatterplots were made. The impact of the discontinuity on the estimation of the output cdf and in the estimation of population parameters has already been observed. The presence of the discontinuity also impacts the sensitivity analysis.

The scatterplots in Figures 14 - 16 indicate that X_2 plays an important role in determining if a breakthrough occurs. Additionally, the scatterplots indicate that the variables that are important, given a breakthrough, are not necessarily the same variables that are important when a breakthrough does not occur. Therefore, since the occurrence or nonoccurrence of a breakthrough has such an influence on the results, it seems reasonable as a first step in a sensitivity analysis to direct efforts toward determining which variables influence "time to breakthrough" rather than concentrating efforts on "rate of dissolution" at each of 20 different time steps. As a second step, it would then seem reasonable to direct sensitivity analysis efforts toward the breakthrough and nonbreak through cases separately. In order to conserve space, these analyses are not presented.

5.6 SECTION SUMMARY

The DNET model was used for comparisons in this section. DNET models dissolution in bedded salt formations and has a feedback mechanism that governs the selection of different submodels for treating various processes. Because of the complexity involved in treating these processes, the governing equations are not solved in an implicitly coupled fashion (i.e., simultaneously), which makes it difficult to implement a differential analysis. Hence, a differential analysis was not performed for the DNET model. For the analyses with LHS and a fractional factorial design, 10 independent variables were considered as input to the model. The model produces nonlinear time-dependent output as a function of each of these input variables, but not known prior to the analysis was the existence of a discontinuity in the output. Some flexibility is required in the analysis to detect the discontinuity after the computer runs are made, as well as to perform meaningful uncertainty and sensitivity analyses on the basis of the runs.

UNCERTAINTY ANALYSIS

The importance of scatterplots for display of input-output relationships as a guide to better understanding of model behavior was mentioned in Section 3, but such plots were not presented until the present section. Their appearance in this section illustrates their usefulness. The side-by-side scatterplots in Figures 14-16 show how three input variables act jointly to affect the output at different points in time. One set of scatterplots is based on 32 computer runs associated with a fractional factorial design and the second set is based on 32 runs associated with LHS. Both sets of plots show that X_3 affects the output conditional on the value of X_2. Additionally, the LHS scatterplot shows a jump of about four orders of magnitude in the output for large values of X_2, but the fractional factorial scatterplot does not reveal this jump. In fact, it is not clear from the fractional factorial scatterplot what happens to the output for intermediate values of X_2. If center points for both X_2 and X_3 are added to the basic fractional factorial design the output would appear to be nonlinear in form, but the jump or discontinuity would still not be apparent. It can only be detected by stratifying the input values across the entire range of X_2.

The discontinuity in the output impacts the entire analysis and can give rise to misleading results if its presence is not detected. For example, the indirect estimate of the cdf in Figure 17 arising from Monte Carlo simulation with the response surface fit gives no indication of problems with discontinuities. Hence, virtually all quantile estimates will be off considerably, as can be seen from the two LHS direct estimates ($n = 32$ and $n = 100$) in Figure 17, which both clearly indicate the presence of the jump in the distribution function. The jump in the output cdf also indicates that an overall estimate of the variance of the output will have little or no meaning; rather, conditional estimates should be made.

SENSITIVITY ANALYSIS

The sensitivity analysis discussion presented in this section did not go into detail comparing various methods of ranking variables as was the case in the previous two sections; rather, the more important issue of the impact of the discontinuity on the analysis was considered. The reason for this is that if the discontinuity is not detected, or ignored if detected, then sensitivity analysis to determine which variables influence the rate of dissolution will most likely not produce meaningful results.

For a sensitivity analysis to provide meaningful results in a situation such as exists with the DNET model, it is probably best to proceed in two stages. The first stage should be concerned with the determination of the variables that influence the occurrence or nonoccurrence of a breakthrough which causes the discontinuity. Such results will provide guidance to the analysis. The second stage would be to perform sensitivity analysis on the breakthrough and nonbreakthrough cases separately, using methods such as have been discussed in the previous sections.

6. ADDITIONAL TECHNIQUES

The purpose of this section is to introduce several additional techniques that have been proposed for uncertainty and senstivity analysis. The adjoint and Green's function techniques are actually methods for use with differential analysis to increase the numerical efficiency with which the necessary partial derivatives can be calculated. The Fourier amplitude sensitivity test is a method which uses techniques from Fourier analysis to simplify direct calculations of expected values and variances.

6.1 ADJOINT TECHNIQUES

As was indicated in Section 4, the repetitive solution of the system of equations in (2.8) and (2.10) can become quite burdensome when a differential sensitivity analysis is performed. An area of active recent investigation is the use of adjoint techniques to reduce the computational requirements associated with differential analysis (e.g., Koda, Dogru, and Seinfield, 1979; Cacuci et al., 1980; Cacuci, 1981a and 1981b; Piepho, Cady, and Kenton, 1981; Hall, Cacuci, and Shlesinger, 1982; Cacuci, Maudlin, and Parks, 1983). Further, additional background can be obtained in various reviews (e.g., Stacey, 1974; Greenspan, 1976; Weisbin, Lewins, and Becker , 1982).

Although a careful discussion of adjoint sensitivity analysis techniques is beyond the scope of this paper, a brief discussion of how such an analysis might be implemented for the MAEROS model will be given. As previously indicated, the model is a system of nonlinear differential equations of the form

$$dY_j(\underset{\sim}{X},t)/dt = f_j[\underset{\sim}{Y}(\underset{\sim}{X},t),\underset{\sim}{X},t] \tag{6.1}$$

with the initial value condition $Y_j(0) = Y_{0j}(\underset{\sim}{X})$ for $j = 1,\ldots,p$. Suppose the dependent variable of interest is defined by

$$I(\underset{\sim}{Y},\underset{\sim}{X},t_F) = \int_0^{t_F} L[\underset{\sim}{Y}(\underset{\sim}{X},t),\underset{\sim}{X},t]\,dt \quad . \tag{6.2}$$

For example, this equation might define an integrated concentration or deposition. It is desired to determine $\partial I/\partial X_i$ for each independent variable X_i. This can be accomplished by introducing and solving the following system of adjoint equations:

$$dY_j^*/dt = \frac{\partial L[\underset{\sim}{Y}(\underset{\sim}{X},t),\underset{\sim}{X},t]}{\partial Y_j} - \sum_{k=1}^{p} \frac{\partial f_j[\underset{\sim}{Y}(\underset{\sim}{X},t),\underset{\sim}{X},t]}{\partial Y_k} Y_k^*$$

$$Y_j^*(t_F) = 0 \tag{6.3}$$

for $j = 1,\ldots,p$. Once the system in (6.3) is solved, each of the desired partial derivatives can be obtained from the relationship

$$\frac{\partial I(\underset{\sim}{Y},\underset{\sim}{X},t_F)}{\partial X_i} = \int_0^{t_F} \frac{\partial L[\underset{\sim}{Y},\underset{\sim}{X},t]}{\partial X_i} dt + \sum_{k=1}^{p} \frac{\partial Y_{0k}(\underset{\sim}{X})}{\partial X_i} \overset{*}{Y}_{0k}(0)$$

$$+ \int_0^{t_F} \sum_{k=1}^{p} \overset{*}{Y}_k(t) \frac{\partial f_k(\underset{\sim}{Y},\underset{\sim}{X},t)}{\partial X_i} dt \qquad (6.4)$$

for $i = 1, 2,\ldots$.

The appeal of the adjoint method lies in the fact that it is only necessary to solve the original equations in (6.1) once and the adjoint equations in (6.3) once. Then, all the desired partial derivatives follow from repetitively performing the less demanding integrations in (6.4). This has the potential to require significantly less computation than repetitively solving the combined system appearing in (2.8) and (2.10). At the outset of this project, our intent was to perform the MAEROS differential analysis with the indicated adjoint techniques. However, it was ultimately decided not to use adjoint techniques for reasons outlined in the next paragraph.

In the performance of an adjoint analysis, the system of equations in (6.1) is solved forward in time from $t = 0$ to $t = t_F$, while the system in (6.3) is solved backward in time from $t = t_F$ to $t = 0$. As the backward solution to (6.3) requires the solution to (6.1), it is necessary to record the solution to (6.1) at selected points in time and to use some type of interpolation procedure in the incorporation of these values into the solution to (6.3). The integrals in (6.4) require the solutions to the systems of equations in (6.1) and (6.3). Thus, it is also necessary to record the solution to (6.3) at selected points in time and to use some type of interpolation procedure in the incorporation of the solutions to (6.1) and (6.3) into the integrals appearing in (6.4). Both the expressions in (6.3) and (6.4) involve partial derivatives, at least some of which must be determined numerically. Finally, the integrals in (6.4) must be evaluated numerically.

Two points emerge from the preceding discussion. First, an adjoint analysis of the MAEROS model is difficult to implement numerically. Due to the successive combining of numerical approximations, it is hard to know and control computational errors. Second, due to the different procedures which must be combined, a large effort is required to develop the software required to run the analysis. The two preceding considerations lead to the decision that it would be better to solve the systems in (2.8) and (2.10) repetitively than it would be to perform an adjoint analysis.

Adjoint analyses are easier to perform for algebraic systems than for differential systems such as the one just discussed. Of course, all differential systems are ultimately implemented as an algebraic system in a computer program.

However, the complexity of the problem and the associated computer program may prevent convenient use of these algebraic equations. A new FORTRAN compiler recently developed at Oak Ridge National Laboratory makes use of the ultimately algebraic structure of models and develops the required partial derivatives needed in an adjoint analysis of the underlying algebraic model associated with a computer program (Oblow, 1983a and 1983b). Although we have not had a chance to work with this program, it is possible that its use could significantly reduce the effort associated with implementing adjoint analyses for certain models.

6.2 GREEN'S FUNCTION TECHNIQUES

Another approach to reducing the computation associated with solving the systems in (2.8) and (2.10) is based on Green's function. As with adjoint techniques, this method is an area of active recent investigation (e.g., Hwang et al., 1978; Dougherty, Hwang, and Rabitz, 1979; Demiralp and Rabitz, 1981a and 1981b; Dacol and Rabitz, 1983). Differential sensitivity analysis revolves around the need to solve the system appearing in (2.10). In matrix notation, this system can be written as

$$d[\partial \underset{\sim}{Y}/\partial X_i]/dt = \partial \underset{\sim}{f}/\partial X_i + \underset{\sim}{J}\, \partial \underset{\sim}{Y}/\partial X_i$$

$$\partial Y(0)/\partial X_i = \partial Y_0(\underset{\sim}{X})/\partial X_i \,, \tag{6.5}$$

where $\underset{\sim}{Y} = (Y_1,\ldots,Y_p)$, $\underset{\sim}{f} = (f_1,\ldots,f_p)$ and $\underset{\sim}{J}$ is the Jacobian matrix for $\underset{\sim}{f}$ with respect to $\underset{\sim}{Y}$. The system in (6.5) must be solved for each X_i. However, it is only the initial-value $\partial \underset{\sim}{Y}(0)/\partial X_i$ and the forcing function $\partial \underset{\sim}{f}/\partial X_i$ that changes from system to system; the Jacobian matrix $\underset{\sim}{J}$ remains the same for all systems. The Green's function technique is based on the separation of the solution of (6.5) into the part that depends on X_i and the part that depends on $\underset{\sim}{J}$. Specifically, the solution to (6.5) can be expressed as

$$\partial \underset{\sim}{Y}(t)/\partial X_i = \underset{\sim}{K}(t,0)[\partial \underset{\sim}{Y}(0)/\partial X_i] + \int_0^t \underset{\sim}{K}(t,\tau)[\partial \underset{\sim}{f}/\partial X_i]d\tau \,, \tag{6.6}$$

where $\underset{\sim}{K}(t,\tau)$is the Green's function defined by

$$\underset{\sim}{K}(\tau,\tau) = \underset{\sim}{I},\ d\underset{\sim}{K}(t,\tau)/dt = \underset{\sim}{J}\underset{\sim}{K}(t,\tau) \text{ for } t \geq \tau \,. \tag{6.7}$$

Use of (6.6) results in the desired separation of the calculation of $\partial \underset{\sim}{Y}/\partial X_i$ into parts dependent on X_i and parts independent of X_i. The Green's function defined in (6.7) can be approximated once and this approximation can then be used repeatedly in the calculation of the desired partial derivatives.

Although use of Green's function techniques may result in a reduction of the computational effort required to repeatedly solve the systems in (2.8) and (2.10), a significant programming effort is still required to implement the method. First, the original system of model equations must be solved. Second, this solution must be used to solve the system in (6.7) that defines the Green's function. Finally, the approximated Green's function must be used repeatedly in the development of approximations to the expressions in (6.6). As with the adjoint techniques, attempts are being made to develop software which will facilitate implementation of Green's function techniques (Kramer et al., 1982). As a careful examination of their development would reveal, adjoint and Green's function techniques are very closely related.

6.3 FOURIER AMPLITUDE SENSITIVITY TEST

The Fourier amplitude sensitivity test (FAST) is another procedure that has been developed for uncertainty and sensitivity analysis (Cukier et al., 1973; Shaibly and Shuler, 1973; Cukier et al., 1975; Cukier et al., 1978). This procedure provides a way to estimate the expected value and variance of a dependent variable and the contribution of individual independent variables to this variance.

As before, suppose $\underset{\sim}{Y} = (Y_1,...,Y_p)$ is a function of $\underset{\sim}{X} = (X_1,...,X_k)$. Further, suppose $X_1,...,X_k$ are random variables described by a probability density function $P(X_1,...,X_k)$ defined on Ω. Then,

$$E(Y_j) = \int_{\Omega} Y_j(\underset{\sim}{X})P(\underset{\sim}{X})d\underset{\sim}{X} \tag{6.8}$$

for $j = 1,...,p$. The central idea of the FAST method is to convert the k-dimensional integral in (6.8) into a one-dimensional integral in s by using the transformation $X_q = G_q(\sin \omega_q s)$ for $q = 1,...,k$. For properly chosen ω_q and G_q,

$$E(Y_j) = \frac{1}{2\pi} \int_{-\pi}^{\pi} Y_j [G_1(\sin \omega_1 s),...,G_k(\sin \omega_k s)] \, ds \ . \tag{6.9}$$

Further, by use of properties of Fourier series,

$$V(Y_j) = \frac{1}{2\pi} \int_{-\pi}^{\pi} Y_j^{\,2} [G_1(\sin \omega_1 s),...,G_k(\sin \omega_k s)] \, ds - E^{\,2}(Y_j)$$

$$= \sum_{i=-\infty}^{\infty} \left(A_i^2 + B_i^2\right) - \left(A_0^2 + B_0^2\right)$$

$$= 2 \sum_{i=1}^{\infty} \left(A_i^2 + B_i^2\right), \tag{6.10}$$

where

$$A_i = \frac{1}{2\pi} \int_{-\pi}^{\pi} Y_j(s) \cos(is)\, ds \tag{6.11}$$

and

$$B_i = \frac{1}{2\pi} \int_{-\pi}^{\pi} Y_j(s) \sin(is)\, ds \ . \tag{6.12}$$

The expressions in (6.9) and (6.10) provide a means to estimate the expected value and variance associated with Y_j. Further, provided the ω_q are integers, the contribution to variance by X_q can be approximated by

$$V_q(Y_j) = 2 \sum_{i=1}^{\infty} \left(A_{i\omega_q}^2 + B_{i\omega_q}^2\right). \tag{6.13}$$

Thus, the ratios $V_q(Y_j)/V(Y_j)$ provide a means to rank individual variable importance on the basis of contribution to variance.

Application of the FAST method involves defining the ω_q and G_q, evaluating the original model at a sufficient number of points to allow numerical evaluation of the integrals in (6.11) and (6.12), and approximation of the sums in (6.10) and (6.13). Applications involving this technique are given by Falls et al. (1979), Koda et al. (1979), Pierce and Cukier (1981), McRae et al. (1981), and Tilden and Seinfeld (1982).

7. SUMMARY AND CONCLUSIONS

7.1 TECHNIQUES AND MODELS USED IN COMPARISONS

Uncertainty analysis and sensitivity analysis are important elements in the development and implementation of computer models for complex processes. Many different techniques have been proposed for performing uncertainty and sensitivity analyses, and published comparisons have been made of some techniques. It is our observation that such comparisons are often made on unrealistic and artificially simple models. For example, one might see a small number of independent input variables used with a simple function. This approach has merit in allowing comparisons against known answers but fails to show the extendibility of the techniques to complex problems. The main aim of this study was to compare several widely used techniques on three models having large uncertainties and varying degrees of complexity in order to highlight some of the problem areas that must be addressed in actual applications.

We are aware that results presented in a study such as this will not satisfy everyone. For example, questions will arise as to the choice of techniques used in the comparisons. We feel that there is adequate justification for the techniques featured in the comparisons, but more importantly, given the documentation on the input and models, it should be possible for other investigators to make comparisons of additional techniques with the results in this study.

Three techniques for performing uncertainty analysis and sensitivity analysis are used in the comparisons made in this paper. These techniques are (1) response surface replacement for the computer model, (2) Modified Monte Carlo as exemplified by Latin hypercube sampling with and without regression analysis, and (3) differential analysis.

Three computer models were used in the comparison of the techniques.

- Pathways - models the environmental movement of radionuclides; consists of a system of four linear, constant coefficient differential equations; requires 20 independent input variables; produces multivariate nonlinear output.

- MAEROS - models multicomponent aerosol dynamics; consists of a system of nonlinear differential equations; requires 21 input variables, eight of which are correlated; produces multivariate time dependent nonlinear output.

- DNET - models dissolution in bedded salt formations; has a feedback mechanism that governs the selection of different submodels; requires 10 independent input variables; produces time-dependent multivariate nonlinear output which is discontinuous with respect to one of the input variables.

The preceding descriptions pertain to the models as used in this comparison. Each of the models is quite general and can be used in configurations that are different from the ones considered here.

7.2. GENERAL SUMMARY OF THE TECHNIQUES

A brief summary of each technique is given in this subsection. This summary is followed in the next subsection by another summary in which the techniques are gauged by particular criteria.

RESPONSE SURFACE REPLACEMENT USING FRACTIONAL FACTORIAL DESIGNS

Fractional factorial designs (FFD) have a proven record of performance and are well documented in the statistical literature. They have provided good results in many experimental situations. They, along with more complex experimental designs, have also been widely used in the construction of response surfaces and are near an optimal choice for input selection if the output behaves in a linear fashion. Even if the output behaves in a nonlinear fashion, the FFD can sometimes be modified to give reasonable results by including center points. The problem in using a FFD to produce a response surface replacement for a computer model of the type considered in this paper lies not so much in the choice of the design but rather in the concept of trying to replace the model with a response surface. Generally speaking, the models are too complex mathematically to be adequately approximated with a response surface. Since indirect estimates of the output cdf(s), the variance of the output variable(s), and variable ranking by contribution to variance are derived from the response surface when using input from a FFD, an inadequate response surface can generate misleading uncertainty analysis and sensitivity analysis results.

The FFD response surface approach provided both good and poor estimates of the output cdfs for the simple Pathways model, but did provide a reliable ranking of the input variables. However, in evaluating rankings for the Pathways model, it should be kept in mind that one input variable tended to dominate each output variable. The response surface approach was not used with the MAEROS model due to the complexity of the multivariate input structure. The response surface approach provided an unreliable estimate of the output cdf with the DNET model largely because the discontinuity in the output went undetected.

DIFFERENTIAL ANALYSIS AND LOCAL BEHAVIOR

A differential analysis is intended to provide information with respect to small perturbations about a point. Excellent information is provided about variable behavior and influence about this point and such information is quite useful in a variety of applications. Problems arise, however, in an uncertainty analysis or in a sensitivity analysis when large uncertainties are present and attempts are made to extend the results from the small perturbations in the input variables, for which the differential analysis is intended, to a broader or global interpretation. For example, estimates of the cdf and variance can be obtained indirectly by using a Monte Carlo simulation with the Taylor series expansion about a basecase point. The results may or may not be sensitive to the choice of this basecase point.

The differential analysis was relatively easy to implement with the Pathways model and a Monte Carlo simulation of the Taylor series expansion about the basecase point produced a cdf in good agreement with the unbiased estimate as shown in Figure 3. However, as illustrated in Figure 4, other choices of basecase

values gave widely varying results. The input variable ranking proved to be in good agreement with the other techniques, but as was mentioned previously, one input variable tended to dominate each output variable. The implementation of the differential analysis with the MAEROS model proved to be another matter entirely. It was extremely difficult and time consuming to do, requiring about six man-months of effort. Moreover, even though the cdf estimates shown in Figures 9-11 all utilized a Taylor series expansion about the same basecase point, the results ranged from reasonably good to poor for three different output variables. The variable rankings shown in Table 14 agreed quite well throughout with the other rankings in the table, but the same was not true in Table 15 where more disparity occurred among the rankings. Due to the complexity of the feedback mechanism governing the selection of different submodels, a differential analysis was not performed with the DNET Model.

LATIN HYPERCUBE SAMPLING

The implementation of LHS is similar to that of simple random sampling and both have a probabilistic basis. In fact, for large sample sizes there is little difference between the two techniques. However, the original intent of LHS was to make more efficient use of computer runs than random sampling for smaller sample sizes. If the output is a monotone function of the input, then LHS has been shown by Iman and Conover (1980) to be more efficient than simple random sampling (i.e., LHS provides a smaller variance for the estimator). If monotonicity is not satisfied, then LHS may or may not be more efficient than simple random sampling. Since LHS has a probabilistic basis, it can provide direct estimates for the cdf and variance. When random pairing is used with LHS, the estimate of the cdf is unbiased while the variance estimate has a small, bounded, but unknown bias. When LHS is used in conjunction with the pairing technique of Iman and Conover (1982a), correlated multivariate structures for the input variables can be input to the computer model in the proper form; something that cannot be done with random pairing in the LHS. However, the property of unbiasedness no longer applies. It is felt that the amount of bias is negligible for the type of problems considered in this study.

LHS was used with all three computer models and produced good estimates of the cdf throughout as measured by comparisons with results from large random samples. For example, for both the Pathways model and the MAEROS model, the LHS estimates with n=50 showed good agreement with random sample estimates with n=100. In the case of the DNET model, the LHS estimate with n=32 was compared against a LHS with n=100 in order to illustrate the small variability associated with LHS estimates. The presence of a discontinuity in the output from DNET was clearly identifiable from the LHS cdf estimate, illustrating the usefulness of LHS in mapping the input space to the output space. The LHS was used with all four methods of ranking indicated in Sections 3 and 4.

7.3 SUMMARY OF TECHNIQUES ACCORDING TO SPECIFIC CRITERIA

There are several specific criteria that are of interest when comparing different techniques for uncertainty and sensitivity analysis. Several such criteria are listed in this subsection along with comments with respect to each of the techniques considered in this study.

EASE OF IMPLEMENTATION

RS - If the number of input variables is small and the variables are independent of one another, then the selection of input values is straightforward with a fractional factorial design. If the variables are not independent, then the design may create pairs of variables that are physically impossible or meaningless. When the number of input variables is large, the development of a suitable design can be difficult. The fitting of the accompanying response surface frequently requires some artistry.

DA - Setup can be very simple, or very difficult, or impossible. Results can vary greatly depending on the choice of a basecase for Taylor series expansion. Monte Carlo simulation of the Taylor series expansion to get cdf estimates and evaluation of the expansion to get variance estimate are both straightforward.

LHS - Setup with either simple or complex multivariate input structures is easy. Output can be processed directly for estimates of the cdf and variance without the need for fitting a response surface. However, the estimate of the variance has a small, but unknown, bias.

FLEXIBILITY

RS - Scatterplots from FFD input provide somewhat limited information. Input values from FFD are orthogonal and as such are not designed to handle correlated input. It is difficult to implement a FFD with a large number of input variables. The input space with a FFD can be under-represented and important points can be missed.

DA - There are scatterplots available A single input point is not affected by correlation in the input variables as long as restrictions among the variables are satisfied. This approach will handle a large number of input variables.

LHS - Scatterplots based on LHS input provide useful information. LHS has the ability to handle correlated input as well as a large number of input variables. The input space is well represented.

ESTIMATION OF THE OUTPUT CDF

RS - The estimate is obtained by using a Monte Carlo simulation with the response surface fit. This indirect estimate can be either good or bad and is dependent on the quality of the fitted response surface.

DA - The indirect estimate is obtained by using a Monte Carlo simulation with a Taylor series expansion about a basecase point. This estimate can vary greatly with the choice of a basecase. Also, the local nature of a Taylor series expansion makes this estimate questionable.

LHS - The cdf estimate is obtained directly from the model output. Further, this estimate has a small associated variance and little, if any, bias.

ADAPTABILITY TO DIFFERENT METHODS OF SENSITIVITY ANALYSIS

RS - All methods of ranking input variables explained in Section 3 can be used. The usefulness of the PRCC is inhibited somewhat by the limited number of fixed points used with each input variable for FFD input.

DA - The PRCC cannot be used. The other three methods of ranking variables as explained in Section 3 are obtained from the Taylor series expansion about the basecase point. The rankings obtained provide local information but do not always extrapolate well to a global interpretation.

LHS - All methods of ranking input variables as explained in Section 3 can be used.

7.4 EXTENSION OF TECHNIQUES TO A SYSTEM ANALYSIS

The input variables have been treated as representing properties associated with a computer model that may itself be only a component in a system of many such models. Such systems are likely to be composed of many different models, some of which will far exceed the complexity of the models considered in this study. For example, the MELCOR program mentioned in the Introduction is one such complex system. Furthermore, it is likely that it will be necessary to apply uncertainty analysis and sensitivity analysis to the entire system. For such applications, the role of some of the input variables will need to change as mentioned in the Introduction, to perhaps represent branch points in the evolution of a process or perhaps different submodels within a larger model. In such case the analysis could be used to identify those models or events that have a significant impact on the system, and in turn may contribute significantly to the uncertainty. Such methodology development is the subject of current research at Sandia National Laboratories, but will build on techniques discussed in this study, in particular, the techniques based on Latin hypercube sampling. One such analysis where LHS has been used in a system analysis is associated with the geologic isolation of radioactive waste as reported in Cranwell et al. (1982).

REFERENCES

Atherton, R. W., Schainker, R. B., and Ducot, E. R. (1975). "On the Statistical Analysis of Models for Chemical Kinetics," AICHE Journal, 21, 441-448.

Barhen, J., Cacuci, D. G., Wagichal, J. J., Bjerhe, M. A. and Mullins, C. B. (1982). "Uncertainty Analysis of Time-Dependent Nonlinear Systems: Theory and Application to Transient Thermal Hydraulics," Nuclear Science Engineering, 81, 23-44.

Baybutt, P., Cox, D. C. and Kurth, R. E. (1982). "Method for Uncertainty Analysis of Large Computer Codes, with Application to Light-Water Reactor Melt-down Accident Consequence Evaluation." Submitted for publication.

Beckman, R. J. and Whiteman, D. N. (1983). "Uncertainty Analysis: Good News and Bad News." Paper presented at the Statistics Symposium on National Energy Issues, October, Rockville, Maryland.

Bishop, T. A. (1983). "The Use of Sensitivity Analysis in Experimental Planning and Design." Paper presented at the 1983 Annual Meeting of the American Statistical Association, Toronto, Canada.

Box, G. E. P. and Behnken, D. W. (1960). "Some New Three Level Designs for the Study of Quantitative Variables," Technometrics, 2, 455-75.

Box, G. E. P. and Draper, N. R. (1959). "A Basis for the Selection of a Response Surface Design," Journal of the American Statistical Association, 54, 622-54.

Box, G. E. P., Hunter, W. G. and Hunter, J. S. (1978). Statistics for Experimenters, An Introduction to Design, Data Analysis, and Model Building, John Wiley and Son, Inc., New York.

Brown, J. B. and Helton, J. C. (1981). "Risk Methodology for Geologic Disposal of Radioactive Waste: Effects of Variable Hydrologic Patterns on the Environmental Transport Model," NUREG/CR-1636, Vol. 4, SAND79-1909, Sandia National Laboratories, Albuquerque, New Mexico 87185.

Cacuci, D. G., Weber, C. F., Oblow, E. M., and Marable, J. H. (1980). "Sensitivity Theory for General Systems of Nonlinear Equations," Nuclear Science and Engineering, 75, 88-110.

Cacuci, D. G. (1981a). "Sensitivity Theory for Nonlinear Systems. I. Nonlinear Functional Analysis Approach," Journal of Mathematical Physics, 22, 2794-2802.

Cacuci, D. G. (1981b). "Sensitivity Theory for Nonlinear Systems. II. Extensions to Additional Classes of Responses," Journal of Mathematical Physics, 22, 2803-2812.

Cacuci, D. G., Maudlin, P. J., and Parks, C. U. (1983). "Adjoint Sensitivity Analysis of Extremum-Type Responses in Reactor Safety," Nuclear Science Engineering.

Cox, N. D. (1977). "Comparison of Two Uncertainty Analysis Methods," Nuclear Science Engineering, 64, 258-265.

Cranwell, R. M., Campbell, J. E., Helton, J. C., Iman, R. L., Longsine, D. E., Ortiz, N. R., Runkel, G. E., and Shortencarier, M. J. (1982). "Risk Methodology for Geologic Disposal of Radioactive Waste: Final Report," NUREG/R-2452, SAND82-2573, Sandia National Laboratories, Albuquerque, New Mexico 87185.

Cranwell, R. M., Campbell, J. E., and Stuckwisch, S. E. (1982). "Risk Methodology for Geologic Disposal of Radioactive Waste: The DNET Computer Code User's Manual," NUREG/CR-2343, SAND81-1663, Sandia National Laboratories, Albuquerque, New Mexico 87185.

Cranwell, R. M., Campbell, J. E., Stuckwisch, S. E., Longsine, D. E., and Finley, N. C. (1983). "DNET Self-Teaching Curriculum," NUREG/CR-2391, SAND81-2256, Sandia National Laboratories, Albuquerque, New Mexico 87185.

Cranwell, R. M., Iman, R. L., and Stuckwisch, S. E. (1985). "Risk Methodology for Geologic Disposal of Radioactive Waste: Sensitivity Analysis of the Dynamic Network (DNET) Model." In preparation.

Cukier, R. I., Fortuin, C. M., Shuler, K. E., Petschek, A. G., and Schaibly, J. H. (1973). "Study of the Sensitivity of Coupled Reaction Systems to Uncertainties in Rate Coefficients. I. Theory," J. Chem. Phys., 59, 3873-3878.

Cukier, R. I., Schaibly, J. H., and Shuler, K. E. (1975). "Study of the Sensitivity of Coupled Reaction Systems to Uncertainties in Rate Coefficients. III. Analysis of the Approximations," J. Comp. Phys., 63, 1140-1149.

Cukier, R. I., Levine, H. B., and Shuler, K. E. (1978). "Nonlinear Sensitivity Analysis of Multiparameter Model Systems," J. Comp. Phys., 26, 1-42.

Cunningham, M. E., Hann, C. R., and Olsen, A. R. (1980). "Uncertainty Analysis and Thermal Stored Energy Calculations in Nuclear Fuel Rods," Nucl. Tech., 47, 457-467.

Dacol, D. K. and Rabitz, H. (1983). "Arbitrary Order Functional Sensitivity Densities for Reaction-Diffusion Systems," J. Chem. Phys., 78, 4905-4914.

Davies, O. L., Ed. (1956). The Design and Analysis of Industrial Experiments, Hafner Publishing Company, New York.

DeBaun, R. M. (1959). "Response Surface Designs for Three Factors at Three Levels," Technometrics, 1, 1-8.

Demiralp, M. and Rabitz, H. (1981a). "Chemical Kinetic Functional Sensitivity Analysis: Elementary Sensitivities," J. Chem. Phys., 74, 3362-3375.

Demiralp, M. and Rabitz, H. (1981b). "Chemical Kinetic Functional Sensitivity Analysis: Derived Sensitivities and General Applications," J. Chem. Phys., 75, 1810-1819.

Dickinson, R. P. and Gelinas, R. J. (1976). "Sensitivity Analysis of Ordinary Differential Equation Systems--A Direct Method," J. Comp. Phys., 21, 123- 143.

Dougherty, E. P., Hwang, J.-T., and Rabitz, H. (1979). "Further Developments and Applications of the Green's Function Method of Sensitivity Analysis in Chemical Kinetics," J. Chem. Phys., 71, 1794-1808.

Downing, D. J., Gardner, R. H. and Hoffman, F. O. (1985). "Response Surface Methodologies for Uncertainty Analysis in Assessment Models," Technometrics. To appear.

Draper, N. R. (1982). "Center Points in Second-Order Response Surface Designs," Technometrics, 24(2), 127-133.

Draper, N. R. and Smith, H. (1981). Applied Regression Analysis, Second Edition, John Wiley & Sons, Inc., New York.

Dunker, A. M. (1981). "Efficient Calculation of Sensitivity Coefficients for Complex Atmospheric Models," Atmospheric Environment, 15, 1155-1161.

Falls, A. H., McRae, G. J., and Seinfeld, J. H. (1979). "Sensitivity and Uncertainty of Reaction Mechanisms for Photochemical Air Pollution," Int. J. Chem. Kinet., 11, 1137-1162.

Finney, D. J. (1960). The Theory of Experimental Design, The University of Chicago Press, Chicago.

Frank, P. M. (1978). Introduction to System Sensitivity Theory, Academic Press, New York, New York.

Gelbard, F. (1982). "MAEROS User Manual," NUREG/CR-1391, SAND80-0822, Sandia National Laboratories, Albuquerque, New Mexico 87185.

Gelbard, F. and Seinfeld, J. H. (1980). "Simulation of Multicomponent Aerosol Dynamics," J. Colloid Interface Sci., 78, 485.

Greenspan, E. (1976). "Developments in Perturbation Theory," Advances in Nuclear Science and Technology, Vol. 9, Academic Press, New York.

Hall, M. C. G., Cacuci, D. G., and Schlesinger, M. E. (1982). "Sensitivity Analysis of a Radiative-Convective Model by the Adjoint Method," Journal of Atmospheric Science, 39, 2038-2050.

Harper, W. V. and Gupta, S. K. (1983). "Sensitivity/Uncertainty Analysis of a Borehole Scenario Comparing Latin Hypercube Sampling and Deterministic Sensitivy Approaches," BMI/ONWI-516, Battelle Memorial Institute, Columbus, Ohio 43201

Helton, J. C., Brown, J. B., and Iman, R. L. (1981). "Risk Methodology for Geologic Disposal of Radioactive Waste: Asymptotic Properties of the Environmental Transport Model," NUREG/CR-1636, Vol. 3, SAND79-1908, Sandia National Laboratories, Albuquerque, New Mexico 87185.

Helton, J. C. and Finley, N. C. (1982). "PATHI Self Teaching Curriculum: Example Problems for Pathways-to-Man Model," NUREG/CR-2394, SAND81-2377, Sandia National Laboratories, Albuquerque, New Mexico 87185.

Helton, J. C. and Iman, R. L. (1980). "Risk Methodology for Geologic Disposal of Radioactive Waste: Sensitivity Analysis of the Environmental Transport Model," NUREG/CR-1636, Vol. 2, SAND79-1393, Sandia National Laboratories, Albuquerque, New Mexico 87185.

Helton, J. C. and Iman, R. L. (1982). "Sensitivity Analysis of a Model for the Environmental Movement of Radionuclides," Health Physics, 42(5), 565-584.

Helton, J. C., Iman, R. L., Johnson, J. D. and Leigh, C. D. (1985). "Uncertainty and Sensitivity Analysis of a Model for Multicomponent Aerosol Dynamics," SAND84-1307, Sandia National Laboratories, Albuquerque, NM 87185. To appear.

Helton, J. C., Iman, R. L., and Brown, J. B. (1985). "Sensitivity Analysis of the Asymptotic Behavior of a Model for the Environmental Movement of Radionuclides," Ecological Modelling. To appear.

Helton, J. C. and Kaestner, P. C. (1981). "Risk Methodology for Geologic Disposal of Radioactive Waste: Model Description and User Manual for Pathways Model," NUREG/CR-1636, Vol. 1, SAND81-1711, Sandia National Laboratories, Albuquerque, New Mexico 87185.

Huber, P. J. (1981). Robust Statistics, John Wiley and Sons, Inc., New York.

Hwang, J.-T., Dougherty, E. P., Rabitz, S., and Rabitz, H. (1978). "The Green's Function Method of Sensitivity Analysis in Chemical Kinetics," J. Chem. Phys., 69, 5180-5191.

Iman, R. L. and Conover, W. J. (1980). "Small Sample Sensitivity Analysis Techniques for Computer Models, with an Application to Risk Assessment," Communications in Statistics, A9(17), 1749-1842. "Rejoinder to Comments," 1863-1874.

Iman, R. L. and Conover, W. J. (1982a). "A Distribution-Free Approach to Inducing Rank Correlation Among Input Variable," Communications in Statistics, B11(3), 311-334.

Iman, R. L. and Conover, W. J. (1982b). "Sensitivity Analysis Techniques: Self-Teaching Curriculum," NUREG/CR-2350, SAND81-1978, Sandia National Laboratories, Albuquerque, New Mexico 87185.

Iman, R. L. and Conover, W. J. (1983). A Modern Approach to Statistics, John Wiley & Sons, Inc., New York.

Iman, R. L. and Conover, W. J. (1985). "A Measure of the Top-Down Correlation," In preparation.

Iman, R. L., Helton, J. C., and Campbell, J. E. (1981a). "An Approach to Sensitivity Analysis of Computer Models, Part 1. Introduction, Input Variable Selection and Preliminary Variable Assessment," Journal of Quality Technology, 13(3), 174-183.

Iman, R. L., Helton, J. C., and Campbell, J. E. (1981b). "An Approach to Sensitivity Analysis of Computer Models, Part 2. Ranking of Input Variables, Response Surface Validation, Distribution Effect and Technique Synopsis," Journal of Quality Technology, 13(4), 232-40.

Iman, R. L. and Shortencarier, M. J. (1984). "A Fortran 77 Program and User's Guide for the Generation of Latin Hypercube and Random Samples for Use with Computer Models," NUREG/CR-3624, SAND83-2365, Sandia National Laboratories, Albuquerque, NM 87185.

Iman, R. L., Shortencarier, M. J. and Johnson, J. D. (1985). "A Fortran 77 Program and User's Guide for the Calculation of Partial Correlation and Standardized Regression Coefficients," NUREG/CR-4122, SAND85-0044, Sandia National Laboratories, Albuquerque, NM 87185.

Kleijnen, J. P. C. (1979). "Regression Metamodels for Generalizing Simulation Results," IEEE Trans. Syst., Man, and Cybern., SMC-9, 93-96.

Koda, M. (1982). "Sensitivity Analysis of the Atmospheric Diffusion Equation," Atmospheric Environment, 16, 2595-2601.

Koda, M., Dogru, A. H., and Seinfeld, J. A. (1979). "Sensitivity Analysis of Partial Differential Equations with Application to Reaction and Diffusion Processes," Journal of Computational Physics, 30, 259-282.

Koda, M., McRae, G. J., and Seinfeld, J. H. (1979). "Automatic Sensitivity Analysis of Kinetic Mechanisms," Int. J. Chem. Kinet., 11, 427-444.

Kramer, M. A., Calo, J. M., Rabitz, H., and Kee, R. J. (1982). "AIM: The Analytically Integrated Magnus Method for Linear and Second Order Sensitivity Coefficients," SAND82-8231, Sandia National Laboratories, Albuquerque, New Mexico 87185.

Lee, K. W., Gieseke, J. A., and Reed, L. D. (1979). "Sensitivity Analysis of the HAARM-3 Code," NUREG/CR-0527, Battelle Columbus Laboratories, Columbus, Ohio 43201.

Lewins, J. and Becker, M., Eds. (1982). "Sensitivity and Uncertainty Analysis of Reactor Performance Parameters," Advances in Nuclear Science and Technology, Vol. 14, Plenum Press, New York.

Marquardt, D. W. and Snee, R. D. (1975). "Ridge Regression in Practice," The American Statistician, 29(1), 3-20.

Marquardt, D. W. (1970). "Generalized Inverses, Ridge Regression, Biased Linear Estimation and Nonlinear Estimation," Technometrics, 12(3), 591-612.

McKay, M. D., Conover, W. J., and Beckman, R. J. (1979). "A Comparison of Three Methods for Selecting Values of Input Variables in the Analysis of Output from a Computer Code," Technometrics, 21(2), 239-245.

McRae, G. J., Tilden, J. W., and Seinfeld, J. H. (1981). "Global Sensitivity Analysis - A Computational Implementation of the Fourrier Amplitude Sensitivity Test," Comput. Chem. Engng., 5.

Morisawa, S. and Inoue, Y. (1974). "On the Selection of a Ground Disposal Site by Sensitivity Analysis," Health Phys., 26, 251-261.

Myers, R. H. (1971). Response Surface Methodology, Allyn and Bacon, Boston.

Nguyen, D. H. (1980). "The Uncertainty in Accident Consequences Calculated by Large Codes Due to Uncertainties in Input," Nucl. Technol., 49, 80-91.

Oblow, E. M. (1983a). "An Automated Procedure for Sensitivity Analysis Using Computer Calculus," ORNL/TM-8776, Oak Ridge National Laboratory, Oak Ridge, Tennessee 37830.

Oblow, E. M. (1983b). "GRESS: Gradient-Enhanced Software System, Version B, User's Guide," ORNL/TM-8339, Oak Ridge National Laboratory, Oak Ridge, Tennessee 37830.

Piepho, M. G., Cady, K. B., and Kenton, M. A. (1981). "An Importance Theory for Nonlinear Ordinary Differential Equations," Report No. HEDL-TME 81-24, Hanford Engineering Development Laboratory, Richland, Washington.

Pierce, T. H. and Cukier, R. I. (1981). "Global Nonlinear Sensitivity Analysis Using Walsh Functions," J. Comp. Phys., 41, 427-443.

Raktoe, B. L., Hedayat, A., and Federer, W. T. (1981). Factorial Designs, John Wiley & Sons, Inc., New York.

Savage, I. R. (1956). "Contributions to the Theory of Rank Order Statistics - the Two-Sample Case," Annals of Mathematical Statistics, 27, 590-615.

Schaibly, J. H. and Shuler, K. E. (1973). "Study of the Sensitivity of Coupled Reaction Systems to Uncertainties in Rate Coefficients. II. Applications," J. Chem. Phys., 59, 3879-3889.

Shampine, L. F. and Watts, H. A. (1980). "DEPAC--Design of a User Orientated Package of ODE Solvers," Report No. SAND79-2374, Sandia National Laboratories, Albuquerque, New Mexico.

Sprung, J. L., Aldrich, D. C., Alpert, D. J., and Weigand, G. G. (1983). Overview of the MELCOR Risk Code Development Program, in Proceedings of the International Meeting on Light Water Reactor Severe Accident Evaluation, pp. TS-10.1-1 to TS-10.1-8, Cambridge, MA, August 28-September 1, 1983.

Stacey, W. M. (1974). Variational Methods in Nuclear Reactor Physics, Academic Press, New York.

Steck, G. P., Dahlgren, D. A., and Easterling, R. G. (1975). "Statistical Analysis of LOCA, FY75 Report, "Technical Report SAND75-0653, Sandia National Laboratories, Albuquerque, NM 87185

Steinhorst, R. K., Hunt, H. W., Innis, G. S., and Haydock, K. P. (1978). "Sensitivity Analysis of the ELM Model." Grassland Simulation Model, edited by G. S. Innis, 231-255, Springer-Verlag, New York, New York.

Tilden, J. W. and Seinfeld, J. H. (1982). "Sensitivity Analysis of a Mathematical Model for Photochemical Air Pollution," Atmospheric Environment, 16, 1357-1364.

Tomovic, R. (1963). Sensitivity Analysis of Dynamic Systems, McGraw-Hill, New York.

Tomovic, R. and Vukobratovic, M. (1972). General Sensitivity Theory, Elsevier, New York.

Division of Technical Information
and Document Control
NRC Distribution Contractor
U.S. Nuclear Regulatory Commission
15700 Crabbs Branch Way
Rockville, MD 20850
250 Copies for RG

USNRC
Division of Risk Analysis and Operations
Washington, DC 20555
M. Cunningham (40)
J. Johnson (5)
L. Lancaster (5)
T. Margulies (5)
D. Rasmuson (5)

Los Alamos National Laboratories (3)
Group S1, MS 606
Los Alamos, NM 87545
H. F. Martz
M. E. Johnson
R. A. Waller

David C. Aldrich
SAIC
1710 Goodridge Drive
P.O. Box 1303
McLean, VA 22102

George Apostolakis
Mechanics and Structures Dept.
UCLA
Los Angeles, CA 90024

Clarence H. Arnett
P.O. Box 702
U.S. Army Combined Army Center
Shawnee Mission, KS 66201

Cory Atwood
EG&G Idaho
P. O. Box 1625
Idaho Falls, ID 83415

William Balson
Decision Focus, Inc.
Los Altos Office Center
Suite 200
4984 El Camino Road
Los Altos, CA 94022

Nathaniel F. Barr
U.S. Department of Energy
Wshington, DC 20545

Steve Bartell
Environmental Sciences Division
Oak Ridge National Laboratory
P.O. Box X
Oak Ridge, TN 37830

Ioannis G. Bartzis
Greek Atomic Energy Commission
Nuclear Research Center Demokritos
Aghia Paraskevi
Attikis
GREECE

Carl B. Bates
U.S. Army Concepts Analysis Agency
8120 Woodmont Ave.
Bethesda, MD 20814

Paul Baybutt
Battelle Laboratories
505 King Avenue
Columbus, OH 43201

Anthony Bayer
Kernforschnungszentrum Karlsruhe G.m.b.H.
Postfach 3640
D-7500 Karlsruhe 1, WEST GERMANY

Carl A. Bennett
Human Affairs Research Center, Battelle
P.O. Box C-5395
Seattle, WA 98105

M. R. Binns
Engineering and Statistical Research Institute
Canada Agriculture, Bldg. 54
Central Experimental Farm
Ottawa, CANADA K1A OC6

Nicholas Birkett
Department of Clinical Epidemiology
& Biostatistics
McMaster University
1200 Main Street
Hamilton, Ontario, L8N 3Z5
CANADA

Thomas A. Bishop
Battelle
505 King Avenue
Columbus, OH 43201

Carla Brofferio
Comitato Nazionale per l'Energia Nucleare
Viale Regina Margherita, 125
Casella Postale N. 2358
I-00100 Roma A.D.
ITALY

Robert Budnitz
Future Resources Associates
734 The Alemeda
Berkeley, CA 94707

Anthony R. Buhl
Technology for Energy Corp.
10770 Dutch Town Rd.
Knoxville, TN 37922

Klaus Burkart
Institut fur Neutronenphysik und
Reaktortechnik (INR)
Kernforschungszentrum Karlsruhe G.m.b.H.
Postfach 3640
D-7500 Karlsruhe 1, WEST GERMANY

D. G. Cacuci
Oak Ridge National Laboratory
Engineering Physics Division
P.O. Box X
Oak Ridge, TN 37830

Pietro Cagnetti
PAS Comitato Nazionale per l'Energia Nucleare
Centro di Studi Nucleari della Casaccia
Via Anguillarese km 1+300
I-00060 Roma
ITALY

James E. Campbell (2)
Intera Environmental Consultants Inc.
11999 Katy Freeway
Houston, TX 77079

S. Chakraborty
Abtielung fur die Sicherheit der Kernanlagen
Eidgenossisches Amt fur Energiewirtschaft
Wurenlingen
SWITZERLAND

Douglas Chambers
Executive Vice President
Senes Consultants Ltd.
499 McNicoll Avenue
Willowdale, Ontario
CANADA M2H 2C9

Lai K. Chan
Department of Statistics
The University of Manitoba
Winnipeg, Manitoba
CANADA R3T 2N2

Alistair D. Christie
Deputy Director, Air Quality and
Inter-Environmental Research Branch
Environment Canada
Atmospheric Environment Service
4905 Dufferin Street
City of North York, Downsview
Ontario, M3H 5T4
CANADA

W. J. Conover (8)
College of Business Administration
Texas Tech University
Lubbock, TX 79409

Michael L. Corradini
University of Wisconsin - Madison
Nuclear Engineering Dept.
145 Engr. Res. Building
1500 Johnson Drive
Madison, WI 53706

A. Bruce Crane
The Aerospace Corporation
Suite 4000
955 L'Enfant Plaza, SW
Washington, DC 20024

M. Crick
National Radiological Protection Board
Chilton
Didcot
Oxon. OX11 ORQ
UNITED KINGDOM

Michael Cullingford
P.O. Box 200
A-1400
Vienna, AUSTRIA

J. M. Davenport
Department of Mathematics
Texas Tech University
Lubbock, TX 79409

Felix Dayo
IKE
Universitat Stuttgart
Postfach 801140,
7000 Stuttgart 80
WEST GERMANY

Joseph L. Devary
Battelle Northwest
P.O. Box 999
Richland, WA 99352

Pamela Doctor (2)
Battelle Northwest
P.O. Box 999
Richland, WA 99352

Gordon B. Dobbins
General Dynamics
P.O. Box 748
Fort Worth, TX 76101

Darryl Downing
Computer Sciences
Building 2029, P.O. Box X
ORNL
Oak Ridge, TN 37830

Gene Dutoit
% Commandant
U. S. Army Infantry School
ATTN: ATSH-CD-CS-OR (Dutoit)
Fort Benning, GA 31905

Ove Edlund
Studsvik Energiteknik AB
Studsvik
Fack
S-611 82 Nykoping 1
SWEDEN

Bert T. Eendebak
KEMA Laboratories
Utrechtseweg, 310
Postbus 9035
NL-6800 ET Arnhem
NETHERLANDS

Daniel Egan (2)
Office of Radiation Program s(ANR-460)
U. S. Environmental Protection Agency
Washington, DC 20460

Steve Eide
Energy Inc.
5345 Wyoming N E.
Suite 101
Albuquerque, NM 87109

Oskar M. Essenwanger
Supv. Res. Phys., Aerophysics
Research Directorate
U.S. Army Missile Laboratory
Redstone Arsenal, AL 35898

Lissa Galbraith
Dept. of Industrial Engineering
& Operations Research
Virginia Polytechnic Institute
Blacksburg, VA 24061

Brenda Ganheart
Mainerals Management Service
P.O. Box 7944
Metairie, LA 70010-7944

R. H. Gardner
Environmental Sciences Division
ORNL
Oak Ridge, TN 37830

Larry George
Lawrence Livermore Laboratory
P.O. Box 808 L-140
Livermore, CA 94550

Herb Ginsburg
Westinghouse Electric Corp.
Bettis Atomos Power Lab.
P.O. Box 79
West Mifflin, PA 15122

Dave G. Gosslee (6)
P.O. Box Y, Bldg. 9704-1
ORNL
Oak Ridge, TN 37830

Steve Goldstein
The MITRE Corporation
1820 Dolly Madison Blvd.
McLean, VA 22102

Richard Gunst (5)
Department of Statistics
Southern Methodist University
Dallas, TX 75275

Allan Gutjahr
Department of Mathematics
NMIMT
Socorro, NM 87801

William V. Harper (2)
Performance Analysis Department
Battelle
505 King Avenue
Columbus, OH 43201

Bernard Harris
Dept. of Statistics
1210 W. Dayton St.
Madison, WI 53711

Michael Haynes
United Kingdom Atomic Energy Authority
Safety & Reliability Directorate
Wigshaw Lane
Culcheth
Warrington WA3 4NE
UNITED KINGDOM

Max Henrion
Dept. of Engineering and Public Policy
Carnegie-Mellon University
Pittsburgh, PA 15213

Margaret F. Hickey
Rocky Flats Plant
Energy Systems Group
Rockwell International Corporation
P. O. Box 464
Golden, CO 80401

Edward Hofer
Gesellschaft für Reaktorsicherheit
D-8046 Garching
Federal Republic of Germany

F. O. Hoffman
Health and Safety Research Division
ORNL
Oak Ridge, TN 37830

David Hopper
Senes Consultants Ltd.
499 McNicoll Avenue
Willowdale, Ontario
CANADA M2H 2C9

Stephen C. Hora (8)
College of Business Administration
Texas Tech University
Lubbock, TX 79409

Frank W. Horsch
Kernforschungszentrum Karlsruhe G.m.b.H.
Postface 3640
D-7500 Karlsruhe 1
WEST GERMANY

Audrey Hutchcraft
Travenol Laboratories, Inc.
P.O. Box 490/RLA-3N
Round Lake, IL 60073

Mr. Toshinori Iijima
Division of Reactor Safety Evaluation
Reactor Safety Research Center
Japan Atomic Energy Research Institute
Tokai Research Establishment
Tokai-mura
Naka-gun
Ibaraki-ken 319-11, JAPAN

Janeen Judah
Department of Petroleum Engineering
Texas A&M University
College Station, TX 77843

Geoffrey D. Kaiser
Consulting Division
NUS Corporation
910 Clopper Road
Gaithersburg, MD 20878

Stanley Kaplan
Pickard, Lowe and Garrick, Inc.
17840 Skypark Blvd.
Irvine, CA 92714

Samuel C. Kao (2)
Applied Mathematics, 515
Brookhaven National Laboratory
Upton, NY 11973

Dean C. Kaul
Science Applications, Inc.
Suite 819
1701 East Woodfield Road
Schaumburg, IL 60195

G. Neale Kelly (2)
NII
HSE
Silkhouse Court
Tithebarn Street
Liverpool L2 2LZ
UNITED KINGDOM

K. E. Kemp
Department of Statistics
Kansas State University
Manhattan, KS 66502

Kensake Kobayashi
Risk Analysis Laboratory
Dept. of Nuclear Safety Evaluation
Japan Atomic Energy Research Institute
Tokyo, JAPAN

Robert L. Kolesar
Engelhard
Menlo Park CN28
Edison, NJ 08818

Jan G. Kretzschmar
Studiecentrum voor Kernenergie (SCK/CEN)
Boeretang, 200
B-2400 Mol
BELGIUM

Keith Kussmaul
Westinghouse R & D Center
Pittsburgh, PA 15235

Joseph Lewi (2)
IPSN/DAS/SAED
CEN-FAR
B.P. n° 6
92260 Fontenay Aux Roses
FRANCE

Daniel Manesse
Institut de Protection et de
Surete Nucleaire (IPSN)
Commissariat a l'Energie Atomique
Centre d'Etudes Nucleaires de
Fontenay-aux-Roses
Boite Postale 6
F-92260 Fontenay-aux-Roses, FRANCE

David S. Margoles (2)
Mathematics and Statistics Division
Lawrence Livermore Laboratory
P.O. Box 808 (L-316)
Livermore, CA 94550

David Martin
Atomic Energy Control
P.O. Box 1046
Ottawa, CANADA K1P 5S9

Ali Masleh
Pickard, Lowe and Garrick, Inc.
Engineering Consultants
2260 University Drive
Newport Beach, CA 92660

Scott Mathews
EG&G Idaho
M.S. TSB
P.O. Box 1625
Idaho Falls, ID 83415

Hue McCoy (3)
TRASANA
White Sands Missile Range
White Sands, NM 88002

Fran McMichael
Dept. of Civil Engineering
Carnegie-Mellon University
Pittsburgh, PA 15213

Greg McRae
Dept. of Chemical Engineering
Carnegie-Mellon University
Pittsburgh, PA 15213

Marise Mikulis
Arthur D. Little, Inc.
Alcorn Park
Cambridge, MA 02140

M. Granger Morgan
Dept. of Engineering and Public Policy
Carnegie-Mellon University
Pittsburgh, PA 15213

Bernie Most
Northrop Services, Inc.
Box 12312
Research Triangle Park, NC 27709

John Mular
Dept. of Civil Engineering
Carnegie-Mellon University
Pittsburgh, PA 15213

K. E. Muller
School of Public Health
Department of Biostatistics
The University of North Carolina
Chapel Hill, NC 27514

Robert J. Mulvihill, F40
Fluor Technology, Inc.
3333 Michelson Drive
Irvine, CA 92730

Shan Nair
Research Division
Central Electricity Generating Board
Berkeley Nuclear Laboratories
Berkeley
Gloucestershire GL13 9PB
UNITED KINGDOM

David S. Newman
Boeing Computer Services
565 Andover Park West
MS 9C-01
Tuckwila, WA 98188

William Nixon
United Kingdom Atomic Energy Authority
Safety & Reliability Directorate
Wigshaw Lane
Culcheth
Warrington WA3 4NE
UNITED KINGDOM

Warner North
Decision Focus, Inc.
Los Altos Office Center
Suite 200
4984 El Camino Real
Los Altos, CA 94022

E. M. Oblow
Oak Ridge National Laboratory
Engineering Physics Division
P.O. Box X
Oak Ridge, TN 37830

Neal Oden
BEAD - Building 475
Brookhaven National Laboratory
Upton, NY 11973

Don Paddleford
Westinghouse
P.O. Box 355
Pittsburgh, PA 15230

Robert Pavur
College of Business Administration
Dept. of BCIS
North Texas State University
Denton, TX 76203

Derek J. Pike
Department of Statistics
The University of Reading
Whiteknights
Reading RG6 2AN
ENGLAND

Kurt H. Porn
Probabilistic Risk and Reliability Assessment
Nuclear Division
Studsvik Energiteknik AB
S-611 82 Nykoping
SWEDEN

Robert P. Rathmacher
Lilly Research Laboratories
Greenfield, IN 46140

Norman C. Rasmussen (3)
Dept. of Nuclear Engineering
Massachusetts Institute of Technology
77 Mass Avenue
Cambridge, MA 02139

Mark Reeves (3)
Intera Environmental Consultants
11511 Katy Freeway
Suite 630
Houston, TX 77079

Sam Rod
Westinghouse Electric Corporation
Waste Technology Services Division
Madison, PA 15663-0286

Ilkka Savolainen
Technical Research Centre of Finland
Nuclear Engineering Laboratory
P. O. Box 169
SF-00181 Helsinki 18
FINLAND

Fritz Seiler
Inhalation Toxicology Research
Institute
Lovelace Biomedical and Environmental
Research Institute
Albuquerque, NM 87185

Sebastiano Serra
ENEL-DCO
Ente Nazionale per l'Energia Elettrica
Via G.B. Martini, 3
Casella Postale N. 386
I-00186 Roma
ITALY

Robert Sewell
P. O. Box 4990
Stanford, CA 94305

Juan Bagues Somonte
Junta de Energia Nuclear
Ciudad Universitaria
Avenida Complutense, 22
Madrid-3
SPAIN

David A. Stanners
Commission on European Communities
Joint Research Center
Ispra Establishment
21020 Ispra (Varese)
ITALY

John R. D. Stoute
Health Physics Division
Energieonderzoek Centrum Nederland (ECN)
Westerduinweg, 3
Postbus 1
NL-1755 Petten ZG
NETHERLANDS

Marian Stubna
Nuclear Power Plants
Research Institute
VUJE
919 3 Jaslovske Bohunice
orkes Trnava
CZECHOSLOVAKIA

Donald M. Swingle
P.O. Box 160
Las Cruces, NM 88004

Soren Thykier-Nielsen
Health Physics Department
Riso National Laboratory
Postbox 49
DK-4000 Roskilde, DENMARK

Alfred Torri
Pickard, Lowe and Garrick, Inc.
2260 University Drive
Newport Beach, CA 92660

Ulf Tveten (Technical Secretary)
Institutt for Energiteknikk
Postboks 40
N-2007 Kjeller, NORWAY

C. F. H. Van Ryn
Royal Dutch/Shell Laboratory
Dept. MSE/5
P. O. Box 3003
1003 AA Amsterdam
NETHERLANDS

Jussi K. Vaurio
Argone National Laboratory, Bldg. 207
9700 South Cass Avenue
Argonne, IL 60439

W. E. Vesely
Risk Safety and Reliability Section
Battelle Laboratories
Columbus, Ohio 43201

I. B. Wall
Electric Power Research Institute
3412 Hillview Avenue
P.O. Box 10412
Palo Alto, CA 94303

Norio Watanabe
Risk Analysis Laboratory
Japan Atomic Energy Research Institute (JAERI)
Tokai-mura, Naka-gun, Ibaraki-Ken
JAPAN

Stephen Watson
Decision Science Consortium
7700 Leesburg Pike
Suite 421
Falls Church, VA 22043

Keith Woodard
Pickard, Lowe & Garrick, Inc.
1200 18th Steet, N.W.
Suite 612
Washington, DC 20036

Jon Young
Energy Incorporated
515 West Harrison
Suite 220
Kent, WA 98031

Shelly Zacks
Dept. of Math Sciences
SUNY - Binghamton
Binghamton, NY 13901

Eric R. Ziegel
Standard Oil Company (Indiana)
Amoco Research Center
P.O. Box 400
Naperville, IL 60566

Auguste Zurkinden
Abteilung fur die Sicherheit
der Kernanlagen
Bundesamt fur Energiewirtschaft
CH-5303 Wurenlingen
SWITZERLAND

2564	G. W. Smith
3141	C. M. Ostrander (5)
3151	W. L. Garner
6246	H. P. Stephens
6312	R. R. Peters
6312	M. S. Tierney
6334	D. R. Anderson
6400	A. W. Snyder
6410	J. W. Hickman
6411	A. S. Benjamin
6412	A. L. Camp
6412	M. P. Bohn
6414	D. M. Ericson
6415	D. J. Alpert
6415	R. P. Burke
6415	J. M. Griesmeyer
6415	F. E. Haskin
6415	J. C. Helton
6415	R. L. Iman (11)
6415	C. D. Leigh
6415	R. M. Ostmeyer
6415	J. L. Sprung
6417	D. D. Carlson
6422	J. E. Brockmann
6422	J. E. Gronager
6430	N. R. Ortiz
6431	R. M. Cranwell
6432	L. D. Chapman
6444	J. M. McGlaun
6444	S. W. Webb
6449	K. D. Bergeron
6449	K. K. Murata
7223	R. G. Easterling
7223	M. J. Shortencarier
7223	F. W. Spencer
8024	M. A. Pound

NRC FORM 335 (12-84) NRCM 1102, 3201, 3202

U.S. NUCLEAR REGULATORY COMMISSION

SEE INSTRUCTIONS ON THE REVERSE

BIBLIOGRAPHIC DATA SHEET

1 REPORT NUMBER (Assigned by TIDC and Vol. No., if any)

NUREG/CR-3904
SAND84-1461

2 TITLE AND SUBTITLE

A Comparison of Uncertainty and Sensitivity Analysis Techniques for Computer Models

3 LEAVE BLANK

4 DATE REPORT COMPLETED

MONTH: January — YEAR: 1985

5 AUTHOR(S)

Ronald L. Iman and Jon C. Helton

6 DATE REPORT ISSUED

MONTH: March — YEAR: 1985

7 PERFORMING ORGANIZATION NAME AND MAILING ADDRESS (Include Zip Code)

Sandia National Laboratories
Albuquerque, NM 87185

8 PROJECT/TASK/WORK UNIT NUMBER

9 FIN OR GRANT NUMBER

A-1339

10 SPONSORING ORGANIZATION NAME AND MAILING ADDRESS (Include Zip Code)

Division of Risk Analysis and Operations
Office of Nuclear Regulatory Research
U. S. Nuclear Regulatory Commission
Washington, DC 20555

11a TYPE OF REPORT

Technical

b PERIOD COVERED (Inclusive dates)

12 SUPPLEMENTARY NOTES

13 ABSTRACT (200 words or less)

Uncertainty analysis and sensitivity analysis are important elements in the development and implementation of computer models for complex processes. Typically, there are many uncertainties associated with both the development and the application of such models. Understanding of these uncertainties and their causes is required to effectively interpret model behavior. Many different techniques have been proposed for performing uncertainty and sensitivity analyses. The objective of the present study is to compare several widely used techniques on three models having large uncertainties and varying degrees of complexity in order to highlight some of the problem areas that must be addressed in actual applications. The following approaches to uncertainty and sensitivity analysis are considered: (1) response surface methodology based on input determined from a fractional factorial design, (2) Latin hypercube sampling with and without regression analysis, and (3) differential analysis. These techniques are compared on the basis of (1) ease of implementation, (2) flexibility, (3) estimation of the cumulative distribution function of the output, and (4) adaptability to different methods of sensitivity analysis. With respect to these criteria, the technique using Latin hypercube sampling and regression analysis gives the best results overall. The models used in the comparisons are well documented, thus making it possible for researchers to make comparisons of other techniques with the results in this study.

14 DOCUMENT ANALYSIS - a KEYWORDS/DESCRIPTORS

b IDENTIFIERS/OPEN ENDED TERMS

15 AVAILABILITY STATEMENT

GPO Sales and NTIS

16 SECURITY CLASSIFICATION

(This page) Unclass.

(This report) Unclass.

17 NUMBER OF PAGES

18 PRICE

☆ U.S. Government Printing Office 1985-576-051/20,040